Digital Implementation of a Soliton System

Digital Implementation of a Soliton System

By

Qiuyuan Huang
M. E. University of Science and Technology of China
B. E. University of Science and Technology of China

A Thesis
Submitted to the Department of Electrical and Computer Engineering
and the School of Graduate Studies
in Partial Fulfilment of the Requirements
for the Degree of
Master in Applied Science

McMaster University

©Copyright by Qiuyuan Huang, December 2007

Master of Applied Science (2007) McMaster University
Electrical and Computer Engineering Hamilton, Ontario

TITLE: Digital Implementation of A Soliton System

AUTHOR: Qiuyuan Huang

SUPERVISORS: Dr. Kon Max Wong, Dr. Steve Hranilovic

NUMBER OF PAGES: xv, 130

Abstract

Solitons and soliton systems have introduced many interests in the applications of signal processing and communication systems due to their special properties. To facilitate the various applications, a digital soliton system is designed to overcome the inherent drawbacks of traditional analog soliton systems in this thesis. Wave digital theory is employed to design a digital model of the nonlinear Toda lattice circuit. The designed model is implemented in Simulink, and numerical results of the simulation verifies the important properties of the digital model and show it to be a good digital soliton system simulator.

Moreover, an example of a soliton communication system is provided to demonstrate the digital soliton system simulator can work as well in soliton communication systems, avoiding the inherent problems of analog implementations.

In addition, the digital Toda lattice circuit modelled in Simulink can be customized to run in DSP and FPGA. Such hardware co-processing will highly improve the speed of the simulation processes.

Acknowledgements

I would like to express my deep and sincere gratitude to my supervisor, Dr. Kon Max Wong. The guidance and encouragement from him are predominant to the completion of this work. His rigorous attitude to research inspired me to my growth of independent research.

I am deeply indebted to my co-supervisor, Dr. Steve Hranilovic. His stimulating suggestions and brilliant ideas helped me in all the time of research for and writing of this thesis.

I would like to thank Dr. Jiankang Zhang and Dr. Shahin Sirouspour for their carefully reviewing my thesis and constructive comments on this thesis. My gratitude also goes to my colleagues at Electrical and Computer Engineering Department for their support. I would like to thank Rong Chai for her helpful discussions regarding this work. So many thanks to all of my best friends for their friendship and support.

Finally, I give my deepest gratitude and love to my family. My parents Yazhou Huang and Ling Jin have always been my source of love and support. Especially, I would like to give my special thanks to my husband Dong Yang whose patient love enabled me to complete this work. My thanks also goes to my parents-in-law and my sister-in-law for their care and encouragement.

Contents

List of Figures

Chapter 1

Introduction

1.1 Context

Solitons are a special class of signals, which propagate with a constant shape and velocity in a corresponding nonlinear dispersive system. From a mathematical standpoint, solitons are stable solutions to a class of nonlinear wave equations which can represent the corresponding nonlinear systems [1].

Since their discovery by J. Scott Russel in 1834 [1], there has been great interest in the study of solitons and the systems exhibiting soliton solutions. A variety of solitons exist in nature, such as in shallow water, in gas plasmas, in nonlinear transmission lines and in nonlinear optics [1, 6]. Most soliton systems share the following special properties: (i) an input pulse dissolves into many solitons, each travels at its own velocity, (ii) a soliton of higher amplitude travels faster than one of lower amplitude, (iii) solitons can pass through one another without changing their shapes and velocities, (iv) during overlap, their joint amplitude decreases [1]. These unique properties facilitate the application of solitons in diverse areas, especially in signal processing and communication systems. Traditional signal

processing and communication systems are based on linear time-invariant systems. Such systems are attractive for their tractable mathematical analysis by linear techniques and are conveniently processed by Fourier methods. The application of soliton nonlinear systems to signal processing and communications requires an extension of classical processing techniques. The special properties of solitons give them unique qualities in most of applications.

Electrical and optical solitons are of practical interest in many applications [6, 7, 10, 11]. Optical solitons have been observed and studied extensively in optical communications. In optical communications, loss and dispersion along optical fibres are the most important effects which limit transmission reliability. Fibres have inherent dispersion, and solitons are stable under the balance between nonlinearity and dispersion. Therefore, optical solitons can propagate in nonlinear fibres without suffering distortion [11]. Much research has focused on the application of solitons in optical communications [10, 11, 18]. In soliton-based optical communications, solitons are used to carry information to achieve the transmission of high-speed digital signals over large distances.

Electrical solitons have been observed in nonlinear transmission lines and nonlinear Toda lattice circuits [1, 6, 7]. In signal processing and communication systems with linear channels, electrical solitons are attractive since the Toda lattice circuit is tractable for realization and manipulation [2]. Some research has been done in soliton communication systems by employing solitons as carrier signals for modulation or multiplexing schemes [2, 3, 4, 5, 8, 9, 19, 20].

1.2 Motivation

A variety of research on applying solitons in signal processing and communication systems has excited much attention. In the application of soliton signals, the corre-

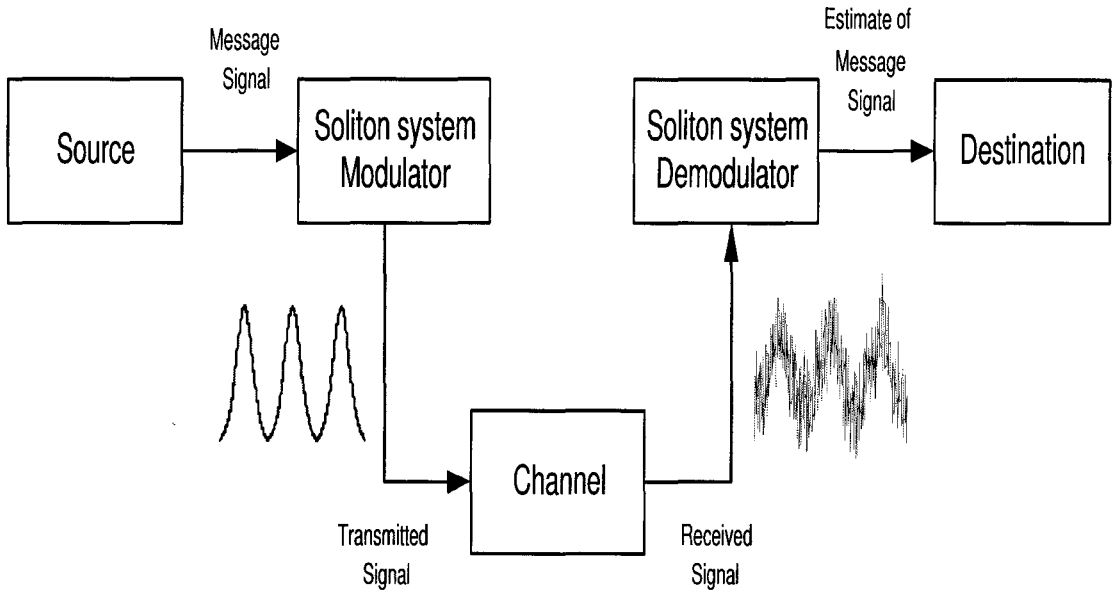

Figure 1.1: General soliton communication system

sponding soliton-supporting systems are employed to generate or process solitons. For example, in electrical communication systems, solitons are typically used as information carrier waveforms in modulation schemes [8, 9]. The overall process is illustrated schematically in Figure 1.1. There are two Toda lattice circuits are utilized. The first one generates sequences of soliton signals and modulates the amplitudes [8] or phases [9] of solitons with the source information at the transmitter. The second one demodulates the signals at the receiver.

For the general application of solitons, the corresponding systems exhibiting solitons must be realized. Traditional solitons and soliton-supporting systems are physical, and so analog. Therefore, all work on solitons and soliton-supporting systems are realized in analog environments and thus sensitive to physical effects such as temperature variations, mechanical vibrations and component tolerances.

Digital systems are more robust, offering greater tolerance to random distur-

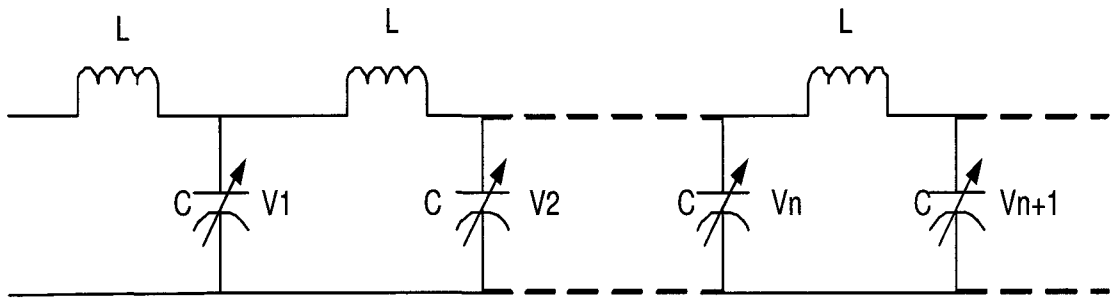

Figure 1.2: Toda LC lattice

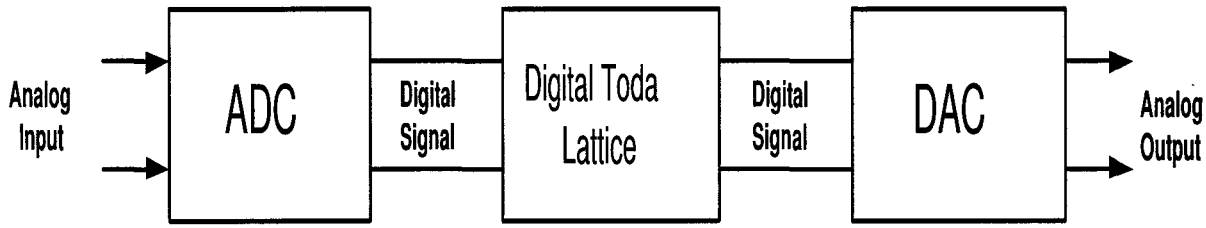

Figure 1.3: Equivalent digital realization of analog Toda lattice circuit

bances or variations. Moreover, when a digital model is designed to realize a soliton system, the digital model can be implemented in high-performance digital signal processors, which improves the operation speed of signal processing. The soliton-supporting Toda LC lattice circuit is illustrated in Figure 1.2. An ideal Toda LC lattice is composed of an infinite number of nodes. Every node consists of a series linear inductor and a shunt nonlinear capacitor. Such infinite structure is not realizable in practice and a finite structure can be adopted with an equivalent impedance to terminate the lattice [7]. Converting an analog soliton-supporting system to a digital version requires sampling and analog to digital conversion (ADC) as well as analog to digital conversion (ADC), as shown in Figure 1.3. However, since the analog systems that exhibit solitons are nonlinear, the realization of a digital soliton system model is not straightforward.

1.3 Research Direction

In this thesis, a digital system is presented to generate and process digitized soliton signals. Electrical solitons and Toda lattice circuits are emphasized since digital circuit design methods can be applied to approach a digital model that has the similar functions to the Toda lattice circuit. The Toda LC lattice is a nonlinear ladder-type circuit [7] equivalent to the exponential lattice which was invented by Toda [6], and possesses electrical soliton solutions. Such electrical circuits are tractable and can be exploited as blocks in signal processing and communication systems.

The goal of this work is to design a digital circuit structure to realize a finite length Toda lattice circuit. The general digital realization of linear circuits can be approached by direct transformations of the impulse response in the time domain or the frequency response in the frequency domain. However, the Toda lattice circuit is nonlinear, and there is no impulse response or transfer function to describe the analog Toda lattice circuit. Therefore, transformations for linear systems are not directly available to this nonlinear case.

Wave digital filter (WDF) theory is considered to design a digital model of the Toda lattice in this thesis. Wave digital filter theory is a digital filter design technique based on the topological structure of the reference analog circuit, not the transfer function [27]. Moreover, WDF theory is not limited to application of filters only. In general, such principles can be applied to circuit realizations, and is also called wave digital circuit (WDC) theory.

The design methodology of WDC is approached by block-based modelling. Therefore after the digital model is designed by WDC theory, a block-based signal flow diagram can be achieved. Such a model of the digital soliton system simulator can be built by various tools. In this thesis, Simulink [57], a block-diagram-based

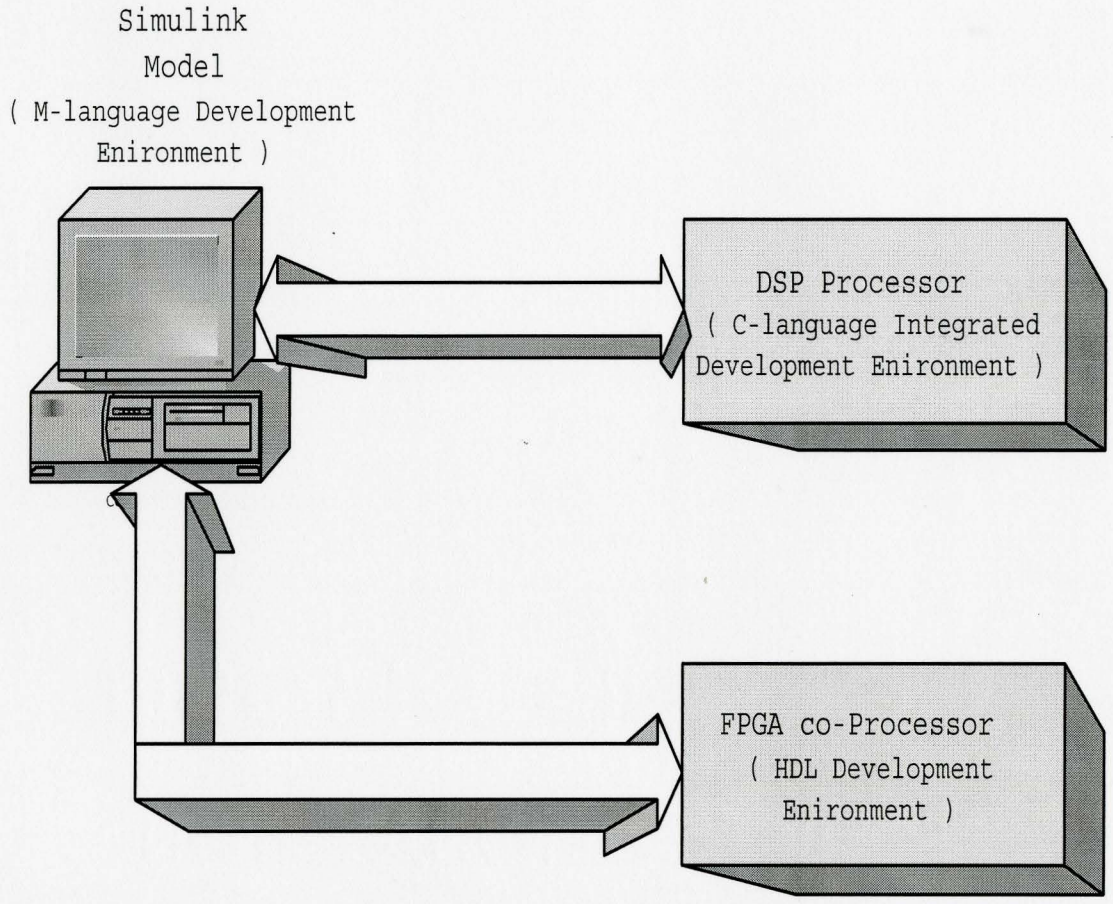

Figure 1.4: Simulink to DSP and FPGA flow diagram

tool which runs within Matlab is utilized. Simulink is a software package used widely in academia and industry to model and simulate dynamic systems. The implementation of the digital model in Simulink can be achieved with high-level system language, which facilitates the implementation procedure. Furthermore, Simulink models can be customized to generate the C code by the Target Language Compiler (TLC), which can run on digital signal processors (DSPs) for faster simulation processes. Using additional tools [52, 53], a digital model built in Simulink can be translated to a Hardware Description Language (HDL), which is a structural specification in order to generate a hardware implementation in field-programmable gate arrays (FPGAs). Consequently, the speed of the simulation processes is highly improved in such real-time systems.

The process of hardware implementation of the digital Simulink models is sketched in Figure 1.4. The digital model designed in Simulink can be implemented in DSP or FPGA by specific tools to improve the simulation speed, and the results can be transferred back to display. Such co-processing technique has also been applied in many fields for computing intensive tasks. One of the most popular applications is video game consoles, such as PlayStation, XBox to model physics-based motion [22, 23]. In academic field, the real-time simulations of a variety of systems are approached by the co-processing technique [54, 55].

1.4 Thesis Structure

Chapter 2 reviews the work that has been done in the area of the applications of solitons and soliton systems in signal processing and communications. Additionally, a survey on the general methods of the digital implementation of analog circuits is addressed, focusing on wave digital filters.

Chapter 3 describes the system design of the digital soliton system simulator.

The design procedure is investigated and the signal flow diagram of the model is presented. The selection of specific parameters is discussed in Chapter 4. Simulation results are given to verify that the performance of the digital model is close to the analog Toda lattice circuit. An example of a soliton communication system is proposed to demonstrate that the digital Toda lattice model can be used to substitute for an analog Toda lattice circuit in a digital soliton communication system.

Finally, this thesis concludes in Chapter 5 with a summary of the work and directions for future work.

Chapter 2

Background

This chapter reviews the components of digital soliton systems that will be drawn upon throughout the thesis. Basic ideas and concepts of general communication systems are introduced. Then the evolution of soliton theory and its applications to communication systems is reviewed, with emphasis on electronic solitons. Finally, a survey on the general methods of the digital implementation of analog circuits is addressed, with attention on the wave digital filters for the aim of designing a digital model of a Toda lattice.

2.1 Communication Systems

2.1.1 General Communication System Model

In this section, general communication systems are briefly described, and modulation and multiplexing techniques are introduced. In the following chapters, these techniques will be extended to soliton-supporting systems.

Figure 2.1 presents a schematic of a general communication system [41, 40]. The design of the transmitter and receiver is a fundamental problem in communi-

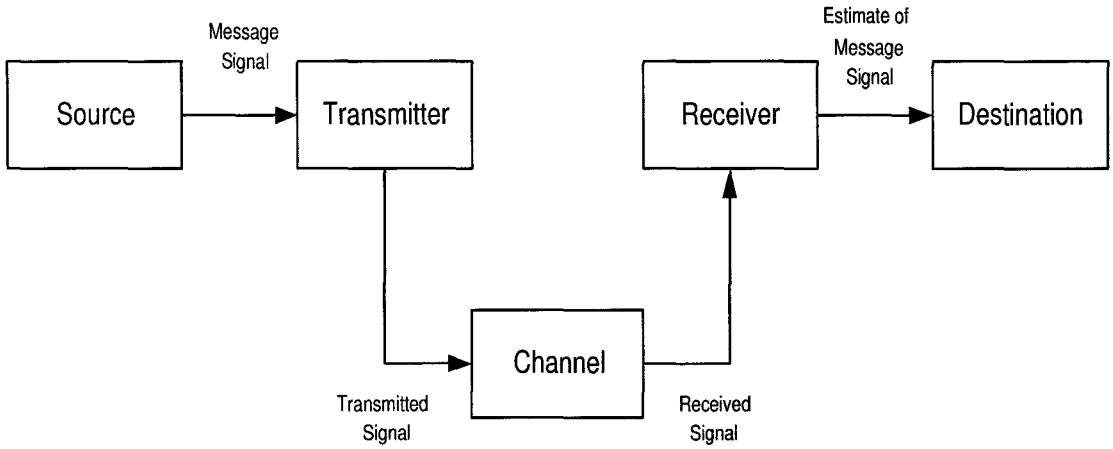

Figure 2.1: Generalized communication system

cation system specification. Two primary options exist for communication system design: digital or analog. For analog communication systems, data are transmitted directly by varying the amplitude, phase or frequency of a carrier in regards to the message. The design of analog communication systems, although conceptually simple, is difficult to build due to the sensitivity of such systems to the components used [39]. Digital communication systems overcome many of the difficulties at the expense of a more complex implementation. The systematic diagram of a digital system is shown in Figure 2.2 [39]. The source encoder performs a mapping from a data source to bits, and the channel encoder maps from bits to codewords to achieve an economical and reliable transmission of bits over a channel [43]. The digital modulator transfers a digital bit stream over an analog channel by varying some parameters of a carrier signal in accordance with the codewords. This procedure will be introduced using soliton-supporting system in Sec. 2.3. The receiver processes the received signal in reverse order to the transmitter, thereby reconstructing the original source message signal [39, 42]. In this thesis, only digital communication systems are considered.

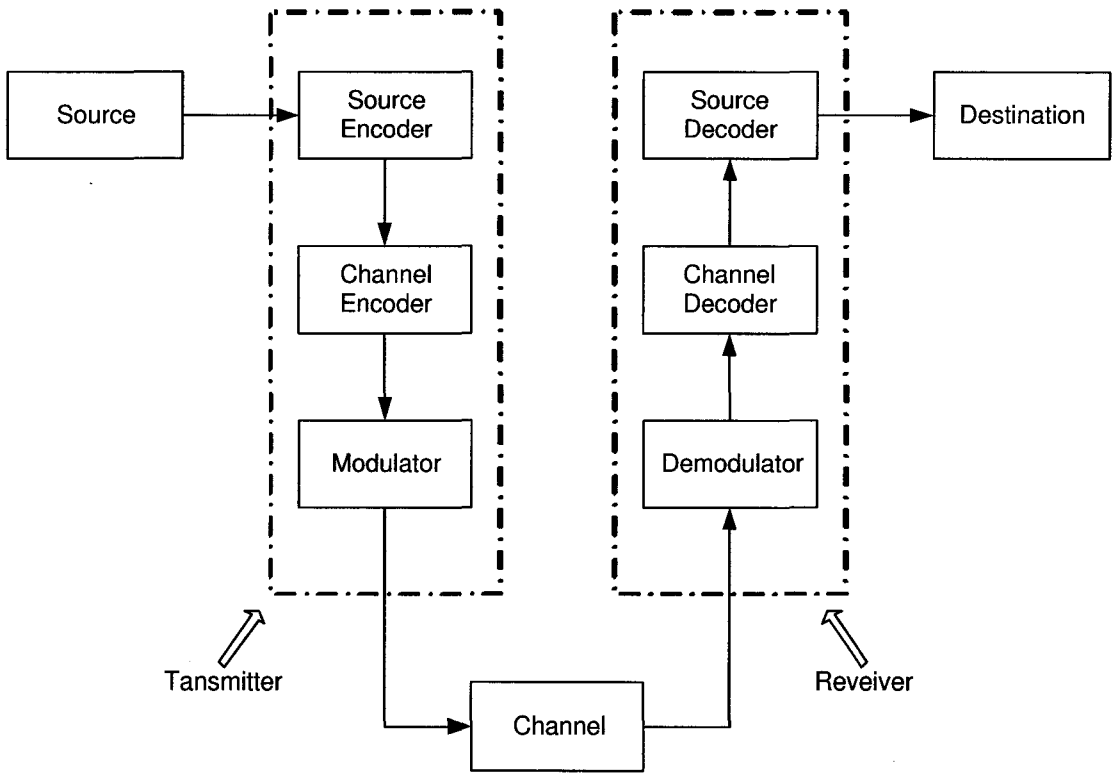

Figure 2.2: Digital communication system

2.1.2 Modulation Schemes

In this subsection some background knowledge of digital modulation techniques are introduced, which is the starting point of the application of solitons to communication systems. Whether analog or digital communication system, the modulation/demodulation part is indispensable. The function of modulation is to represent the data in a continuous waveform well suited to the channel characteristics. In this thesis, low pass baseband channels are considered.

2.1.2.1 Modulation Methods

There are two large families of modulation from the standpoint of carriers: continuous-wave modulation and pulse modulation. Continuous-wave modulation includes two basic families: amplitude modulation and angle modulation. In amplitude modulation (AM), the amplitude of the carrier wave is varied in accordance with the message signal continuously. Angle modulation has two forms: frequency modulation(FM) and phase modulation(PM). In FM, the frequency of carrier is varied with the message signal and similarly in PM, the phase is varied continuously [39, 42].

Pulse modulation modulates a pulse train instead of continuous-wave signals to carry the message. It includes pulse amplitude modulation (PAM), pulse duration modulation (PDM), pulse position modulation (PPM) and pulse code modulation (PCM) and any others. Pulse modulation can be either analog modulation or digital modulation, dependent on the message is analog signals or digital bits. For example, digital amplitude modulation is also called amplitude-shift keying (ASK). In digital modulation, an analog carrier signal is modulated by a digital bit stream. The most commonly used digital modulation methods include on-off keying (OOK),amplitude-shift keying(ASK), phase-shift keying (PSK) and

frequency-shift keying (FSK) [39, 42].

2.1.2.2 Signal Space Representations

Consider a collection of M signals which lie in a vector space. According to the Gram-Schmidt procedure, the M signals can be represented as a linear combination of N orthonormal basis functions, where $N \leq M$. If an N-dimensional Euclidean space is formed with axes being the N orthonormal basis functions, then each of the M signals can be represented geometrically in this space as a linear combination of the basis. This N-dimensional Euclidean space is called a signal space. Note that in the signal space, the squared Euclidean distance between any signal and the origin is the energy of that signal.

Suppose that $\{s_i(t), i = 1, 2, \cdots M\}$ is a set of real-valued signals, and $\phi_j(t), j = 1, 2, \cdots N$ is a set of real-valued orthonormal basis functions. All $s_i(t)$ and $\phi_j(t)$ are time limited to $D_t = [0, T_s]$. The signals can be represented as

$$s_i(t) = \sum_{j=1}^{N} s_{ij}\phi_j(t) \quad i = 1, 2, \cdots M \tag{2.1}$$

where the coefficients s_{ij} are the inner product of $s_i(t)$ and $\phi_j(t)$.

$$s_{ij} = \langle s_i(t), \phi_j(t) \rangle = \int_{D_t} s_i(t)\phi_j(t)dt \tag{2.2}$$

Therefore each $s_i(t)$ can be determined and represented by the vector S_i,

$$S_i = [s_{i1}, s_{i2}, \cdots s_{iN}] \quad i = 1, 2, \cdots M \tag{2.3}$$

Thus, for a given set of basis functions $\phi_i(t)$, the signal $s_i(t)$ can be specified by a vector in an N-dimensional Euclidian space.

2.1.2.3 Digital Modulation Methods

As indicated above, a digital modulator maps a sequence of binary digits into a set of corresponding signal waveforms. Here digital pulse amplitude modulation(PAM) is considered as an example to illustrate the representation of digitally modulated signals.

In baseband digital PAM, the signal waveforms are represented as

$$s_i(t) = I_i g(t) \quad i = 1, 2, \cdots M \quad , \tag{2.4}$$

where $g(t)$ is a real-valued signal pulse whose shape influences the spectrum of the transmitted signal, which will be observed later. Assume that the symbol is time-limited to $t \in [0, T_s]$, and there are a total of $M = 2^k$ possible messages to be modulated. Let $\{I_i, i = 1, 2, \cdots M\}$ denote the set of M possible amplitudes corresponding to M possible k-bit blocks of symbols. In every T_s interval a k-bit block symbol is transmitted, and so the symbol rate is denoted as $R_s = 1/T_s$ symbol/second. So the bit rate is $R = kR_s$ bits/second.

Typically, the signal amplitude I_i takes the discrete values as [42]:

$$I_i = (2i - 1 - M)\, d \quad i = 1, 2, \cdots M \quad , \tag{2.5}$$

where $2d$ is the distance between adjacent signal amplitudes. Now the signal space concepts are applied to explain the PAM modulated signals. As shown in (2.4) and (2.5), the M-PAM signals are one-dimensional ($N = 1$). From (2.1),

$$s_i(t) = s_i \phi(t) \quad i = 1, 2, \cdots M \quad , \tag{2.6}$$

where

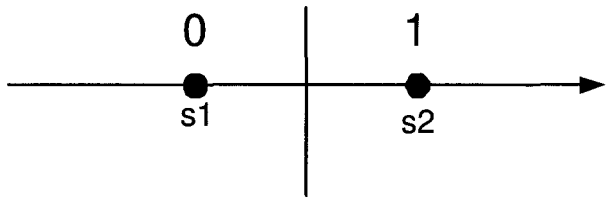

Figure 2.3: Constellation of 2-PAM

$$\phi(t) = \sqrt{\frac{2}{E_g}} g(t) \quad , \tag{2.7}$$

$$s_i = I_i \sqrt{\frac{E_g}{2}} \quad i = 1, 2, \cdots M \quad , \tag{2.8}$$

and E_g is the energy of $g(t)$. In special case of $M = 2$ signals, $s_1 = -\sqrt{\frac{E_g}{2}}, s_2 = \sqrt{\frac{E_g}{2}}$.

A constellation diagram is a representation of a signal modulated by a digital modulation scheme. It is defined as the collection of all signal vectors. Figure 2.3 is the constellation of 2-PAM, the Euclidean distance between these two signal points is

$$d_{2PAM} = |s_1 - s_2| = \sqrt{2E_g} \quad , \tag{2.9}$$

where the operator $|v| = \sqrt{< v, v >}$. In 2-PAM, this is also the minimum Euclidean distance due to only two points in the constellation. This distance is useful to analyze the performance of different modulation methods. Other digital modulation techniques have a similar analysis to PAM.

2.1.3 Signal Design for Band-limited Channels

In the previous subsection, the modulation techniques are discussed. In this subsection, the frequency characteristics of digitally modulated signals is discussed and then the signal design for a band-limited channel is considered.

2.1.3.1 Spectral Characteristics of Digitally Modulated Signal

Based on (2.4), a general form for PAM is

$$s(t) = \sum_{n=-\infty}^{+\infty} I^n g(t - nT_s) \quad , \tag{2.10}$$

where $\{I^n\}$ represents the sequence of symbols that results from mapping $k-$bit blocks into corresponding signal points selected from the appropriate signal space diagram. The sequence of information symbols $\{I^n\}$ is assumed to be wide-sense stationary with mean μ_i here. Therefore $s(t)$ is a stochastic process, which is a cyclostationary process, i.e. it has periodic statistics.

The power spectral density (PSD) of a random signal describes how the power is distributed with frequency. The PSD is the Fourier transform of the autocorrelation function $R(\tau)$ of a signal if the signal can be treated as a wide-sense stationary random process. The PSD of $s(t)$ is

$$\Phi_{ss}(f) = \frac{1}{T_s}|G(f)|^2 \Phi_{ii}(f) \quad , \tag{2.11}$$

where $G(f)$ is the Fourier transform of $g(t)$, and $\Phi_{ii}(f)$ denotes the PSD of the information sequence [42]. From (2.11), the spectral characteristics of $s(t)$ depends on the design of the pulse shape $g(t)$ and the correlation characteristics of the information sequence. If the information symbols are equally likely and symmetrically positioned in the constellation, i.e. the mean $\mu_i = 0$,

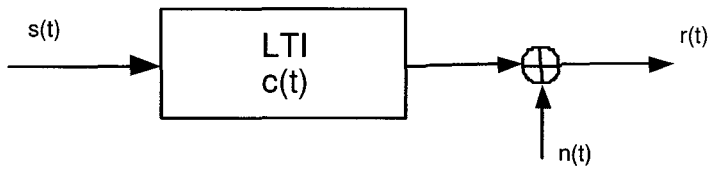

Figure 2.4: The communication channel model

$$\Phi_{ss}(f) = \frac{\sigma_i^2}{T_s}|G(f)|^2 \quad , \tag{2.12}$$

where σ_i^2 is the variance of an information symbol. Thus the PSD of the signal to be transmitted over a channel is only controlled by the design of $g(t)$.

2.1.3.2 Pulse Shaping

The communication channel considered in this work is band-limited to a specified bandwidth of W Hz. Such a channel can be modelled as Figure 2.4, and by a linear time-invariant filter with an equivalent low-pass frequency response $C(f)$ which is zero for $|f| > W$. Additionally, the channel is assumed to be flat in the transmission bandwidth.

The design of the pulse $g(t)$ for a bandlimited channel is termed pulse shaping. The following requirements should be considered to design the pulse shape of $g(t)$. Pulse $g(t)$ should have most of the energy in the $|f| < W$ to avoid the intersymbol interference (ISI) among adjacent received symbols. The ISI is the distortion of a signal caused by the temporal spreading of the transmitted signals over the channel.

Nyquist Criterion states a necessary and sufficient condition for zero ISI [42], namely

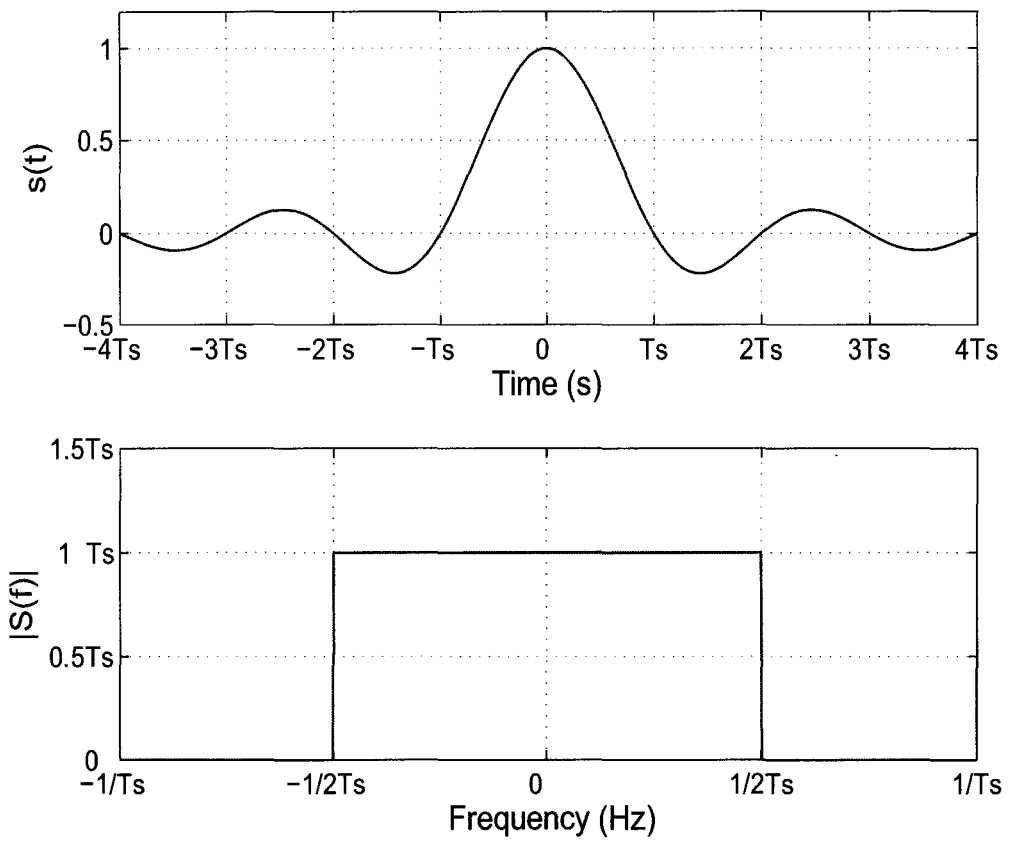

Figure 2.5: A sinc-shaped pulse in time domain and its magnitude spectrum

$$g(t = kT_s) = \begin{cases} 1 & k = 0 \\ 0 & k \neq 0 \end{cases} . \tag{2.13}$$

The Fourier transform $G(f)$ satisfies

$$\sum_{m=-\infty}^{\infty} G(f + m/T_s) = T_s \tag{2.14}$$

Considering these two requirements and the Nyquist criterion, an example of a pulse is shown in Figure 2.5. At every sample time T_s, the other symbols are zeros,

only the current symbol has non-zero value. So if this signal does not experience temporal spreading over channel, there is no ISI. Otherwise the frequency magnitude spectrum indicates the compact spectral of this pulse. So it also satisfies the first requirement. If the bandwidth of the channel is W, indicated by Figure 2.5, when $1/2T_s \leq W$ is satisfied, the Nyquist criterion is satisfied [42], therefore the symbol rate $R = 1/T_s \leq 2W$. From Figure 2.5, the tails of this sinc-shaped $g(t)$ decay as $1/t$, so a small mistiming error in sampling at the receiver results in series of ISI components. In the next chapter, the properties of solitons in terms of the signal design for band-limited channels will be discussed. In this thesis, solitons will be utilized as pulse sequences and the performance in a communication system will be quantified.

2.1.4 Multiplexing Techniques

In this subsection, we introduce multiplexing techniques briefly, which relates to another possible application of solitons in communication.

Multiplexing is a process where multiple message signals are combined into one signal for sharing the communication resource. By certain means this multiplexed signal can be separated into the signals at demultiplexer.

The channel can be orthogonally shared in frequency or time domain respectively and jointly. In a multiplexing system, the two basic methods are frequency-division multiplexing (FDM) and time-division multiplexing (TDM). Furthermore, wavelength-division multiplexing (WDM) is another multiplexing technique in fibre-optic communications. By FDM technique, different source signals are multiplexed with different frequency resource allocation. Similarly, a TDM system allocates different timeslots to transmit different signals in one channel. WDM uses different wavelengths (colors) of laser light to carry different signals. Since

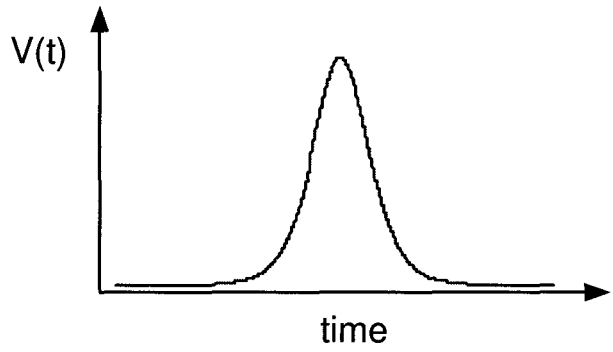

Figure 2.6: One soliton signal in the time domain

wavelength and frequency are inversely proportional, WDM is just another form of FDM. In recent years, another technique–Orthogonal Frequency-Division Multiplexing (OFDM) is popular in wide band digital communication systems, which uses a large number of closely-spaced orthogonal sub-carriers [39, 42].

Soliton systems have also been proposed for multiplexing of digital data streams [3, 19, 20]. In this work, the implementation issues with such systems are considered and previous work are reviewed in Section 2.3.2.

2.2 Solitons and the Systems Supporting Solitons

The term *soliton* is coined to describe a solitary wave [12]. Figure 2.6 presents an example soliton signal measured from voltage through the nonlinear capacitor in a Toda lattice circuit [6]. Solitons belong to a special class of stable nonlinear dispersive wave entities, which can propagate with constant shape and velocity in nonlinear dispersive systems.

2.2.1 Discovery Of Soliton

A soliton was first observed by J. Scott Russel in 1834 [1]. In his report to the British Association [13], he described the waves of water rolled forward along the channel without change of form or decrease of speed when a rapidly moving boat stopped suddenly on the Edinburgh-Glasgow canal. Such singular phenomenon excited much research interest. In 1895, Korteweg and deVries [1] provided a analytic solution to explain this unusual motion of shallow water waves. This work was the foundation of the analytical method of solution for soliton systems. Later, in the course of a numerical study of the ergodicity on a weakly nonlinear lattice, Fermi, Pasta, and Ulam (FPU) [14] found a recurrence phenomenon: for a variety of sinusoidal initial conditions, they observed that the wave recovered its initial state after some lapse of time. Zabusky and Kruskal finished the numerical study of the Korteweg-deVries (KdV) equation, which is a continuum approximation to the weakly nonlinear lattice studied by FPU [15]. The dramatic balance between dispersivity and nonlinearity ensures the stability of soliton, as is discussed in the next section.

2.2.2 Mathematical Explanation of Soliton

To comprehend the soliton's unique properties, some knowledge of nonlinear dispersive equations should be introduced. From a mathematical standpoint, solitons are stable solutions to a class of nonlinear dispersive wave equations which can represent the corresponding nonlinear systems [1]. Consider the equation $f(s(x,t)) = 0$. If $s_s(x - \mu t)$ is a solution to this equation, $s_s(x - \mu t)$ is a solitary wave that can propagate stably in the corresponding system. The system is nonlinear if and only if $f(C_1 a(x,t) + C_2 b(x,t)) \neq C_1 f(a(x,t)) + C_2 f(b(x,t))$. Moreover, if the phase velocity of the wave $s_s(x - \mu t)$ depends on its frequency,

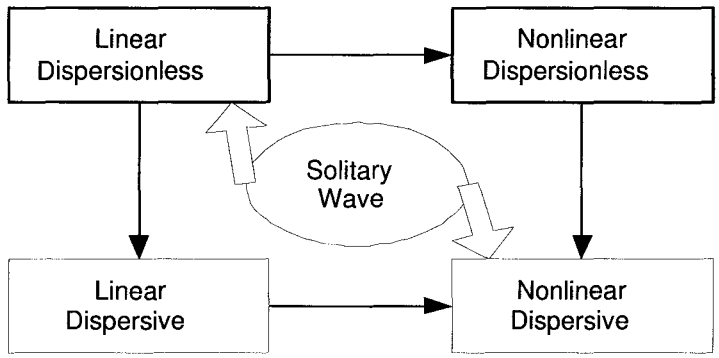

Figure 2.7: Conditions under which solitary wave solutions exist

this system is considered to have dispersive effect [21]. If f represents a linear dispersionless system, a solitary wave solution can be obtained. Also a nonlinear dispersive wave equation f can exhibit a solitary wave solution [12]. This situation is illustrated in Figure 2.7. The term *Soliton* is used to indicate only the solitary wave solution to nonlinear dispersive equations.

2.2.3 Systems that Exhibit Solitons

In the evolution of soliton theory, the inverse scattering transform plays significant role [1, 2, 6]. Given an initial condition of a nonlinear system, the solution can be explicitly determined for all time by inverse scattering theory [2]. Solitons are eigenfunction solutions with discrete eigenvalues. There has been a large class of nonlinear wave equations that have similar solutions with KdV. The solutions to these equations can be obtained by a nonlinear superposition of a variety of soliton solutions. This class of equations are called systems exhibiting solitons [12]. Here a few of this rich class that has potential applications are briefly presented.

2.2.3.1 Korteweg-deVries (KdV) Equation

KdV solitons (2.15) were first derived by Korteweg and deVries to explain the lossless propagation of shallow water waves [1],

$$\phi_t + \alpha\phi\phi_x + \phi_{xxx} = 0 \tag{2.15}$$

where $\phi = \phi(x,t)$ is a real function of two real variables x and t, and α is a real-valued constant parameter. The operator p_q in this thesis denotes partial differential $\frac{\partial p}{\partial q}$. Here the nonlinearity and dispersive effect of KdV equation is analyzed as an example to comprehend the soliton systems.

According to the mathematical background introduced previously,

$$\phi_t + \alpha\phi_x = 0 \tag{2.16}$$

is linear and dispersionless, and

$$\phi_t + \alpha\phi\phi_x = 0 \tag{2.17}$$

is nonlinear and dispersionless due to the nonlinear term $\alpha\phi\phi_x$.

Due to the dispersive term ϕ_{xxx},

$$\phi_t + \alpha\phi_x + \phi_{xxx} = 0 \tag{2.18}$$

is linear and dispersive. The solitary wave solution of KdV equation is

$$\phi(x,t) = \frac{3u}{\alpha}\text{sech}^2\left(\frac{\sqrt{u}}{2}(x-ut)\right) \quad , \tag{2.19}$$

where u is an arbitrary constant, $\phi(x,t)$ is the eigenfunction of equation(2.15) with the eigenvalue u.

The KdV equation is very useful in many studies of the balance effect between a simple nonlinearity and a simple dispersive effect. Besides the classical water wave problem, it can be used in many applications [1, 12], namely ion-acoustic waves in plasma, waves in a rotating atmosphere, the anharmonic lattice, thermally excited phonon packets in low-temperature nonlinear crystals and pressure waves in a liquid-gas bubble mixture.

2.2.3.2 the Sine-Gordon(SG) Equation

The sine-Gordon equation [1, 2] is

$$\phi_{xx} - \phi_{tt} = \sin\phi \quad ,$$

where $\phi = \phi(x,t)$ is a real function of x and t. The corresponding soliton solution is

$$\phi(x,t) = 4\arctan\left(\exp\pm\left(\frac{x-ut}{\sqrt{1-u^2}}\right)\right)$$

where u is arbitrary constant. The sine-Gordon equation has been used to describe a variety of physical phenomena [1, 2]: the propagation of a crystal dislocation, a unitary theory for elementary particles and the propagation of magnetic flux along a Josephson strip line. The sine-Gordon soliton is also called 'kink' soliton since it corresponds to a rotation in ϕ by 2π as x goes from $-\infty$ to $+\infty$.

2.2.3.3 the Nonlinear Schrödinger (NLS) Equation

The nonlinear Schrodinger(NLS) equation is another soliton-supporting system,

$$i\phi_t + \phi_{xx} + k|\phi|^2\phi = 0 \quad , \tag{2.20}$$

where k is a real-valued constant parameter, $i^2 = -1$, $\phi = \phi(x,t)$ is a complex function of x and t. The Nonlinear Schrodinger is even more generally useful than the KdV equation. It has been used as a model to describe the propagation of lightwave pulses in nonlinear optics, the propagation of a heat pulse in a solid and Langmuir waves in plasmas and many other applications [1, 2]. It admits envelope solitary wave solutions of the form

$$\phi(x,t) = \phi_0 \text{sech}\left(\sqrt{\frac{k}{2}}\phi_0 (x - u_e t)\right) \cdot \exp\left(i\left(\frac{u_e}{2}\right)(x - u_c t)\right) \tag{2.21}$$

where ϕ_0, u_e, u_c are arbitrary real constants. Here u_e and u_c are the envelope and carrier velocity respectively.

2.2.3.4 Toda Lattice Equation

The Toda lattice is one of the simplest nonlinear system models supporting soliton solutions [2]. Toda first derived an equation to describe motion on a one-dimensional lattice with the nearest neighbor interaction[6, 16] and found the existence of a 'lattice soliton'. Then Hirota and Suzuki [7] constructed a nonlinear network which is an equivalent system to a one-dimensional nonlinear lattice based on Toda's results. This network is actually a lumped nonlinear transmission line, which consists of a ladder-type LC circuit,as shown in Figure 1.2.

At every node of the network, the inductor is linear and the capacitor is voltage-dependent with the capacitance is represented by

$$C(V_n) = \frac{C_0 V_0}{V_n} \log\left(1 + \frac{V_n}{V_0}\right) \tag{2.22}$$

where C_0 and V_0 are constant capacitance and voltage respectively and V_n is the voltage difference across the nonlinear capacitor at the nth node.

The voltage propagation in the network can be represented by

$$LC_0 \frac{d^2}{dt^2} \log\left(1 + \frac{V_n(t)}{V_0}\right) = \frac{V_{n+1}(t)}{V_0} + \frac{V_{n-1}(t)}{V_0} - 2\frac{V_n(t)}{V_0} \quad , \tag{2.23}$$

where L is a constant inductance. Actually the Toda lattice equation is a discrete version of KdV equation by discretizing the spatial axis x to the number of nodes n. Then the behavior of the Toda lattice is easily understood by KdV approximation.

A solitary wave solution of (2.23) was given in [7] which corresponds to the one found by Toda:

$$V_n(t) = V_0 \cdot \beta^2 \mathrm{sech}^2\left(\beta\tau - Pn - \eta^0\right) \qquad \tau = \frac{t}{\sqrt{LC_0}}, \beta = \sinh P \quad , \tag{2.24}$$

where β is the corresponding eigenvalue, which is an arbitrary real constant, P is the velocity with which soliton propagates in the lattice, η^0 is the initial phase shift of the soliton. Such electrical solitons have been of significant use in applications to communication and signal processing because of the tractability of Toda lattice circuit [2, 3, 4, 8, 9, 19, 20].

2.3 Soliton Communication Systems

2.3.1 Properties

The soliton-supporting systems discussed in the previous section have the following properties: [6, 7, 1]

1. A pulse signal input at any given position dissolves into many solitons, each of which travels at its own velocity.

2. A soliton can travel with invariant velocity and stable shape and a soliton of higher amplitude travels faster than one of lower amplitude in the corresponding

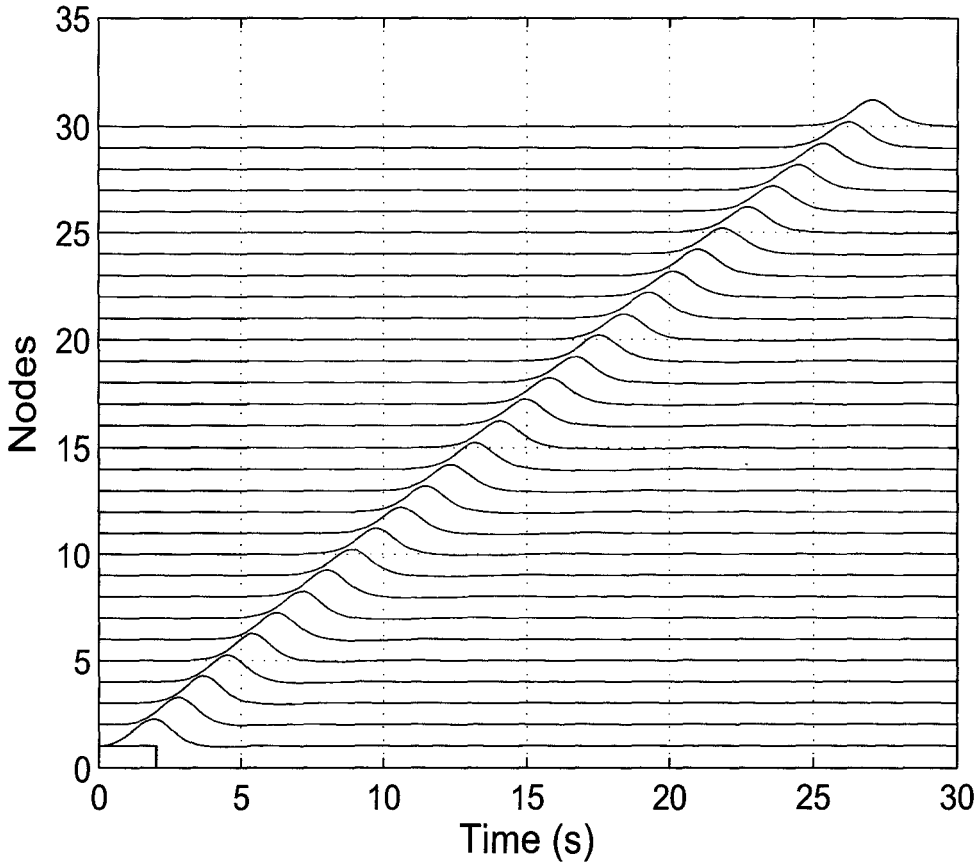

Figure 2.8: The propagation of pulse in the Toda lattice (Amplitude=1 V, Duration=2 s)

supporting systems.

3. And solitons can pass through one another without changing their shapes and velocities.

4. During the overlapping, the joint amplitude of the signal decreases, i.e. the energy of the overlapped solitons decreases.

All the simulation results shown in the figures in this section are obtained by

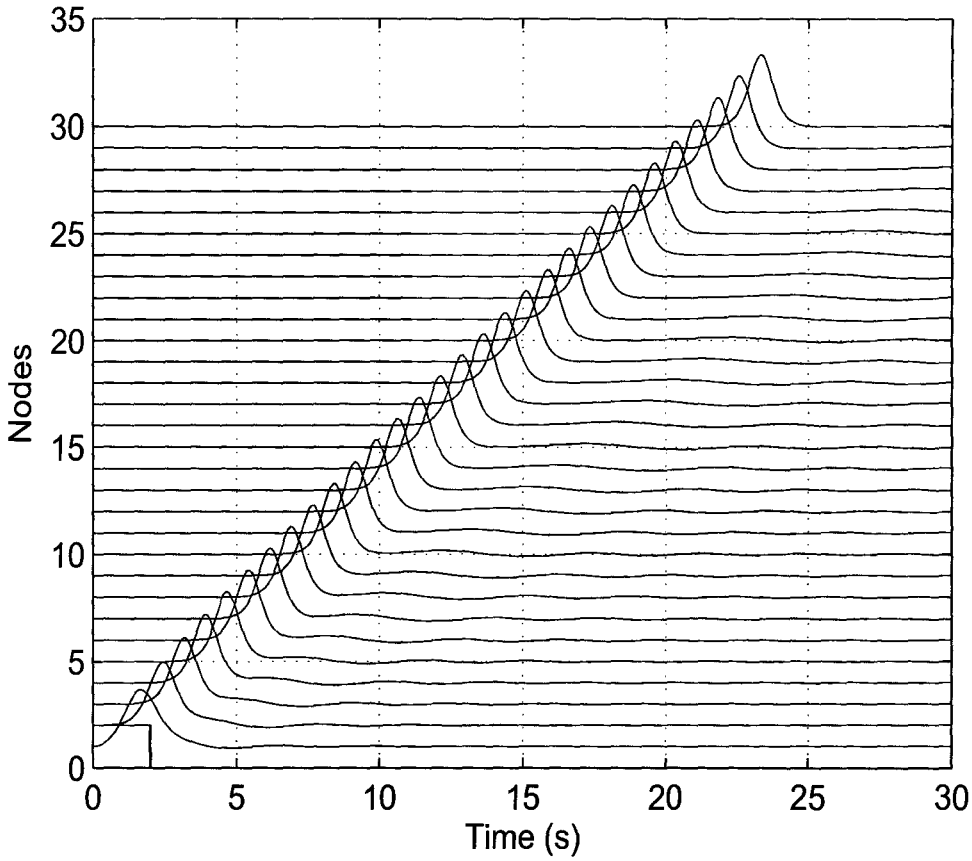

Figure 2.9: The propagation of pulse in the Toda lattice (Amplitude=2 V, Duration=2 s)

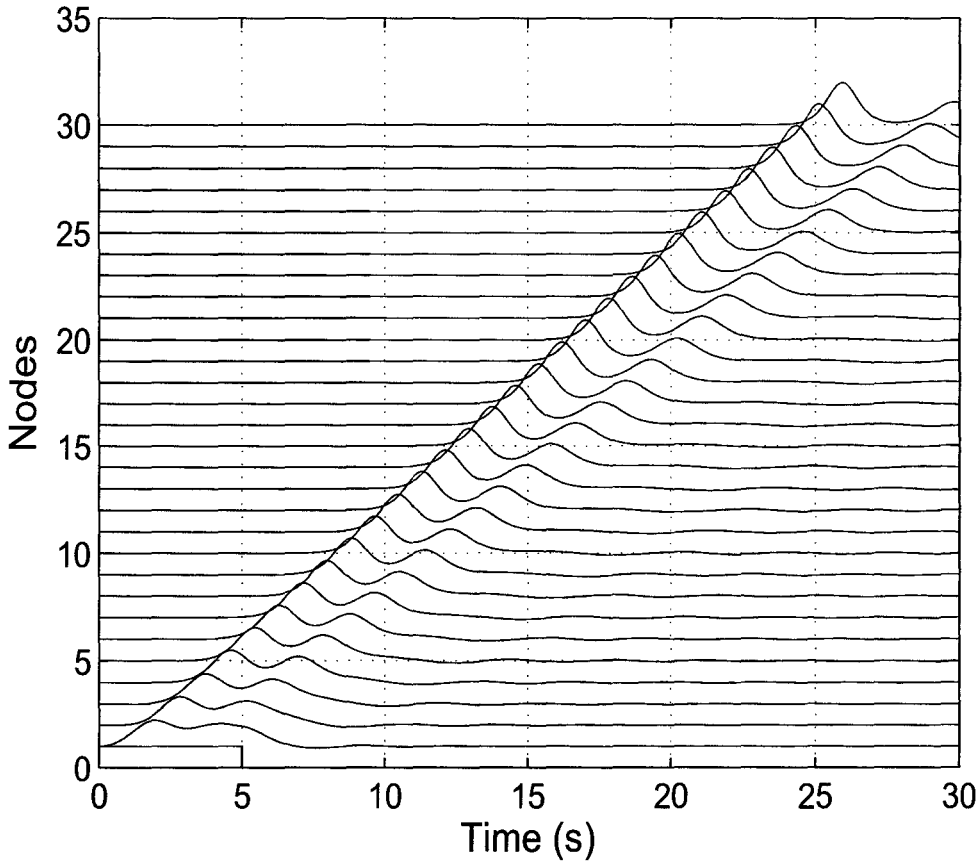

Figure 2.10: The propagation of pulse in the Toda lattice (Amplitude=1 V, Duration=5 s)

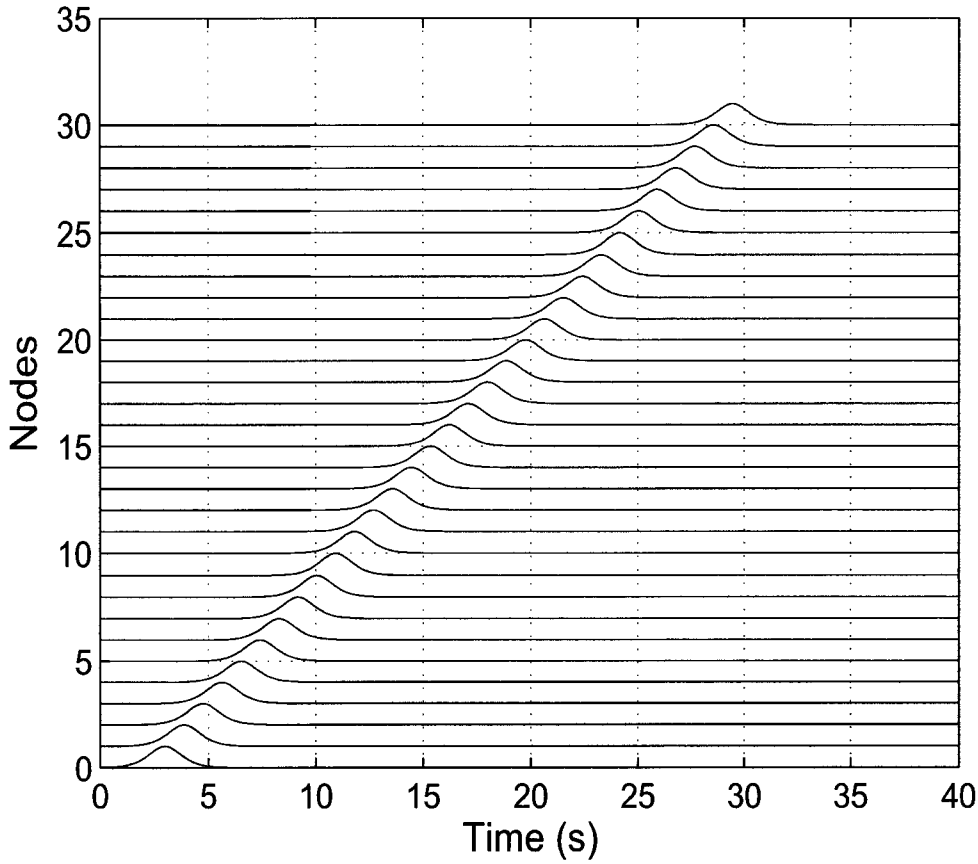

Figure 2.11: The propagation of single soltion in the Toda lattice ($\beta = 1$)

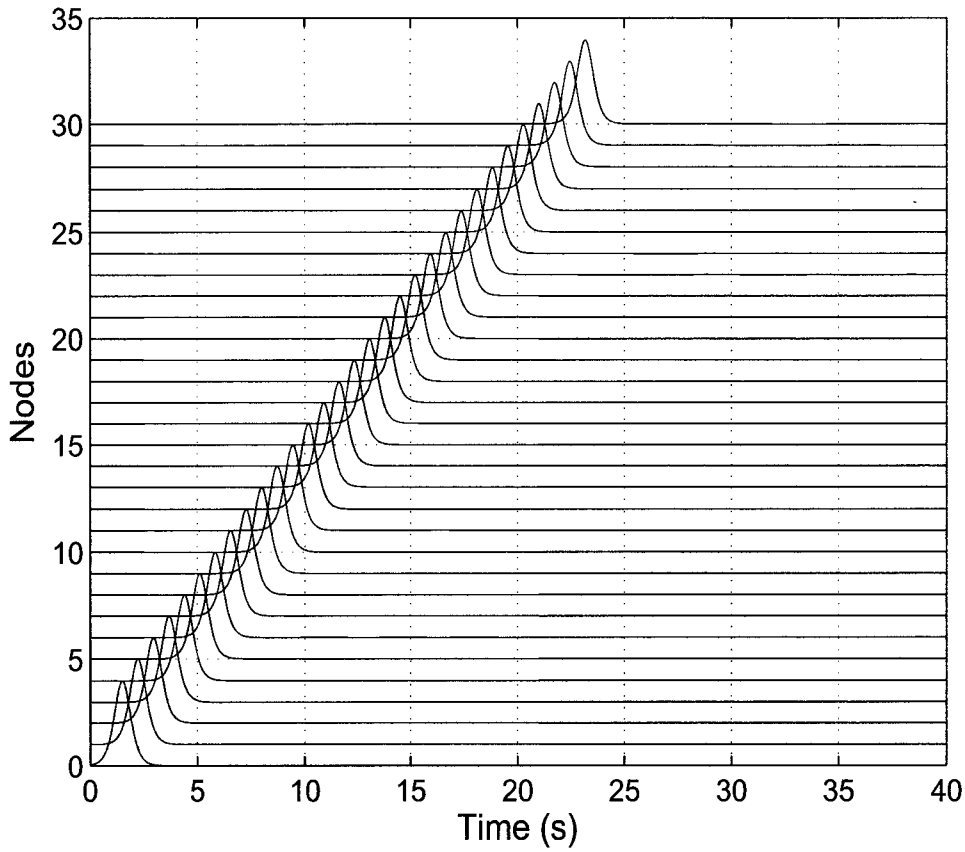

Figure 2.12: The propagation of single soltion in the Toda lattice ($\beta = 2$)

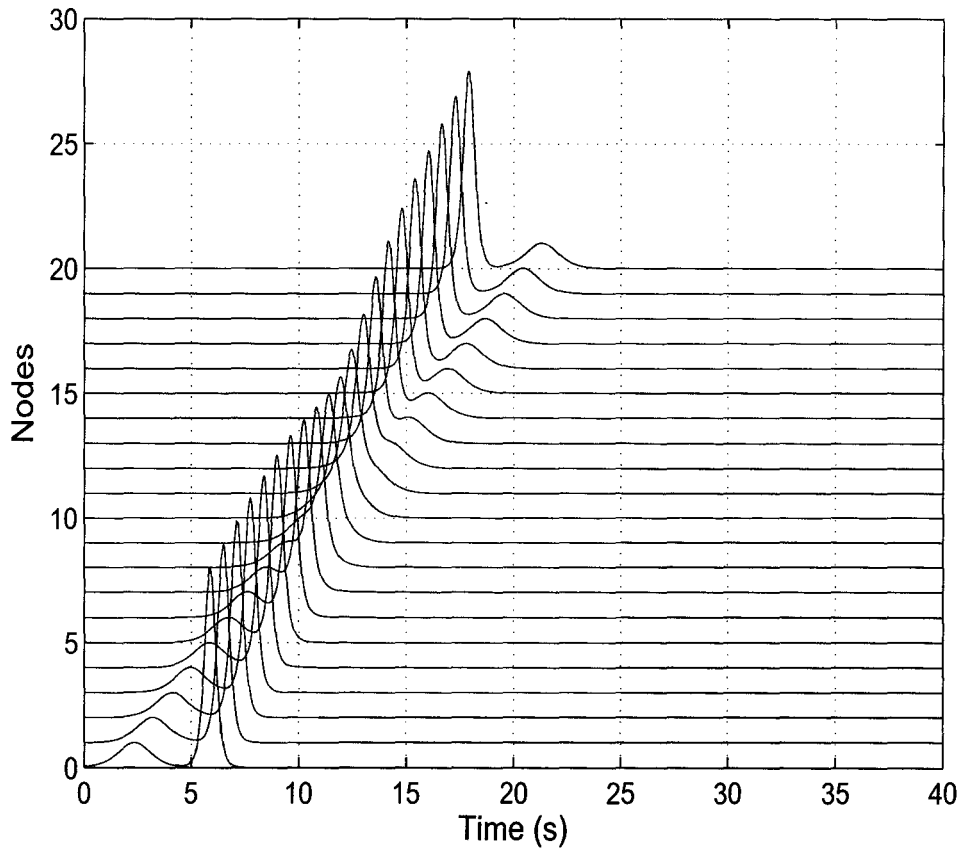

Figure 2.13: Two solitons interaction in the Toda lattice ($\beta_1^2 = 1, \beta_2^2 = 8$)

using ordinary differential equation (ODE) function to realize the Toda lattice equation in Matlab. Figure 2.8, Figure 2.9 and Figure 2.10 show the first property that pulse will dissolve into solitons when propagating in Toda lattice. Figure 2.11 and Figure 2.12 illustrate the second property that pulse shape is preserved and velocity depends on amplitude. The third and the forth properties are shown in Figure 2.13, which clarifies the situation of two different solitons simultaneous propagation in Toda lattice. The solitons maintain their shapes and velocities in propagation even though passing through each other and when the solitons overlap in the Toda lattice, the amplitude of the resulting signal will be less than the higher amplitude of these two solitons.

These special properties have been applied to signal processing and communication systems [10, 11, 18, 9, 8, 3, 4, 5]. Solitons can be used as information carrier signals due to its stable propagation and independence. In the next subsection, we will review the work that have been done in this field.

2.3.2 Realization of Soliton Communication Systems

Optical and electrical solitons share the special properties mentioned above, and have extensive applications in communication systems. In 1973, Hasegawa and Tappert theoretically demonstrated the existence of optical soliton in lossless fibers [11]. Since then, much research has focused on the realization of solitons in optical communications [10, 11, 18]. In optical communication, loss and dispersion along the optical fibres are the most important effects which limit transmission. Fibres have inherent dispersion, and solitons are stable under the balance between nonlinearity and dispersion. Thus, solitons can be transmitted in nonlinear fibres without suffering distortion [11]. Conventional communications using optical fibers require repeaters to regenerate optical pulses which have been distorted by fiber dispersion

and loss. The distances between repeaters are chosen to be as large as possible. In soliton-based optical communications, the repeaters only need to compensate the loss in fibre because the dispersive effect has been balanced by the nonlinearity. Therefore in soliton's optical communication, the repeater distance can be large and the transmission distance can be long. Some work has shown [10, 11, 18] that solitons can be used to achieve transmission of high-speed digital signals by $20Gb/s$ over large distances ($150km$) in optical communication. A comprehensive review of solitons in optical communication can be found in [10, 11, 18].

In traditional communication systems, electrical solitons are more attractive since the Toda lattice circuit is tractable as tuned transmitters and receivers [2]. Usually solitons are used as information carrier waveforms in modulation by modulating their amplitudes (AM) [8] or phases (PM) [9]. According to the Toda soliton equation (2.24), the amplitude and the phase of the soliton signal both depend on the parameter β. Therefore the parameter modulation of soliton carriers can achieve AM and PM simultaneously. On the other hand, giving rise to a scale modulation rather than a pure amplitude modulation was introduced in A. Singer's PhD dissertation [2]. Similarly, an analog of PM or pulse-position modulation (PPM) could be achieved by modulating the relative position of each soliton in a given period, which was demonstrated in [2]. As a simple extension of soliton modulation, multi-user systems can apply different solitons as carrier signals of different users for multiplexing [2, 3, 19, 20]. Different solitons with different β can be nonlinearly superimposed in the corresponding nonlinear system. Such composite soliton can be transmitted as multiplexed signal, which provide increased energy efficiency. This technique is particularly attractive for a broad range communication contexts over power-limited channels including wireless and satellite communication. Recent work on Soliton Amplitude Division Multiplexing (SADM) schemes has been done in [19, 20]. The spectral properties and the energy

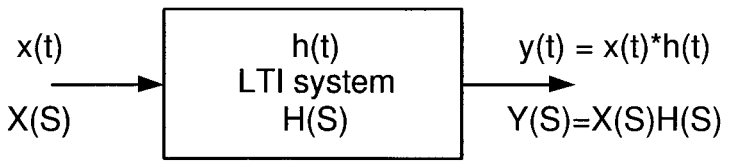

Figure 2.14: LTI system sketch

content of the composite soliton was analyzed and these properties in the context of multiplexing were discussed in [19, 20]. In these communication systems, the Toda lattice circuit is employed as a carrier generator, modulator/demodulator or multiplexer/demultiplexer. In [8, 9, 2, 3, 19, 20], it was assumed that an analog Toda lattice is available for implementation.

The Toda lattice circuit is an analog circuit, and therefore it is sensitive to physical effects (temperature variations, mechanical vibrations and component tolerances). However, digital circuits are more robust, offering greater tolerance to random disturbances or variations. So a digital model of a Toda lattice circuit is required to implement the same functions as Toda lattice in digital communication systems. In the next section, some general background knowledge about digital implementation of analog circuit will be introduced.

2.4 Wave Digital Circuits

2.4.1 General Methods to Implement Digital Filters from Analog Filters

Digital implementation of analog filters can be approached in the time domain or in the frequency domain. Figure 2.14 presents a sketch of a linear time-invariant(LTI) system. It illustrates that the impulse response $h(t)$ or transfer function $H(S) = L\{h(t)\}$ can describe the corresponding LTI system completely,

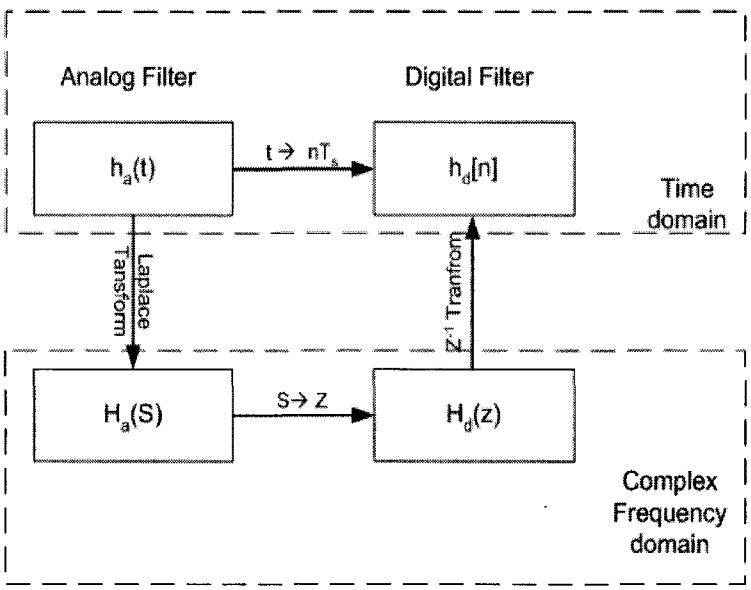

Figure 2.15: Transformations from analog to digital LTI filters

where $L\{\cdot\}$ is the Laplace operator. Therefore, for analog LTI filters the digital realization is usually achieved by direct transformations of the impulse response in time domain or the transfer function in complex frequency domain [24, 37]. Figure 2.15 is a diagrammatic sketch showing the transformations from analog to digital LTI filters.

In time domain, a common transformation is the impulse-invariant transformation

$$h_d(n) = h_a\left(t = nT_s\right) \quad , \tag{2.25}$$

where T_s is the sample time. In complex frequency domain, a common transform method is bilinear transformation

$$H_d(z) = H_a\left(\frac{2}{T_s}\frac{1-z^{-1}}{1+z^{-1}}\right) \quad . \tag{2.26}$$

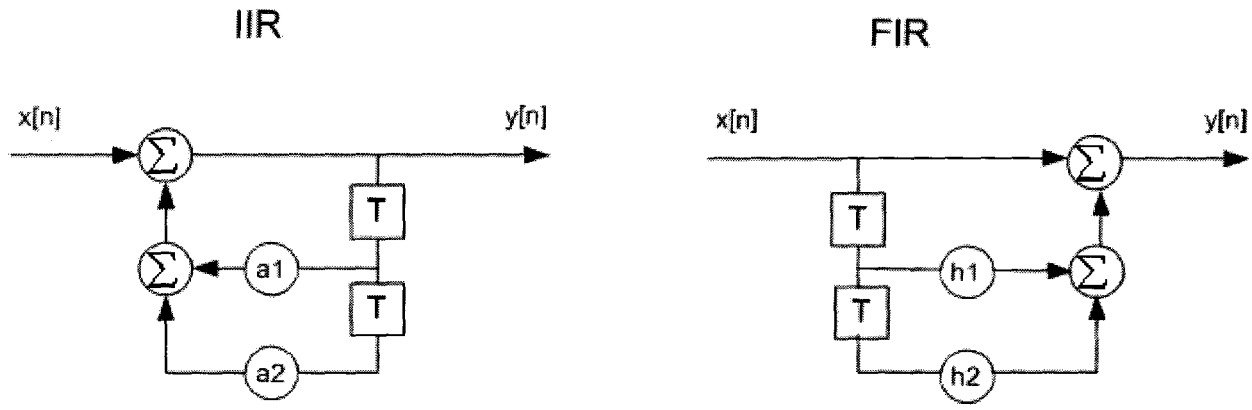

Figure 2.16: Simple IIR and FIR signal flow diagram

The transfer function $H_d(z)$ can often be written in rational form

$$H_d(z) = \frac{\sum_{i=0}^{P} b_i z^{-i}}{\sum_{j=0}^{Q} a_j z^{-j}} \quad , \tag{2.27}$$

where $a_j, b_i \in \mathbb{R}$. If $a_j = 0, \quad j = 1, \cdots Q$, $H_d(z)$ represents a finite impulse response (FIR) filter. Finite here means its response to an impulse ultimately settles to zero. If not all $a_j, \quad j = 1, \cdots Q$ equals zero, this filter is termed an infinite impulse response (IIR) type, which has an impulse response function which is non-zero over an infinite length of time. Figure 2.16 is a signal flow diagram to show a simple example of IIR and FIR filters, where the signal flow diagram is the basic description of digital filter circuit.

However, since the convolution law does not apply for nonlinear systems, there is no impulse response or transfer function to describe the nonlinear analog circuit. Thus, all the transformations introduced for the linear systems above are not directly available to nonlinear case. However, extensions to this linear system case will be discussed in the following sections.

2.4.2 Introduction to Wave Digital Filters

Wave digital filter (WDF) theory is a digital filter design technique based on the topological structure of a circuit, not the transfer function [27]. It was first described in 1970 [25] and there has been significant work done on this subject itself and its many relationships with other areas, especially in the signal processing fields [27, 30, 31, 32, 33, 34]. In [27], a detailed review of WDF theory was given by Fettweis. This classical paper is a valuable guide to the design of WDFs especially in the application of signal-processing field. Fettweis [27] treats the basic WDF principles and does not take into account of nonlinear cases. In [33], the WDF modelling of nonlinear circuits is proposed as an extension of the classic WDFs. Profiting from block-based modelling, WDFs also have great applications in the physical modelling for digital sound synthesis [34].

A wave digital filter is a kind of digital filter based on physical modelling principles. It is closely related to classical networks [28]. As described by V. Belevitch in *Classical Network Theory* [28], an electrical network is a system composed of a finite number of interconnected elements such as resistances, capacitances, inductances and generators. A WDF can be regarded as a digital representation of a classical network by modelling every element and interconnection. It is a physical modelling methodology based on the topology.

Differential equations are commonly used to describe classical analog filters, and the bilinear transformation is known as a complex frequency mapping from analog to digital domain based on the integral of differential equation. The bilinear transformation is also selected as the frequency variable transform method in wave digital principles. On this basis, for the sake of maintaining realizability from reference structure to digital realization, according to scattering parameter of classical network theory [28], wave quantities are used as signal variables in-

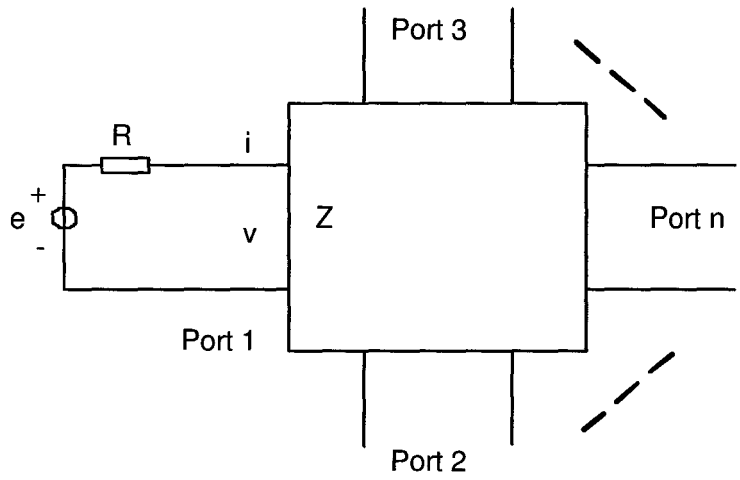

Figure 2.17: A n-port element block

stead of voltages and currents. These principles will be described in the following subsections specifically.

Note that wave digital principles are not limited to application of filters only. In general, such principles can be applied to circuit realizations.

2.4.3 Definitions

Before the basic principles are described for wave digital circuit (WDC) theory, definitions fundamental to WDCs are present in this section.

2.4.3.1 N-port Element

An n-port element is the basic model in classical network theory [28]. From the analysis of a n-port element, some important parameters can be defined to study the WDC theory clearly.

Figure 2.17 shows an n-port element. Assume that Port 1 is interconnected with a resistive voltage source. Here R is termed *the port resistance* of Port 1, and

Z is termed *the internal impedance* of Port 1. The reflectance of Z relative to R is defined as

$$\gamma = \frac{Z-R}{Z+R} = \frac{v/i-R}{v/i+R} \quad . \tag{2.28}$$

Here γ is defined as a scattering parameter of Port 1, which describes the reflectance of the internal impedance to the port resistance. For the entire n-port element, the reflectance of every internal impedance with respect to every port resistance Γ will be controlled into a scattering matrix.

2.4.3.2 Wave Quantities

Wave quantities are the signal variables in WDC theory. In classical electrical circuit theory, all the variables such as voltage, current, charge, energy are constrained by Kirchhoff laws, so these variables and circuit's topology are termed to be in Kirchhoff domain. Wave quantities and the circuit topology realized by wave digital principles are called in wave digital (WD) domain. Instead of the corresponding variables in analog circuits, voltage,current and power wave quantities are used in wave digital circuits [27]. Just as the names imply, voltage wave quantities have the same unit as voltage, and similarly current and power wave quantities have the same unit as current and power respectively.

The voltage wave quantities are defined in detail to show the description of wave quantities. For example, in reference to the n-port element shown in Figure 2.17, consider Port 1, the port voltage is v and the port current is i, and R is the port resistance.

In time domain, the incident wave (forward wave) is

$$a = v + Ri \quad , \tag{2.29}$$

and the reflected wave (backward wave) is

$$b = v - Ri \quad . \tag{2.30}$$

In complex frequency domain,

$$A = V + RI \tag{2.31}$$

and

$$B = V - RI \quad . \tag{2.32}$$

The description of wave quantities in complex frequency domain could be in s-domain for analog circuit and in z-domain for the converted digital circuit. This frequency transformation from s to z domain will be addressed in the next subsection.

Using the scattering parameter γ in (2.28), this relation between a and b can be written as

$$b = \gamma a \quad . \tag{2.33}$$

For clarity, these definitions can be understood by their analogy in transmission line theory [29]. In transmission line theory, the voltages and the currents can be decomposed as forward-travelling and backward-travelling. Figure 2.18 is a simple example to illustrate the two-direction voltages and currents by transmission line. An equivalent resistive voltage source representation can be derived for a one-port generator. This one-port is interconnected with a load resistance. This case can be treated as a voltage source E is connected to a transmission line which characteristic resistance is R_c, and terminated by a load resistance R_L. Here

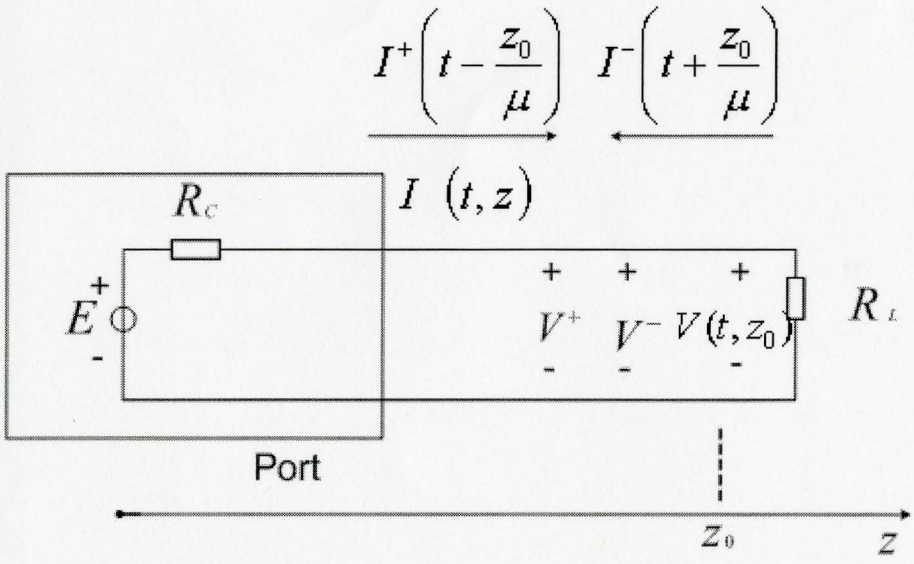

Figure 2.18: Explanation of the incident and reflected signals from a transmission line point of view.

$$V(t, Z_0) = R_c I(t, Z_0) \quad , \tag{2.34}$$

where Z_0 is the coordinate of the load resistance in z-axis and for the forward-travelling direction is

$$V^+(t - \mu Z_0) = R_c I^+(t - \mu Z_0) \quad , \tag{2.35}$$

where μ is the parameter of the transmission line. Similarly for the backward-travelling direction

$$V^-(t - \mu Z_0) = R_c I^-(t - \mu Z_0) \quad . \tag{2.36}$$

So the reflectance from R_L to R_c is

$$\gamma_L = \frac{R_L - R_c}{R_L + R_c} = \frac{V^-(t - \mu Z_0)}{V^+(t - \mu Z_0)} \quad . \tag{2.37}$$

The total voltage is

$$V(t, Z_0) = V^+(t - \mu Z_0) + V^-(t - \mu Z_0) = (1 + \gamma_L)\, V^+(t - \mu Z_0) \quad . \tag{2.38}$$

Defining $a = 2V^+(t - \mu Z_0)$ and $b = 2V^-(t - \mu Z_0)$, applying the above relations given,

$$a = V(t, Z_0) + R_c I(t, Z_0) \tag{2.39}$$

and

$$b = V(t, Z_0) - R_c I(t, Z_0) \quad . \tag{2.40}$$

Comparing (2.39) and (2.40) with (2.29) and (2.30), the equivalence between these two pairs of variables is easily recognized. Therefore the incident voltage wave quantity a in WDC theory is equivalent to the forward-travelling voltage in transmission line theory and similarly the reflected voltage wave quantity is equivalent to the backward-travelling voltage.

2.4.4 Frequency Transformation

In order to establish the correspondence between a WDC and its reference filter, an appropriate frequency transformation is required from the analog reference domain to the digital wave domain. The bilinear transform is based on the integral of a differential equations, as discussed in Section 2.4.2, therefore it is an appropriate method to be applied in WDF's frequency transformation. Here the procedure of transforming a first-order ordinary differential equation (ODE) to a difference equation by bilinear transform is introduced. A higher-order ODE can

be represented by several first-order ODEs. Therefore this procedure demonstrates how the bilinear transform can be applied for the discretization of general ODEs. Consider a continuous-time system represented by a first-order ODE,

$$y'(t) + cy(t) = dx(t) \tag{2.41}$$

where c, d are constants, $y'(t)$ denotes $\frac{dy}{dt}$. The transfer function of this system is

$$H_a(s) = \frac{d}{s+c} \quad . \tag{2.42}$$

The sampled signal $w(nT_s)$ can be represented by

$$w(t = nT_s) = \int_{(n-1)T_s}^{nT_s} w'(\tau)d\tau + w\left((n-1)T_s\right) \quad .$$

Employ the trapezoidal rule to approximate the integral,

$$w(nT_s) - w\left((n-1)T_s\right) = \frac{T_s}{2}\left(w'\left(nT_s\right) + w'\left((n-1)T_s\right)\right) \quad . \tag{2.43}$$

According to (2.41), let $t = nT_s$ and $t = (n-1)T_s$, subtract $y'((n-1)T_s)$ from $y'(nT_s)$, and substitute (2.43) to eliminate the derivatives, a difference equation can be gotten

$$y[n] - y[n-1] = \frac{T_s}{2}\left[-c\left(y[n] + y[n-1]\right) + d\left(x[n] + x[n-1]\right)\right] \quad . \tag{2.44}$$

The transfer function of the discrete-time system described by (2.44) is

$$H_d(z) = \frac{d}{\frac{2}{T_s}\frac{z-1}{z+1} + c} \quad . \tag{2.45}$$

Comparing (2.42) with (2.45), if the relation between s and z satisfies

$$s = \frac{2}{T_s}\frac{1-z^{-1}}{1+z^{-1}} = \frac{2}{T_s}\tanh(pT_s/2) \quad z = e^{pT_s} \tag{2.46}$$

where p is the actual complex frequency. Notice that $H_d(z)$ in (2.45) and $H_a(s)$ in (2.42), differ only by the substitution in (2.46).

Although all wave digital circuits (WDC) use the bilinear transform as the basic principle, there are still particular differences. In some references, another choice of frequency variable's transformation is [27, 30, 31, 32, 33]

$$s = \frac{1-z^{-1}}{1+z^{-1}} = \tanh(pT_s/2), \quad z = e^{pT_s} \tag{2.47}$$

This transformation is also bilinear, and only differs by a scaling factor from (2.46). In (2.46), the complex frequency in reference domain s and in WD domain p are equivalent in small frequency range, i.e. $s \approx p$ for small values of p whereas this equivalence does not hold in (2.47).However (2.47) is still employed in many WDC applications, because the implementation of one-port elements is more tractable than (2.46), which will be explained in the discussion of realization. In our wave digital model, (2.46) is employed as the frequency transform.

2.4.5 Realizability

A digital filter can be fully described mathematically by a system of difference equations. The mathematical description of a digital filter can equivalently be represented by a signal-flow diagram. For all digital filters, not only for WDCs, realizability is achieved when the following conditions are satisfied [27]:

1. The system operates at a constant rate $F_s = 1/T_s$
2. The total delay in every loop must be equal to a multiple of T_s
3. No delay-free directed loops exist in the signal-flow diagram

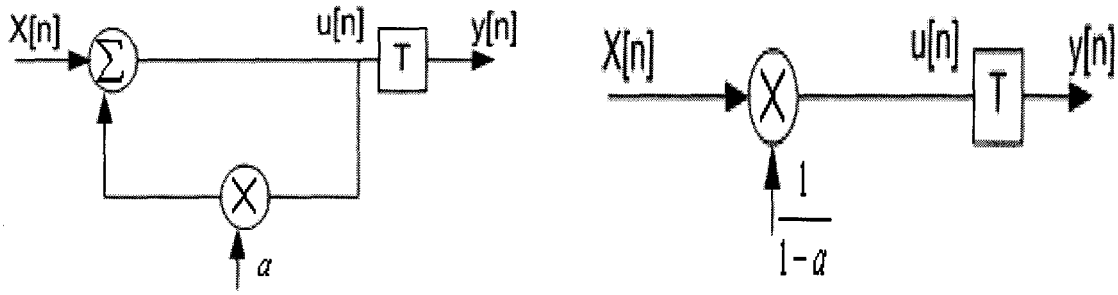

(a) (b)

Figure 2.19: Removal of a delay-free directed loop

The first two conditions are straightforward since any digital system requires that every operation can be ordered periodically at a constant rate. When a digital filter is designed, these two conditions are easily satisfied. The last condition is the most difficult one because in many cases the delay-free directed loops may exist in recursive filter structures. Delay-free directed loop (DFDL) is such a feedback loop without any delays. Such a loop is not realizable in real operation since that it forms an algebraic loop. Figure 2.19(a) is an example of a system with a DFDL. This DFDL in a signal-flow diagram is also described by

$$u[n] = x[n] + au[n] \quad . \tag{2.48}$$

From (2.48), the current value of $u[n]$ is dependent on itself, therefore it causes algebraic loop. However in this example, the DFDL problem can be solved by the modification of the signal-flow structure. Reformulating (2.48) as

$$u[n] = \frac{1}{1-a}x[n] \quad a \neq 1 \quad ,$$

and the signal-flow diagram in Figure 2.19(a) can be modified to a new structure, as shown in Figure 2.19(b), where no DFDL exists. However, not every DFDL

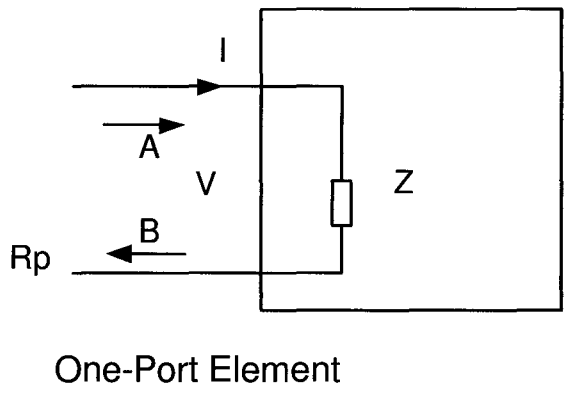

Figure 2.20: One port element

problem can be solved by such manipulation. Solving the DFDL problem is a key issue in the design of complete WDCs and a new approach is discussed in Chapter 3.

2.4.6 Realization of One-port Element

Having defined the basic principles of WDC, the realization of the simplest linear one-port element in WD domain is discussed.

In a classical circuit, if the Laplace transform is employed for steady-state analysis, the impedances of major elements can be represented as $Z = RS^{\lambda}$. For a resistance, $\lambda = 0$, for a linear inductance, $\lambda = 1$ and for a linear capacitance, $\lambda = -1$. The port resistance is denoted as R_p. Referring to the wave quantities defined in (2.31) and (2.32),

$$A = V + R_p I \qquad B = V - R_p I$$

and

$$\frac{V}{I} = Z = RS^{\lambda} \quad .$$

Therefore in reference to the definition of the scattering parameter in Section 2.4.3, the reflectance of Z to the port resistance, denoted as γ can be gotten as

$$\gamma = \frac{RS^{\lambda} - R_p}{RS^{\lambda} + R_p} \quad ,$$

A useful simplifying feature would be that the scattering parameter of one-port element γ is independent of R. Therefore, the appropriate value of R_p should be appointed. The two bilinear transforms discussed in Section 2.4.4 are employed respectively.

Using the bilinear transform in (2.46), the scattering parameter γ_{WD} in WD domain can be formed as

$$\gamma_{WD} = \frac{R\left(\frac{2}{T_s}\frac{1-z^{-1}}{1+z^{-1}}\right)^{\lambda} - R_p}{R\left(\frac{2}{T_s}\frac{1-z^{-1}}{1+z^{-1}}\right)^{\lambda} + R_p} \quad . \tag{2.49}$$

To have γ_{WD} independent of R, the port resistance should be selected as

$$R_p = \left(\frac{2}{T_s}\right)^{\lambda} R \quad . \tag{2.50}$$

By the transform of (2.47), γ_{WD} will be

$$\gamma_{WD} = \frac{R\left(\frac{1-z^{-1}}{1+z^{-1}}\right)^{\lambda} - R_p}{R\left(\frac{1-z^{-1}}{1+z^{-1}}\right)^{\lambda} + R_p} \quad ,$$

$$R_p = R \tag{2.51}$$

can keep the scattering parameter independent of R. Comparing (2.51) and (2.50), the appointment of the port resistance from the first transform in (2.46) is more complicated than the second transform in (2.47). In the following introduction to WDC, the second transform in (2.47) is employed.

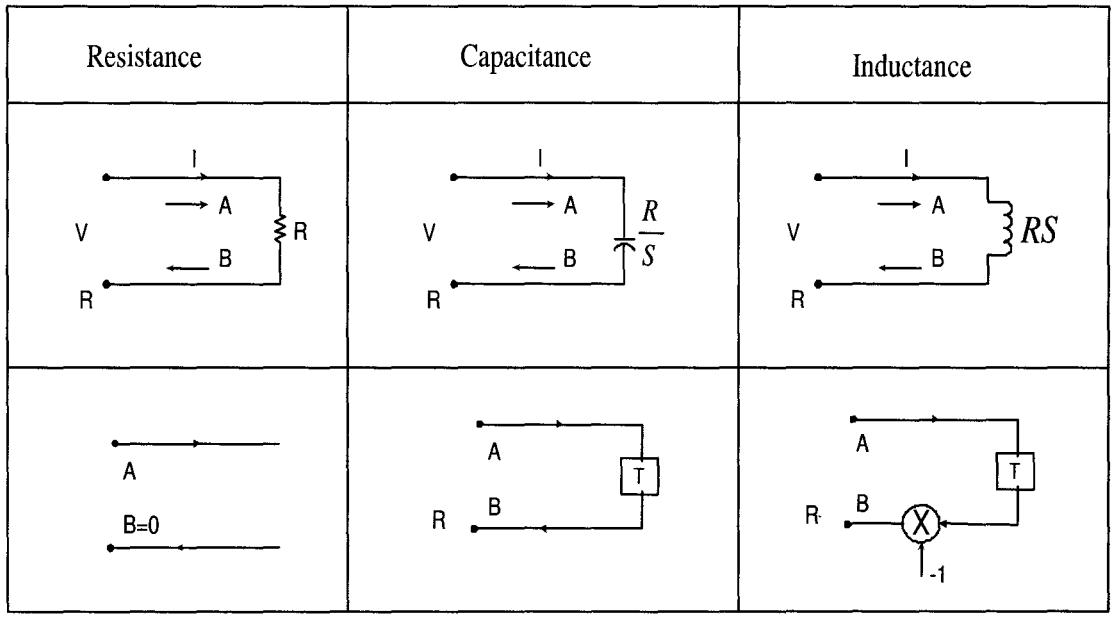

Figure 2.21: Major linear one-port elements and their realization in the WD domain

An example of linear inductance is given to illustrate the realization of one-port element in WDC. For a linear inductance, $Z = RS$, if the port resistance is appointed as $R_p = R$, (2.49) can be simplified as

$$\gamma_{WD} = z^{-1} \quad ,$$

where z^{-1} in z-domain is equivalent to the operation of unit delay in time domain. Therefore by appointing an appropriate port resistance, a linear inductance in reference domain can be realized by a unit delay element in WD domain. Using a similar technique, the realization of one-port components is shown in Figure 2.21 [27].

2.4.7 Interconnections of Elements

In order to construct a WDC, the interconnection of individual components must be introduced. The basic topological connections are parallel and series. Parallel adaptors is introduced in detail, the series adaptors have a similar development outlined in [27]. Note that the Kirchhoff laws in reference domain are still satisfied in WD domain.

2.4.7.1 Parallel Adaptors

Consider N ports which have port resistance $R_k, k = 1, ...N$ respectively are parallel connected. The Kirchhoff laws must be satisfied as

$$v_1 = v_2 = ... = v_N \tag{2.52}$$

and

$$i_1 + i_2 + ... + i_N = 0 \quad . \tag{2.53}$$

Based on WDC principles, the equations of wave quantities can be derived from the equations of voltages and currents. Substitute $v_i = (a_i + b_i)/2$, $i_i = (a_i - b_i)/(2R)$ into (2.52) and (2.53) to give

$$b_k = (\gamma_1 a_1 + \gamma_2 a_2 + ... + \gamma_N a_N) - a_k, \qquad k = 1, ..., N \tag{2.54}$$

where the scattering parameter γ_k is also called the multiplier coefficient of port k, which is formed as

$$\gamma_k = \frac{2G_k}{\sum_{l=1}^{N} G_l} \qquad k = 1, ..., N \quad , \tag{2.55}$$

where $G_k = 1/R_k$ is the port conductance of port k.

2.4.7.2 Series Adaptors

If N ports which has port resistance $R_k, k = 1, ...N$ respectively are series connected, the wave quantities can be related as

$$b_k = a_k - \gamma_k(a_1 + a_2 + ... + a_N) \qquad k = 1, ..., N \quad , \tag{2.56}$$

where

$$\gamma_k = \frac{2R_k}{\sum_{l=1}^{N} R_l} \qquad k = 1, ..., N \quad . \tag{2.57}$$

2.4.7.3 Special Ports

Besides the basic adaptors, two special ports in interconnections must be explained before wave digital principles are applied for digital implementation.

In order to implement a N-port adaptor, N multiplier coefficients are needed from the discussion above. However from (2.55) and (2.57),

$$\gamma_1 + \gamma_2 + \cdots + \gamma_N = 2 \tag{2.58}$$

regardless of whether a parallel or series adaptor is used. Thus, there are $N-1$ independent coefficients. Any port coefficient γ_k can be eliminated by (2.58), and is termed as a *the dependent port.* For an N-port adaptor, there are in total N degrees of freedom to decide which port is dependent. In order to minimize the sensitivity of the coefficient realized implicitly, the coefficient of the dependent port should not be smaller than any of the others. Since when the other coefficients are modified, it will suffer a relatively small change [27].

A *reflection-free port* is such a port where the reflection is absent, i.e. the port coefficient satisfies

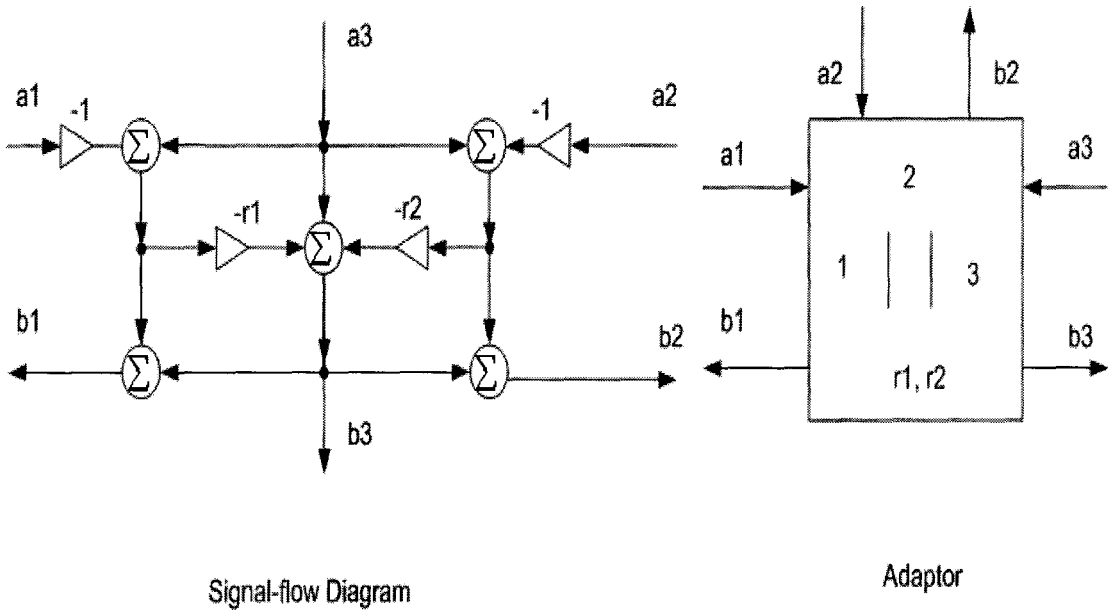

Figure 2.22: A unconstrained three-port parallel adaptor and corresponding signal-flow diagram

$$\gamma_k = 1 \quad . \tag{2.59}$$

Referring to (2.56) and (2.54), the reflection wave of this port b_k is independent of the incident wave of this port a_k. From (2.57) and (2.55), reflection-free port has another interpretation: the port resistance is equal to the input resistance at this port if the other ports are terminated by their respective port resistances. If a reflection-free port exists, the adaptor is termed to be *constrained* [27].

2.4.7.4 Examples

Consider the unconstrained 3-port parallel adaptor in Figure 2.22, as well as the corresponding signal flow diagram. The structure of the signal-flow diagram refers to the description of parallel adaptors in (2.54). In this adaptor, Port 3 is depen-

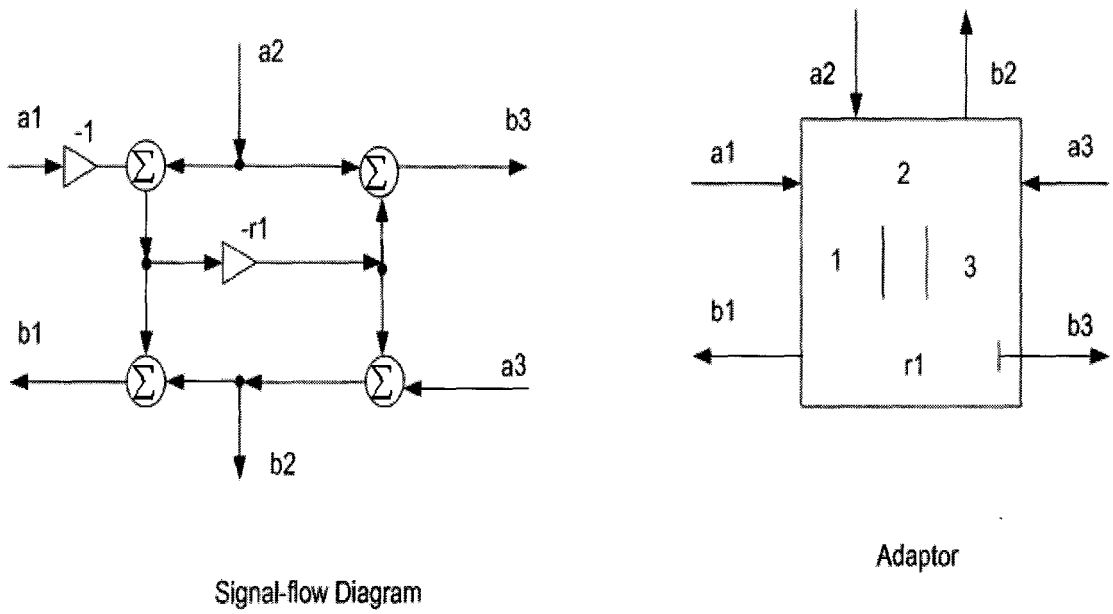

Figure 2.23: A constrained three-port parallel adaptor and corresponding signal-flow diagram

dent port and there are no constraints on this adaptor. Figure 2.23 is a constrained 3-port parallel adaptor with Port 3 reflection-free. In this adaptor, Port 2 is dependent port. The reflection-free port is represented symbolically by a stroke at the output of this port, as shown in Figure 2.23.

2.4.8 Realization of Circuits

In the previous two subsections, the issues of how to realize the various building blocks and how to realize the interconnections for WDF have been addressed. In this section, the general principles for realization of circuits are concluded. Firstly, the WD building blocks must be interconnected in the same way as their corresponding analog elements. Secondly, for every two ports connected to each other, the corresponding waves must flow in the same direction. Thirdly, for any

two ports thus combined, the two port resistances must be the same. As shown in Figure 2.24,

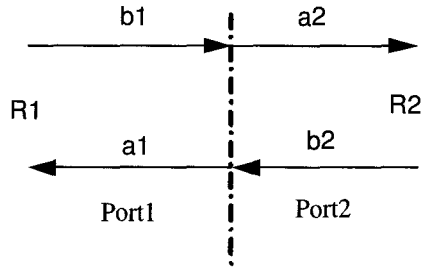

Figure 2.24: Interconnection of two wave ports

$$b_1 = a_2$$

$$a_1 = b_2$$

$$R_1 = R_2$$

Finally, the realizability conditions that were expressed in Sec. 2.4.5 must be satisfied.

To illustrate the WD techniques consider the digital implementation of the analog low pass filter in Figure 2.25. The source voltage E, the resistor R_0 and

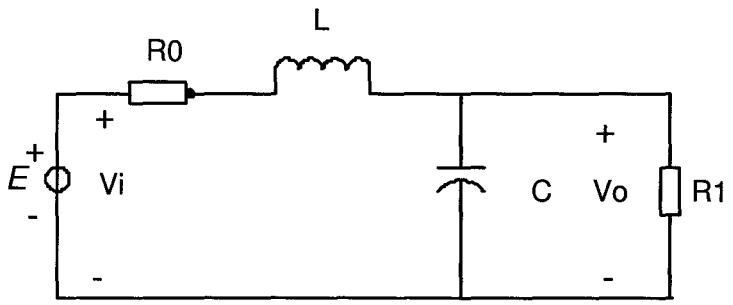

Figure 2.25: A low pass filter in analog domain

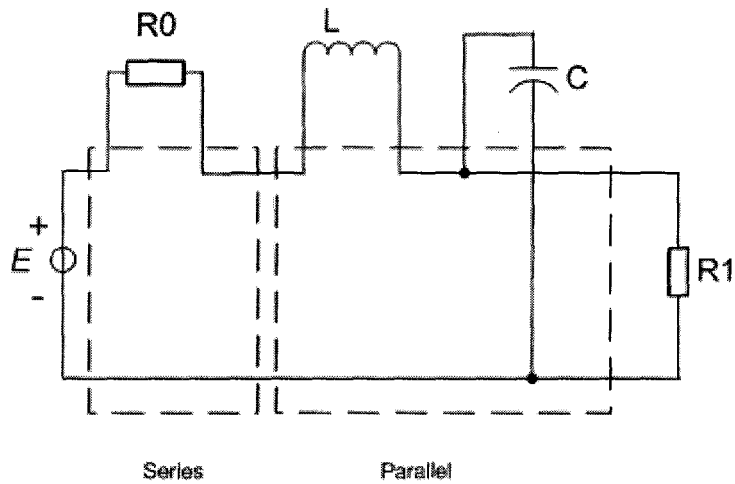

Figure 2.26: Circuit analysis of the analog filter

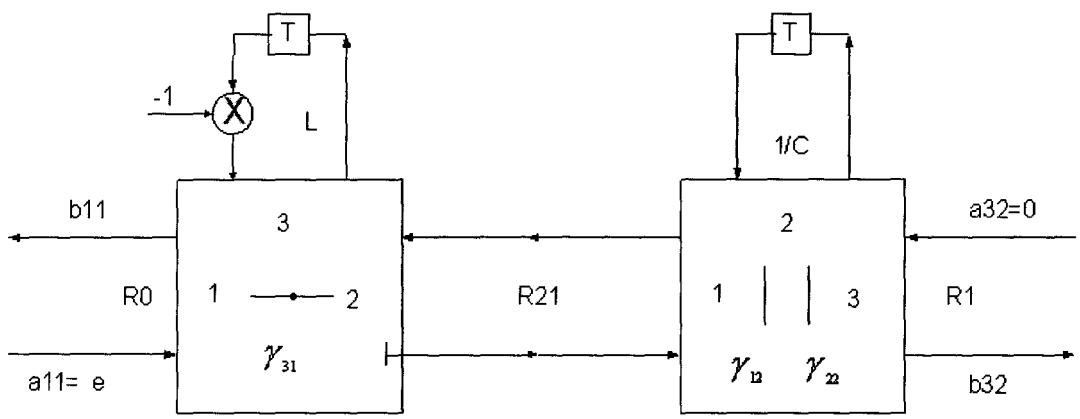

Figure 2.27: The corresponding low pass filter in wave digital domain

the remaining part of the circuit are connected in series, and the capacitor C, the resistor R_1 and the remaining part of the circuit are parallel connected, as shown in Figure 2.26. In series connection 1, the port resistance of Port 1 $R_{11} = R_0$ for matching the resistor R_0, the port resistance of Port 3 $R_{31} = L$ for matching the inductor L according to Figure 2.21. Port 2 is designated as a reflection-free port, since R_{21} is not specified a priori and is a degree of freedom. Thus, $\gamma_{21} = 1$, following (2.57), the port resistance of Port 2 is

$$R_{21} = R_{11} + R_{31} = R_0 + L \quad .$$

Select Port 1 as dependent port, so the multiplier constant of this series adaptor is

$$\gamma_{31} = \frac{R_{31}}{R_{31} + R_{11}} = \frac{L}{R_0 + L} \tag{2.60}$$

In parallel connection 2, the port conductance of Port 2 $G_{22} = C$, for Port 3, $G_{32} = 1/R_1$, and for Port 1, $G_{12} = 1/R_{21}$. Select Port 3 as dependent port, The multiplier constants are

$$\gamma_{12} = \frac{2G_{12}}{G_{12} + G_{22} + G_{32}}, \qquad \gamma_{22} = \frac{2G_{22}}{G_{12} + G_{22} + G_{32}} \tag{2.61}$$

So, one wave digital realization of this low pass analog filter shown in Figure 2.25 is built as Figure 2.27.

In general, the WD implementation of an analog circuit is not unique. In this example, Port 2 of connection 1 can be designated as reflection-free or not. And in connection 2, there are three options of the dependent port: Port 1, 2 or 3. Therefore even for one analog circuit, there are still several corresponding WD structures.

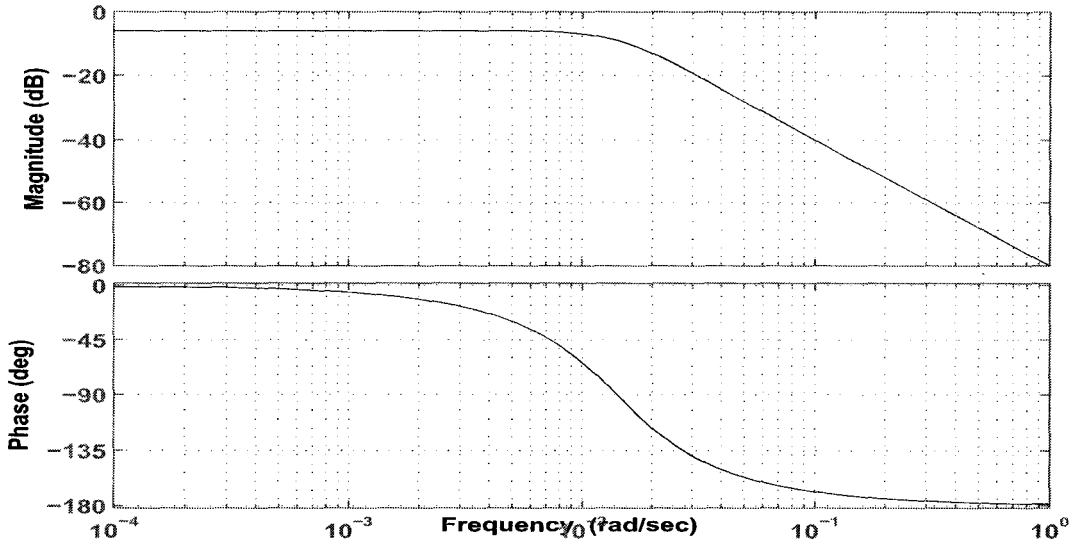

Figure 2.28: Bode diagram of the analog low-pass filter

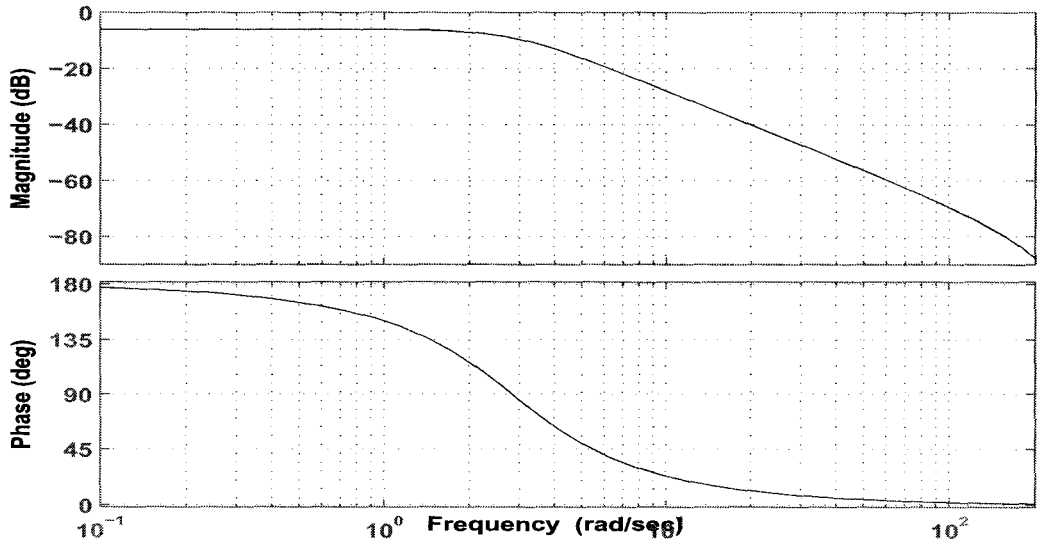

Figure 2.29: Bode diagram of the wave digital low-pass filter

Figures 2.28 and 2.29 are the Bode diagram of the low pass filter in analog domain and in wave digital domain. The parameters are set as the following: $R_0 = 1$, $R_1 = 1$, $L = 10^2$, $C = 10^2$, $T_s = 10^{-2}$. Notice good agreement, these two figures illustrate that the corresponding WD structure has the similar low-pass frequency property with the analog filter in the frequency range scaled by $2/T_s$. This result agrees with (2.47).

2.4.9 Nonlinear Wave Digital Circuits

Since WDCs are designed based on circuit topology, they can be used to realize a wide range of circuits. By far, linear circuits realization is the most well studied, however, nonlinear circuits can also be considered. In this subsection, some work is reviewed that has been done in nonlinear wave digital circuits which is related to our prescribed design work on Toda lattice circuits.

In 1992, Meerkotter and Felderhoff first proposed a structure of nonlinear transmission lines by wave digital filter principles [30]. A linear capacitance and an ideal transformer whose turns ratio is variable dependent on the voltage over the capacitor are employed to realize the nonlinear capacitance. However, such implementation of nonlinear capacitor requires an iterative algorithm solve an implicit equation for the turns ratio variable and the wave quantities. In that paper, the wave digital model of transmission line is symmetric, which is not the same as Toda LC lattice which is needed for the soliton communication system. Furthermore, unit elements are inserted in that model to cut the delay-free directed loops (DFDLs). In that structure, the minimal operational time is $T' = T/15$, T is the sampling time. Therefore oversampling fractional delays are required, reducing efficiency greatly. Felderhoff continued his work on a new wave description for nonlinear elements [38]. A method similar to the well-known Jacobi's method

was applied to cut the DFDLs [32]. However, the whole circuit model remained the same as in [30], and the implementation of the nonlinear capacitor was also unchanged. Some techniques to realize that nonlinear capacitor without iterative algorithm is attractive. And a new structure to implement the Toda lattice circuit is required for this model. In 1999, Sarti and De Poli proposed a detailed and thorough method toward nonlinear wave digital filters [33]. In next chapter, an implementation of the nonlinear capacitor in Toda lattice is presented based on the description of [33]. As well, a new structure for the Toda lattice circuit is presented.

2.5 Conclusions

In this chapter, the fundamental knowledge of communication systems is reviewed. Solitons and the systems exhibiting solitons are introduced, and due to their special properties, the applications of optical and electrical solitons in signal processing and communication systems are proposed. Some work on this subject is surveyed and the realization of the soliton communication systems is introduced. In the application of signal processing and communication systems, the electrical solitons are attractive due to the tractability of the Toda lattice circuit for realization and manipulation. Since traditional soliton-supporting systems are physical, they are analog. Thus, they are sensitive to the physical effects such as temperature variations, mechanical vibrations and component tolerances. So a digital model of the Toda lattice circuit is required to substitute the analog Toda lattice in the applications. A survey is presented on the methods of digital implementation of analog circuits. Furthermore, due to the nonlinearity of the Toda lattice, wave digital theory is advanced to achieve the digital realization of nonlinear circuits. The fundamental principles are introduced and some work related to the realization

of nonlinear circuits is mentioned. The design and implementation of the digital Toda lattice will be presented on the basis of WDCs theory.

Chapter 3

Wave Digital Implementation of a Soliton System

In this chapter the design and implementation of a digital soliton system is presented to overcome many of the difficulties of analog soliton systems. Here the Toda lattice circuit is considered since wave digital circuit design methods can be applied to approach a digital model that has nearly equivalent functions with the Toda lattice circuit.

This chapter describes the implementation of a digital soliton simulation system. Some definitions are specified for analysis and measurement. In the design of such a system, the implementation of a digital Toda lattice circuit is the major concern. By means of wave digital circuit theory, introduced in Chapter 2, a new digital representation of Toda lattice circuit is proposed. The detailed design of this wave digital model is addressed. This digital model of a soliton system can be employed as a digital soliton system simulator, which has the potential to be applied in the research of soliton systems, such as in optical communications, and soliton multiplexing systems.

3.1 Definitions

3.1.1 Time-frequency Analysis

From the Fourier transform, a signal with limited bandwidth must be unlimited in time and vice versa. From a signal processing standpoint, a signal that is transmitted must start at some initial time and stop at some terminating time. Such signals can not be band-limited in frequency. However, bandwidth is a precious resource, and must be tightly controlled. Real signals are thus unlimited both in time and in frequency domain. The definition of the time and frequency bandwidth of a signal must be defined on the whole real line.

In Slepian's classical paper [45], the time and frequency bandwidth are specified based on the measure of energy distribution in time and frequency. Define the energy of a continuous-time signal $s(t)$ as

$$E_s = \int_{-\infty}^{\infty} s^2(t)dt \quad . \tag{3.1}$$

From Parseval's theorem,

$$E_s = \int_{-\infty}^{\infty} |S(f)|^2 df \tag{3.2}$$

where $S(f)$ represents the continuous Fourier transform of $s(t)$ and the operation $|.|$ is the magnitude of a signal.

Consider a real signal $s(t)$ of finite energy E_s, given in (3.1) and (3.2). Such a signal is termed time-limited to the interval $(-T/2, T/2)$ at level ε if

$$E_s - E_T \leq \varepsilon$$

where

$$E_T = \int_{-T/2}^{T/2} s^2(t)dt$$

and T is defined as the duration of $s(t)$ at level ε, or is commonly called the fractional energy duration. For example, if $\varepsilon = 10^{-2}$, T is 99% energy duration of $s(t)$.

Similarly, $s(t)$ is band-limited to $(-W, W)$ at level ε if

$$E_s - E_{2W} \leq \varepsilon$$

where

$$E_{2W} = \int_{-W}^{W} |S^2(f)|df$$

and W is termed the fractional energy one-sided bandwidth of $s(t)$ and $2W$ is the corresponding two-sided bandwidth.

These definitions lead to a useful consequence that all signals of finite energy are both band-limited to some finite bandwidth W and time-limited to some finite duration T at some level ε. At least N_s independent functions are needed to represent such signal $s(t)$ from the point of view of representing $s(t)$ with normalized error energy less than ε [45]. The approximate dimension is defined as

$$N_s = 2WT \quad .$$

The dimension N_s of a signal $s(t)$ is the number of degrees of freedom in $s(t)$, i.e., $s(t)$ which is limited in T seconds and W Hz can be specified by a sequence of $2WT$ independent values at level ε when energy is measured [40, 43]. For robust result,

$$N_s = 2WT + 1 \quad .$$

This consequence is of great importance to representation of a signal in a digital system.

3.2 Introduction to Digital Soliton Communication Systems

This section discusses the time-frequency characteristics of Toda soliton signals using the definitions of Section 3.1.1 and introduces a digital soliton communication system as a possible application.

3.2.1 Time-frequency Analysis of Soliton Signals

In this subsection, the bandwidth and time duration of a soliton signal are analyzed, which are crucial to the design of the soliton simulation system. Here the 99% energy bandwidth and duration are applied in reference to Section 3.1.1.

Chapter 2 introduced several kinds of solitons and their corresponding soliton systems. The Toda soliton is selected in this work as specified in (2.24) due to close link to circuit theory. For a single soliton signal, the duration and bandwidth are independent of the phase. So for simplification, a soliton with zero phase which matches normalized Toda lattice circuit is analyzed,

$$s(t) = \beta^2 \mathrm{sech}^2(\beta \mathrm{t}) \tag{3.3}$$

where β can be any positive real value. According to Section 2.2.3.4, the normalized Toda lattice circuits have unit inductance $L = 1$ and unit capacitance parameter $C_0 = 1, V_0 = 1$. The Fourier transform of the Toda soliton is [7],

$$S(f) = \frac{2\pi^2 f}{\sinh(\frac{\pi^2 f}{\beta})} \quad . \tag{3.4}$$

The total energy of a single soliton can be shown to be

$$E_s = \int_{-\infty}^{\infty} |s(t)|^2 \mathrm{dt} = \frac{4}{3}\beta^3 \quad . \tag{3.5}$$

Following early definitions, the 99% fractional energy duration is

$$\int_{-T/2}^{T/2} |s(t)|^2 \mathrm{dt} = 0.99\mathrm{E_s} \quad , \tag{3.6}$$

and 99% fractional energy bandwidth is

$$\int_{-W}^{W} |S(f)|^2 \mathrm{df} = 0.99\mathrm{E_s} \quad . \tag{3.7}$$

For a given soliton, (3.6) and (3.7) can be solved by numerical integration to give $T = 3.1422/\beta$ and $W = 0.3937\beta$ respectively. So the Nyquist rate B must satisfy $B > 0.7874\beta$ in order to avoid aliasing.

From this result, some useful conclusions are apparent. Firstly, in reference to the definition in Section 3.1.1, the effective dimension of a single Toda soliton signal in the normalized lattice is independent of β, i.e.,

$$2WT = 2 \times \frac{\beta}{0.3937} \times \frac{3.1422}{\beta} = 2.4742 \quad .$$

Therefore, the effective dimension of all of the soliton signals is the same. Secondly, for a given band-limited channel with two-sided bandwidth $2W$, the allowable solitons transmitted in this channel have the parameter $\beta < W/0.3937$. Thirdly, to sample a given soliton signal, the sampling rate must satisfy $T_s < 1/0.7874\beta$.

The time and frequency representation of a Toda soliton signal with $\beta = 2$ is illustrated in Figure 3.1, where the 99% energy is time-limited in $(-T/2, T/2)$ and band-limited in $(-W, W)$ are shown. The figure shows that the soliton is a pulse-like signal with compact energy both in time-limited duration and band-limited

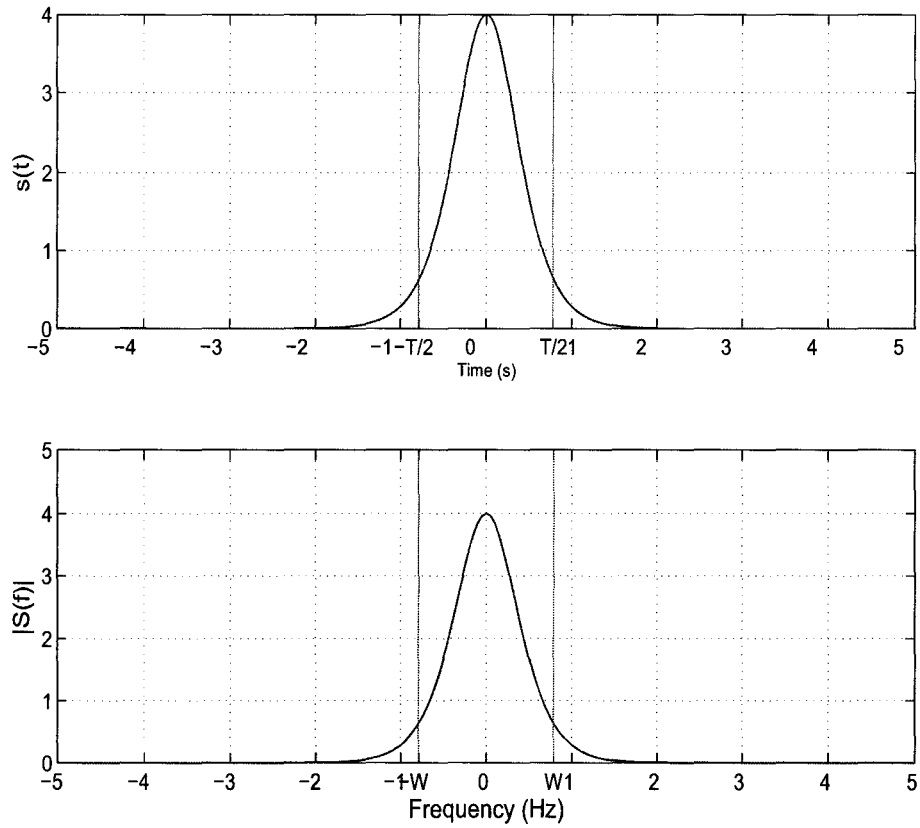

Figure 3.1: Time and frequency analysis of soliton ($\beta = 2$)

bandwidth. Therefore, soliton signals are amenable to efficient representation in digital systems.

3.2.2 Example of Digital Soliton Communication System

After the time-frequency analysis of Toda solitons, the soliton has been shown suitable to carry information for transmission in a band-limited channel. One possible application of a soliton system is for a communication system. A schematic diagram of a general soliton communication system is shown in Figure 1.1. Solitons are used as carrier signals to carry information in a soliton communication system. A soliton-supporting system is required to act as digital modulator and demodulator. As an extension of soliton modulation, different solitons can be also used to multiplex signals of different users due to the separability of different solitons. Traditional soliton-supporting systems are physical systems, as introduced in Section 2.2, and are analog systems and thus sensitive to the physical effects (temperature variations, mechanical vibrations). However digital systems are more robust, offering greater tolerance to random disturbances or variations. Therefore, a digital model of an analog soliton-supporting system is required to provide more robust performance in a digital soliton communication system. Among these systems, the Toda lattice circuit is the most tractable for digital modelling since the methods of digital implementation of analog filters can be applied.

3.3 Digital Toda Lattice Circuit

According to the discussion of the digital soliton communication system in the previous section, a digital Toda lattice circuit is required to act as digital modulator-demodulator or multiplexer-demultiplexer. From the overview of wave digital cir-

cuits in Section 2.4, the fundamental theory has been introduced and wave digital circuits are known to have advantages to represent nonlinear analog circuits. In this section, a new model of a digital Toda lattice is proposed using wave digital principles. For the synthesis of linear circuits, the classical wave quantities described in (2.29),(2.30) are sufficient to represent the circuits as introduced in Chapter 2. Whereas for the sake of modelling nonlinear circuit elements, new types of waves have been proposed in the literature [33, 38], and will be applied to Toda lattice circuits here.

3.3.1 General Wave Variables

Instead of classical voltage wave quantities, general voltage wave quantities with memory can be applied in the digital implementation of nonlinear analog elements [33]. In time domain,

$$a^g(t) = m(t) + \mu n(t) \tag{3.8}$$

$$b^g(t) = m(t) - \mu n(t) \quad . \tag{3.9}$$

Here $m(t)$ is a filtered voltage, i.e. $m(t) = f_v(v(t))$ and $n(t)$ is a filtered current, i.e. $n(t) = f_i(i(t))$. And $f_v(\cdot)$, $f_i(\cdot)$ are linear time-invariant (LTI) mappings. The value μ is the port reference parameter. From the bilinear transform from s to z domain introduced in Section 2.4.4, in z domain,

$$A^g(z) = H_v(z)V(z) + \mu H_i(z)I(z) \tag{3.10}$$

$$B^g(z) = H_v(z)V(z) - \mu H_i(z)I(z) \tag{3.11}$$

where $H_v(z)$ is the transfer function of the digital voltage filter corresponding to the analog filter f_v and similarly $H_i(z)$ is of the current filter. If this one-port element is resistive, $m(t) = k_m v(t)$, $n(t) = k_n i(t)$; if capacitive, $m(t) = k_m v(t)$, $n(t) = f_i\left(\int i(t)dt\right)$; if inductive, $m(t) = f_v\left(\frac{dv}{dt}\right)$, $n(t) = k_n i(t)$.

By using this pair of general wave variables, the characteristic of inductors and capacitors can be transformed to that of resistors. As known, inductive and capacitive nonlinearities are described by differential equations and likewise, resistive nonlinearities are represented by algebraic equations. Handling nonlinearities described by algebraic equations is easier than the nonlinearities described by differential equations [33]. Therefore, the characteristics of nonlinear capacitors in the Toda lattice circuit are expected to be reformed to resistive nonlinearities. This will be presented in the next subsection.

3.3.2 Specific Wave Variables for Nonlinear Capacitors in the Toda Lattice

By adopting general wave quantities stated previously, specific wave quantities can be defined for the nonlinear capacitors in the Toda lattice. In the Toda lattice, the nonlinearity is due to the nonlinear capacitor [2], the amount of charge stored in this nonlinear capacitor

$$q = c(v)v = C_0 V_0 \log\left(1 + \frac{v}{V_0}\right) \tag{3.12}$$

where v is the voltage difference across the capacitor, C_0, V_0 are parameters described in Section 2.2.3.4.

Thus, a new pair of wave variables can be defined as:

$$a^c = v + \mu q \tag{3.13}$$

$$b^c = v - \mu q \tag{3.14}$$

These definitions and (3.12) demonstrate that the characteristics are resistive in variables v and q. From the definitions of the wave quantities in (3.13) and (3.14),

$$v = \frac{a^c + b^c}{2}$$

and

$$q = \frac{a^c - b^c}{2\mu}$$

can be derived. Substituting these two expressions into (3.12), and then the nonlinear characteristic can be represented in a function of a and b,

$$f(a^c, b^c) = C_0 V_0 \log(1 + \frac{a^c + b^c}{2V_0}) - \frac{a^c - b^c}{2\mu} = 0 \quad . \tag{3.15}$$

So the capacitive nonlinearity becomes resistive. From (3.15), an implicit function of a^c and b^c is obtained to indicate the characteristic of the nonlinear capacitor in wave digital domain. Consider the implicit function $f(a, b) = 0$. Since $f(a, b)$ is continuously differentiable, it is possible to write b as a explicit function of a, i.e. the form $b = g(a)$, when for any fixed point $(a_0, b_0) \in \mathbb{R}^2$ with

$$f(a_0, b_0) = 0$$

and

$$\left.\frac{\partial f}{\partial b}\right|_{(a_0, b_0)} \neq 0 \quad , \tag{3.16}$$

by the implicit function theorem [36]. From (3.15),

$$\frac{\partial f}{\partial b^c} = \frac{C_0 V_0}{a^c + b^c + 2V_0} + \frac{1}{2\mu} \quad .$$

For the sake of satisfying (3.16), the following equation

$$v = \frac{a^c + b^c}{2} \neq -V_0(1 + C_0\mu) \tag{3.17}$$

must hold in order to have an explicit functional relationship between a^c and b^c, where v is the voltage difference across the capacitor. According to the definition in (2.22), $-V_0$ is the breakdown reverse voltage which specifies the capacitor's characteristic.

However, in Toda lattice circuit, the voltage across the nonlinear capacitor always satisfies

$$v > -V_0 \quad ,$$

due to the circuit's property. So the property when $v \leq -V_0$ is undefined. In order to let (3.17) always holds in the Toda lattice circuit,

$$\mu > 0 \tag{3.18}$$

is a sufficient condition. Therefore the inequality(3.18) guarantees $f(a^c, b^c) = 0$ can have an equivalent explicit form $b^c = g(a^c)$.

The wave digital realization of a circuit or an element changes the variables from Kirchhoff domain to WD domain as introduced in Section 2.4.3.2. The nonlinear characteristic of the Toda capacitor in Kirchhoff domain according to (3.12) is shown in Figure 3.2. And Figure 3.3 shows the algebraic nonlinearity between the incident wave and reflected wave with different values of port reference parameter μ according to (3.15). As shown in Figure 3.3, the relationship between a^c and b^c is quasi-linear when μ gets large. Since μ scales the charge q, the voltage $v = \frac{a^c+b^c}{2}$ range decreases with μ increasing according to (3.13) and (3.14). Therefore, when the voltage range is small, the functional relationship between a^c and b^c is quasi-linear. With satisfaction of the condition (3.18), freedom exists to set value of μ.

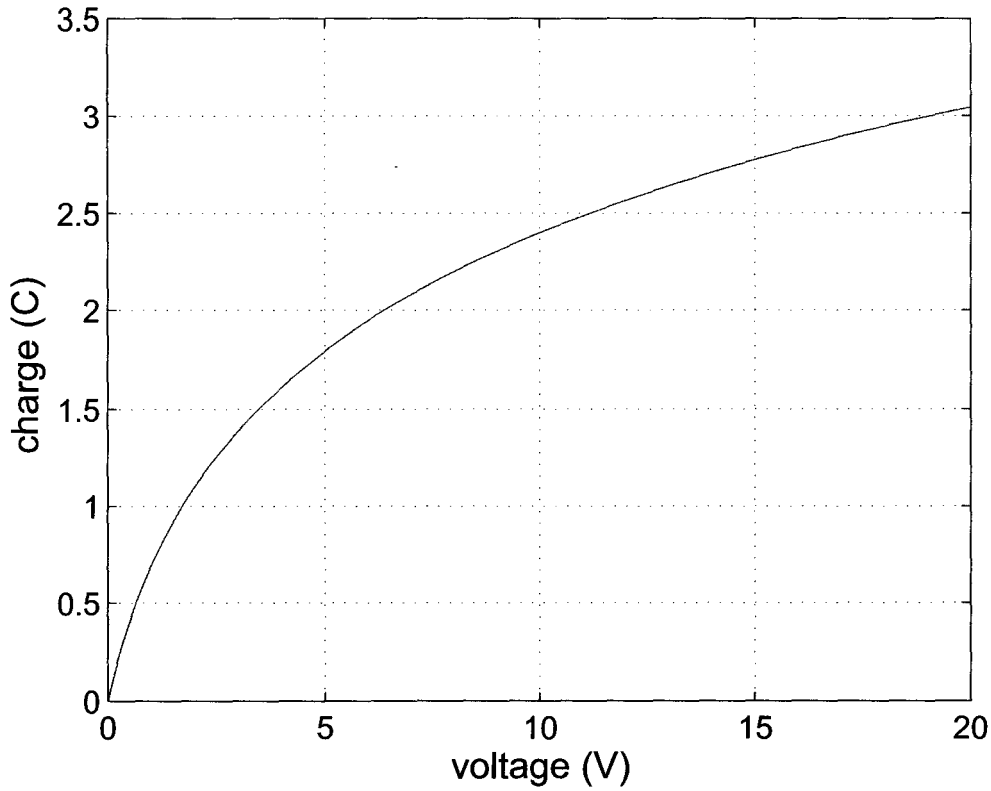

Figure 3.2: Nonlinear characteristic of Toda capacitor in Kirchhoff domain

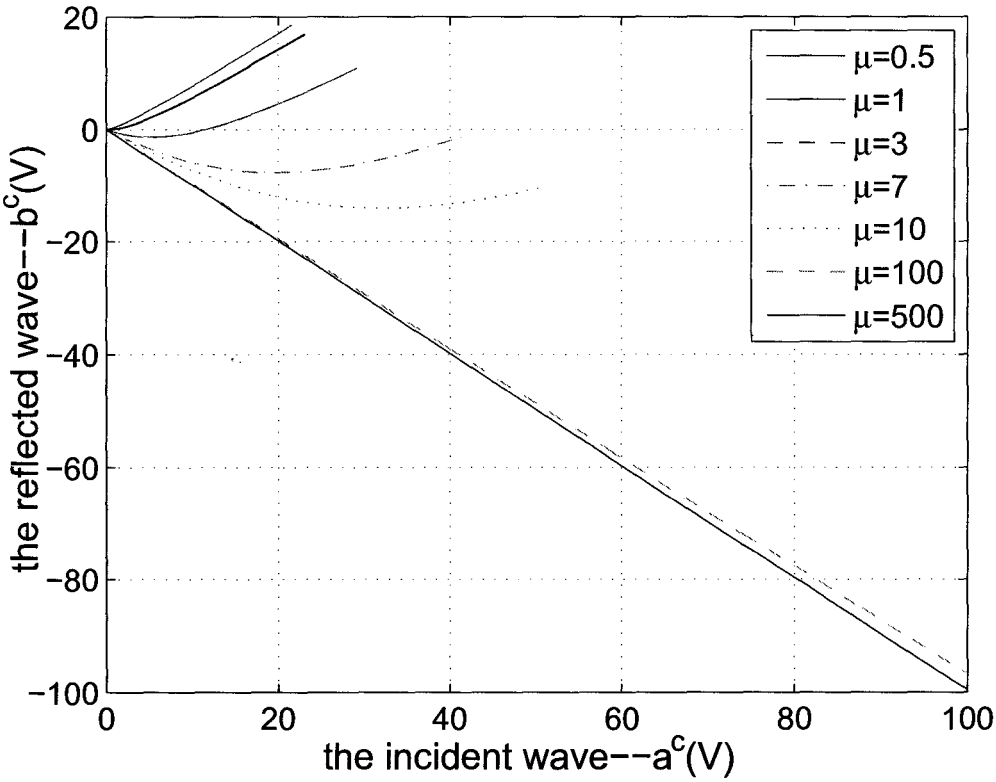

Figure 3.3: Nonlinear characteristic of Toda capacitor in general wave digital domain

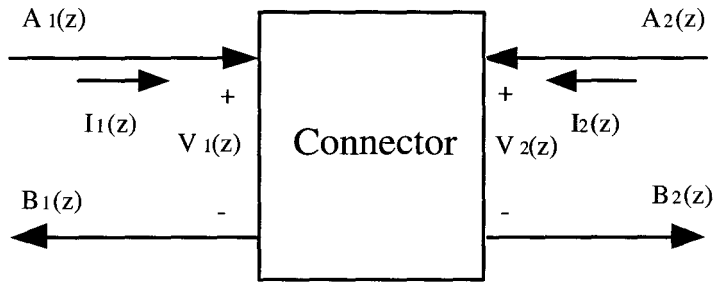

Figure 3.4: Connection between two wave variables of different types

The value of μ in the whole Toda lattice circuit will be discussed when the whole wave digital structure of the Toda lattice is presented in Section 3.3.5. Therefore, using the new wave digital transformation, the nonlinearity of Toda capacitor can be reformed to a resistive nonlinearity, which is quasi-linear. Hereafter, the nonlinear analog capacitor can be represented by some simple implementation in digital domain, such as look-up table, or using piece-wise linear data fitting to represent the dependence of the incident and reflected wave quantities.

3.3.3 Connections between Different Wave Variables

It is often useful to design wave digital circuits that have more than one type of wave quantities in systems. Therefore methods of connecting different wave variables are required to implement complete digital structures. In the implementation of the Toda lattice, the connection method between linear classical wave variables and specific wave variables for nonlinear capacitors are required since the remaining elements are all linear. In this subsection, the general connections of two different wave variables are introduced.

In Figure 3.4, two pairs of wave quantities of different types are interconnected by a connector. Here $A_i(z), i = 1, 2$ and $B_i(z), i = 1, 2$ are the incident and reflected wave quantities of the two different types in complex frequency domain.

$I_i(z), i = 1, 2$ and $V_i(z), i = 1, 2$ are the currents and voltages of these two ports in Z-domain respectively.

These two pairs of different wave quantities are represented as follows:

$$A_1(z) = H_{V1}(z)V_1(z) + H_{I1}(z)I_1(z) \tag{3.19}$$

$$B_1(z) = H_{V1}(z)V_1(z) - H_{I1}(z)I_1(z) \tag{3.20}$$

$$A_2(z) = H_{V2}(z)V_2(z) + H_{I2}(z)I_2(z) \tag{3.21}$$

$$B_2(z) = H_{V2}(z)V_2(z) - H_{I2}(z)I_2(z) \tag{3.22}$$

where $H_{Vi}, i = 1, 2$ are the voltage filter, and $H_{Ii}, i = 1, 2$ are the current filter. In reference to Section 2.4.3, the scattering matrix of two-port junction is defined as:

$$\mathbf{S_{2\times 2}} = \begin{pmatrix} \frac{B_1(z)}{A_1(z)}|_{A_2(z)=0} & \frac{B_1(z)}{A_2(z)}|_{A_1(z)=0} \\ \frac{B_2(z)}{A_1(z)}|_{A_2(z)=0} & \frac{B_2(z)}{A_2(z)}|_{A_1(z)=0} \end{pmatrix} . \tag{3.23}$$

so

$$\mathbb{B}_2 = \mathbf{S_{2\times 2}}\mathbb{A}_2$$

where

$$\mathbb{B}_2 = [B_1(z), B_2(z)]^T$$

$$\mathbb{A}_2 = [A_1(z), A_2(z)]^T$$

Referring to [33], for two port interconnection, the continuity conditions of the two-port junctions must be satisfied: $V_1(z) = V_2(z)$ and $I_1(z) = -I_2(z)$. From

(3.19), (3.20) and (3.21), (3.22), the continuity conditions can be expressed by wave quantities as

$$\frac{A_1(z)+B_1(z)}{2H_{V1}} = \frac{A_2(z)+B_2(z)}{2H_{V2}} \tag{3.24}$$

and

$$\frac{A_1(z)-B_1(z)}{2H_{I1}} = -\frac{A_2(z)-B_2(z)}{2H_{I2}} \quad . \tag{3.25}$$

Reformulate (3.26) and (3.27), the reflected waves can be expressed by incident waves as

$$B_1(z) = K(z)A_1(z) + \frac{H_{V1}}{H_{V2}}\left(1-K(z)\right)A_2(z) \tag{3.26}$$

and

$$B_2(z) = \frac{H_{V2}}{H_{V1}}\left(1+K(z)\right)A_1(z) - K(z)A_2(z) \quad , \tag{3.27}$$

where

$$K(z) = \frac{H_{V1}(z)H_{I2}(z) - H_{V2}(z)H_{I1}(z)}{H_{V1}(z)H_{I2}(z) + H_{V2}(z)H_{I1}(z)} \quad . \tag{3.28}$$

$K(z)$ is the transfer function of the reflection filter that characterizes the scattering junction with memory. The scattering matrix of this two port junction can be simplified to

$$\mathbf{S_{2\times 2}} = \begin{pmatrix} K(z) & \frac{H_{V1}(z)}{H_{V2}(z)}\left(1-K(z)\right) \\ \frac{H_{V2}(z)}{H_{V1}(z)}\left(1+K(z)\right) & -K(z) \end{pmatrix} \tag{3.29}$$

3.3.4 R-C Mutators in the Toda Lattice

Following the connections between different wave quantities stated in the previous subsection, the corresponding connections can be defined between classical waves, formulated in (2.29) and (2.30), for linear elements and specific waves, formulated in (3.13) and (3.14), for nonlinear capacitors in Toda lattice. A scattering junction is required between nonlinear capacitor and the remaining circuit.

The wave digital implementation of the nonlinear capacitor in the Toda lattice has been proposed in Section 3.3.2. From the Laplace transformation of (3.13) and (3.14), the wave quantities in S-domain are

$$A^c(s) = V(s) + \mu\frac{I(s)}{s} \tag{3.30}$$

and

$$B^c(s) = V(s) - \mu\frac{I(s)}{s} \quad . \tag{3.31}$$

By the bilinear transformation specified in (2.46), the wave quantities of this nonlinear capacitor are indicated in Z-domain as follows:

$$A^c(z) = V(z) + R_c(z)I(z) \tag{3.32}$$

and

$$B^c(z) = V(z) - R_c(z)I(z) \quad , \tag{3.33}$$

where

$$R_c(z) = \frac{\mu T_s}{2}\frac{1+z^{-1}}{1-z^{-1}} \tag{3.34}$$

is the reference transfer function (RTF) of this nonlinear capacitor's port.

Such a junction to be used for connection between a capacitive RTF and a reference resistor is termed as R-C mutator [33]. The scattering matrix of this R-C mutator can be derived in reference to (3.29),

$$\mathbf{S_{RC}} = \begin{pmatrix} K(z) & 1-K(z) \\ 1+K(z) & -K(z) \end{pmatrix} \tag{3.35}$$

where the transfer function of the reflection filter is

$$K(z) = \frac{R_c(z) - R}{R_c(z) + R} \tag{3.36}$$

where R is the port resistance of the resistive port to be connected to the nonlinear capacitive port. Due to the determinant of $\mathbf{S_{RC}}$

$$|\mathbf{S_{RC}}| = 1 \quad ,$$

the R-C mutator is a nondissipative component and therefore lossless. The structure of such digital implementation of the nonlinear capacitor in Toda lattice is shown as Figure 3.5.

In this structure, by denoting

$$R = \frac{\mu Ts}{2}$$

and then according to (3.36),

$$K(z) = z^{-1} \quad .$$

By adopting this $K(z)$, considering only the two-port mutator illustrated in Figure 3.5, there are no delay-free branches from the incident waves a^c, a^1 to the reflected waves b^c, b^1 when no capacitor is interconnected. But when this R-C mutator is interconnected to a block which characterizes the nonlinearity of the capacitor, a

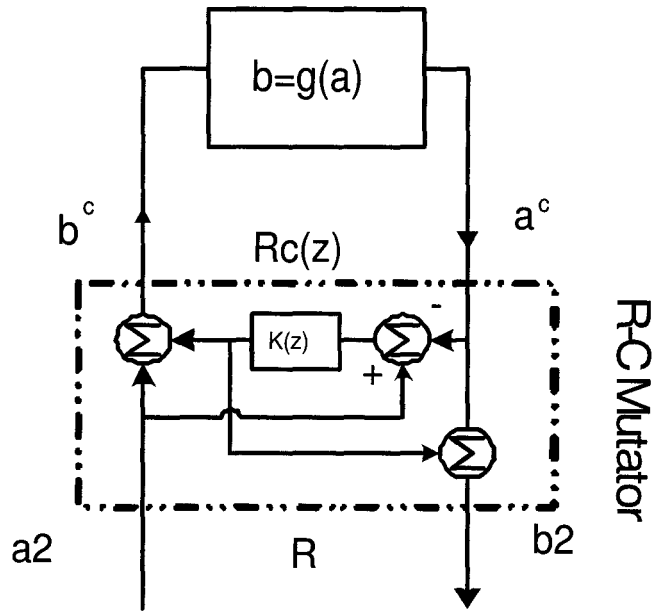

Figure 3.5: New WD implementation of the nonlinear capacitor in Toda lattice

delay-free branch still exists. The delay-free branches give rise to the problem of delay-free directed loops (DFDLs) as discussed in Section 2.4.5, which is very important for the realizability. This problem will be discussed in the next subsection where the whole structure of wave digital Toda lattice is presented.

3.3.5 New Wave Digital Structure of the Toda Lattice

Based on the model of wave digital nonlinear capacitor proposed in Section 3.3.2 and the classical realization of wave digital circuits introduced in Chapter 2, a new wave digital structure of a Toda lattice is built.

3.3.5.1 One Node Structure

The analog Toda lattice is shown in Figure 1.2. One node of the Toda lattice can be constructed by a series adaptor and a parallel adaptor, as illustrated in Figure

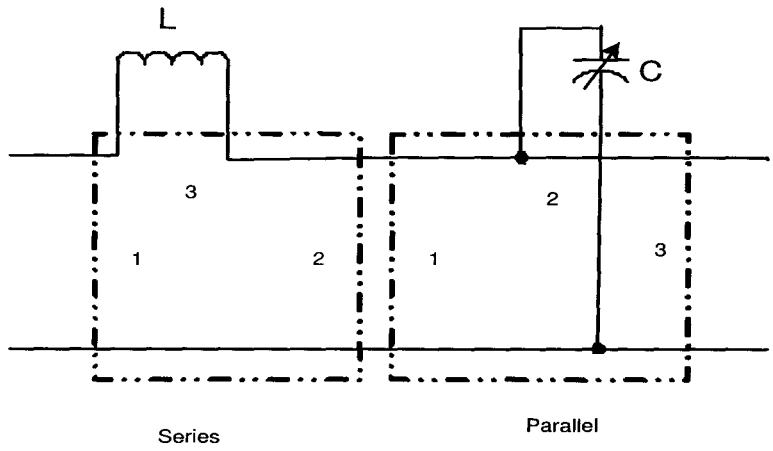

Figure 3.6: Circuit analysis of one node in Toda lattice

3.6. Figure 3.7 is the wave digital model of one node in the Toda lattice. In this model, a piece-wise linear data fitting block is adopted to describe the nonlinear capacitor.

As discussed in Section 2.4, there are freedoms to appoint the reflection-free ports in the adaptors. For example, in the series adaptor of this model as shown in Figure 3.7, except for port 3, port 1 and port 2 both have opportunities to be reflection-free port since port 1 and port 2 do not connect to any element directly as introduced in Section 2.4.7.3. Here port 2 is assigned to be reflection-free in respect that the input and output port resistance are required to be consistent. So this node model can be concatenated without any modification to build the whole Toda lattice. And moreover, the DFDL between a_1 and b_1 is cut by this reflection-free port. Notice that when two nodes are concatenated, from one output port to another input port, there is still the problem of a DFDL. This problem must be solved for the realizability of the digital model referring to Section 2.4.5.

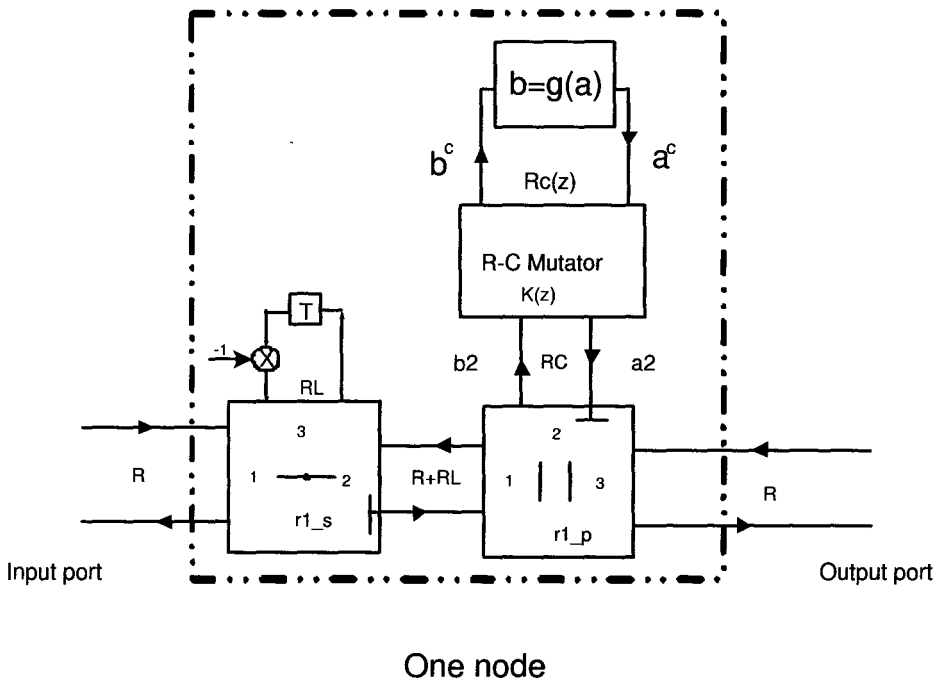

Figure 3.7: New WD implementation structure of one node in Toda lattice

3.3.5.2 Modeling to Cut DFDLs

From a mathematical viewpoint, a DFDL is an algebraic loop. In Section 2.4.5, some discussion has been addressed about DFDLs. The DFDL problem often appears in particular when analog circuits are converted to digital domain. If the circuit is linear, various techniques can be applied to convert an analog system into an equivalent digital system. A linear digital circuit can always be rearranged to a new one in which DFDLs are removed since the linear circuit itself does not lead to algebraic loops, and so if a DFDL exists, it is caused by the configuration. In [48], simple graph-theoretic methods for detecting and locating DFDLs in digital circuit configuration are outlined and the means of partial modification of the signal-flow structure to remove DFDLs is presented. However, such a method is only valid for linear cases.

However, for digital modeling of nonlinear circuits, the DFDL problem can not be solved by manipulation without introducing new blocks or iterative algorithms. The implementation of the nonlinearity introduces delay-free branches which can not be directly eliminated. A general method of efficient computation of nonlinear filter networks with DFDLs is presented in [47], where iterative methods are applied to solve the DFDL problem. The Newton-Raphson method can be applied to iterate a solution. Although possible for short circuit, naturally the impact of error propagation in long Toda lattices limits the applicability of this technique.

Clearly, some filter structure to break the delay-free branches must be added into any path belonging to the DFDL to cut the loop. A common delay element can not be employed directly in a wave digital circuit since the delay is a part of the wave digital block of a component, such as capacitor or inductor in reference to Figure 2.20.

A linear predictor [35] is applied in our model to cut DFDLs. A linear predictor

is an FIR filter that predicts the present value u_n in a sequence from the past inputs $u_{n-k}, k = 1, \cdots M$ as described in

$$\hat{u_n} = -\sum_{k=1}^{M} a_k u_{n-k}$$

where M is the prediction order, $a_k, k = 1, \cdots M$ are the parameters. In the method of least squares the parameters $a_k, k = 1, \cdots M$ are obtained as a result of the minimization of the total squared error

$$E^2 = \sum_{n=-\infty}^{+\infty} \left(u_M + \sum_{k=1}^{M} a_k u_{n-k} \right)^2 \tag{3.37}$$

with respect to each parameter, i.e.

$$\frac{\partial E^2}{\partial a_i} = 0, \quad i = 1, \cdots M \quad . \tag{3.38}$$

From (3.37) and (3.38),

$$\sum_{k=1}^{M} a_k \sum_{n=-\infty}^{+\infty} u_{n-k} u_{n-i} = -\sum_{n=-\infty}^{+\infty} u_n u_{n-i}, \quad i = 1, \cdots M \tag{3.39}$$

can be obtained. To solve (3.39), autocorrelation method can be adopted. Define

$$R(i) = \sum_{n=-\infty}^{+\infty} u_n u_{n-i} \quad ,$$

then (3.39) reduces to

$$\sum_{k=1}^{M} a_k R(i-k) = -R(i), \quad i = 1, \cdots M \quad . \tag{3.40}$$

In practice, the signals are known over only a finite interval, therefore the autocorrelation coefficients must be estimated in finite interval. In our linear predictor model, the previous M signal points $u_{n-k}, k = 1, \cdots M$ are known to predict the

signal u_n. So a window of length M can be applied to truncate the signal by M interval,

$$u'_k = \begin{cases} u_k, & 1 \leq k \leq M \\ 0, & \text{otherwise} \end{cases}$$

Therefore, the autocorrelation function is then given by

$$R(i) = \sum_{n=1}^{M-i} u_n u_{n+i} \quad , \tag{3.41}$$

Substituting (3.41) into (3.40), rewrite in matrix form,

$$\begin{pmatrix} R(0) & R(1) & \dots & R(M-1) \\ R(1) & R(0) & \dots & R(M-2) \\ \vdots & \vdots & \ddots & \vdots \\ R(M-1) & R(M-2) & \dots & R(0) \end{pmatrix} \begin{pmatrix} a_1 \\ a_2 \\ \vdots \\ a_M \end{pmatrix} = \begin{pmatrix} R(0) \\ R(1) \\ \vdots \\ R(M-1) \end{pmatrix} . \tag{3.42}$$

This matrix equation can be solved by Levinson-Durbin algorithm [56] in our linear predictor block. Consequently the present output of the linear predictor is independent of the present input. By adding this block into the DFDL, the delay-free path will be eliminated.

3.3.5.3 Wave Digital Structure of Finite Length Toda Lattice

The ideal Toda LC lattice is composed of an infinite number of nodes, as shown in Figure 1.2 in Chapter 1. Such an infinite structure is not realizable in practice. A finite structure can be adopted with an equivalent impedance to terminate the lattice, as shown in Figure 3.8. To approximate the ideal case, the equivalent impedance, which is resistive, is chosen to terminate the circuit [7], where

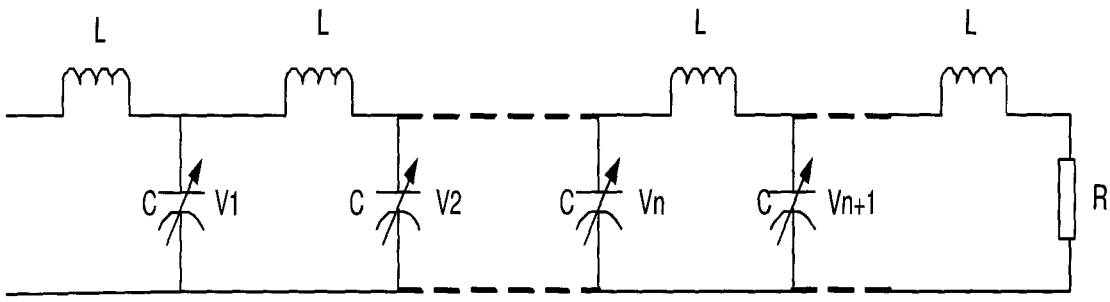

Figure 3.8: Equivalent finite structure of Toda LC lattice

$$R = \sqrt{\frac{L}{C_0}} \quad . \tag{3.43}$$

The wave digital model of the finite Toda lattice is illustrated in Figure 3.9, which is based on the one node model in Figure 3.7.

According to this WD structure of the Toda lattice and the basic principles of WDC introduced in Chapter 2, the parameters of the model are specified as follows with reference to Figure 3.7: R is the same as the terminating resistance in (3.43), and the port resistance of the linear inductor is

$$R_L = \frac{2L}{T_s} \quad ,$$

the port resistance of the $R-C$ mutator is

$$R_C = \frac{1}{\frac{1}{R+R_L} + \frac{1}{R}} \quad ,$$

and the port reference parameter of the nonlinear capacitor is

$$\mu = \frac{2R_c}{T_s} \quad .$$

Therefore, μ is not a free parameter in this WD model of Toda lattice. It depends on the analog circuit's specification and the sample time of this digital system.

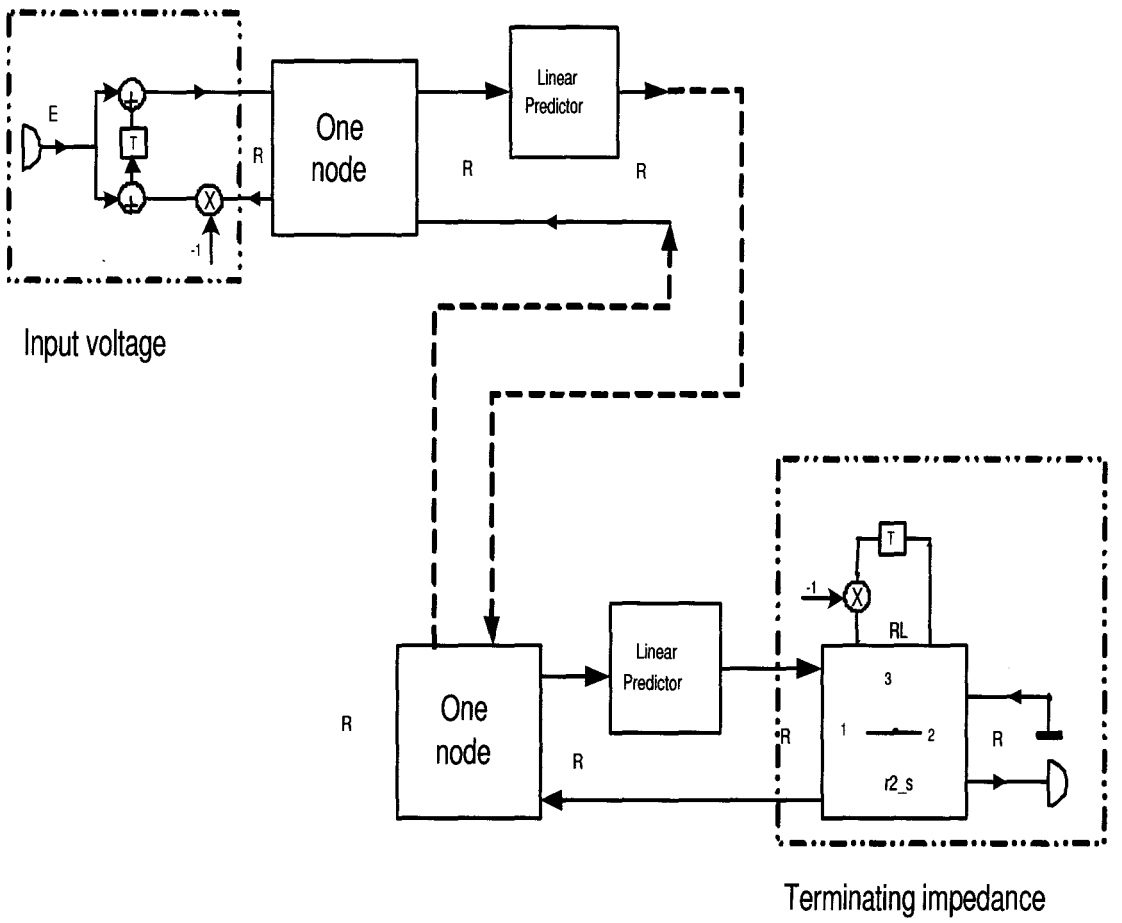

Figure 3.9: New WD implementation structure of a Toda lattice without DFDLs

Because $R_c > 0$ and $T_s > 0$, $\mu > 0$. Thus, this condition guarantees that an explicit function exists to describe the wave quantities of the nonlinear capacitor as discussed in 3.3.2.

3.4 Conclusions

In this chapter, the time-frequency properties of a single Toda soliton signal were analyzed from the measure of energy with regard to the signal model applied in signal processing. Then an example of a digital soliton communication model is provided. In digital soliton communication systems, the digital modulator-demodulator or digital multiplexer-demultiplexer part should have the same function as an analog Toda lattice. Therefore, an equivalent digital model of Toda lattice circuit is required. By means of the wave digital principles that is introduced in Chapter 2, a new wave digital structure of Toda lattice circuit with finite length is proposed for practical applications. This digital soliton system model can be used not only in digital communication systems but also in general research on soliton systems. In the next chapter, simulation results based on the digital model that is presented in this chapter will be provided for comparison with the analog Toda lattice circuit and corresponding parameterdesign will be discussed.

Chapter 4

Simulation and Application of the Digital Soliton System Simulator

In Chapter 3, a digital model of a Toda lattice circuit is proposed with design by wave digital principles. Existing soliton-supporting systems are all analog systems. Therefore, applications of solitons and soliton systems can be accomplished only in analog environments. Since such systems are sensitive to noise and physical effects, digital soliton systems have more advantages than their analog counterparts. This digital model is a digital soliton system simulator, which has potential use in extensive applications of soliton systems.

This chapter presents the numerical results and comparison of the digital model to the analog Toda soliton system. The assumptions and the simulation environment are specified. The parameter selection of the model is discussed with reference to performance. Simulation results are then given to verify that the performance of the digital Toda lattice model is nearly equivalent to the analog Toda lattice circuit. Finally, an example of a soliton communication system is proposed to demonstrate that the digital Toda lattice model can be used to substitute for an

analog Toda lattice circuit in a digital soliton communication system.

4.1 Simulation Environment and Assumptions

4.1.1 Simulation Environment

Digital signal processing (DSP) systems can be described by signal flow diagrams. In Chapter 3, the design procedure for a digital soliton system simulator was presented, and a signal flow diagram was given to describe this digital model visually. The digital soliton system simulator can be built by various tools. In this thesis, Simulink, which runs within Matlab is utilized [57]. Simulink is a block-diagram-based tool for modelling, simulating and analyzing multi-domain dynamic systems, and it is tightly coupled with Matlab and supported by blocksets and extensions. Therefore, it allows designers to model a system with high-level language, which facilitates the modelling. The digital models built in Simulink can be translated to C code by the Target Language Compiler (TLC) in the real-time workshop of Simulink to accelerate the simulation speed. And the code can be downloaded and implemented in digital signal processors (DSPs) to execute real-time simulations. Moreover, some work in the area of hardware synthesis from Simulink models has already been done [52, 53]. By using these tools, a digital model built in Simulink can be translated to Hardware Description Language (HDL), as a structural specification in order to generate a hardware implementation in field-programmable gate arrays (FPGAs). Consequently, the simulation is executed faster in FPGA than in Simulink software.

Our digital soliton system simulator is built up in Simulink version 6.3, Matlab 7.1.0.246. The detailed block diagrams of our model in Simulink is specified in the Appendix.

4.1.2 Assumptions

To measure the performance,the minimum mean square error (MMSE) is employed in this chapter. The minimum of the average of the sum of these errors can be obtained by shifting one vector relative to the other. The relative MMSE between x and y of the same length K is calculated as

$$MMSE(x,y) = min_{i\in[0,K-1]}\left\{\frac{\frac{1}{K}\sum_{k=1}^{K}(x[k]-y[k+i])^2}{\frac{1}{K}\sum_{k=1}^{K}(x[k])^2}\right\} \quad , \tag{4.1}$$

where when $k+i > K, y[k+i] = 0$, i.e. zero padding is applied. This MMSE will be used to measure the errors between the output signals of the digital Toda lattice and the theoretical outputs. According to (2.24), when a soliton

$$V(t) = V_0 \cdot \beta^2 \text{sech}^2\left(\beta\frac{t}{\sqrt{LC_0}} - \eta^0\right)$$

is input to the Toda lattice, the theoretical output signal at the mth node should be

$$V_m(t) = V_0 \cdot \beta^2 \text{sech}^2\left(\beta\frac{t}{\sqrt{LC_0}} - \text{asinh}(\beta)\text{m} - \eta^0\right) \quad .$$

Therefore, theoretically the output at the mth node is still a soliton with the delay in time

$$\Delta_m = \frac{\text{asinh}(\beta)}{\beta}m \tag{4.2}$$

with respect to the input soliton.

Referring to Section 3.3.5, the parameters L, V_0, C_0 are decided by the elements in the analog Toda lattice circuit. For all the related simulations in this thesis, the normalized lattice is selected. These parameters are set as $L = 1, V_0 = 1, C_0 = 1$. Different values may be chosen for the different applications of the Toda lattice.

Except for these three parameters, sample rate T_s, linear predictor order L_{lpc} and the total number of nodes in the Toda lattice circuit N are free parameters. All the other coefficients that are specified in Section 3.3.5 are dependent on these six parameters. The selection of these parameters will be discussed in the next section.

4.2 Parameter Design

Following the signal flow diagram presented in Chapter 3, a model of our digital soliton system simulator can be established. Before exploiting this model for simulation, some important parameters must be selected. This section discusses the parameter design problem.

4.2.1 Sampling Rate

For the implementation of a digital system, the sampling rate is among the most important specifications. From Nyquist's theorem, the sampling interval to sampling a continuous bandlimited signal to make a discrete signal depends on the bandwidth of this signal. In the digital soliton system simulator, the transmitted signals may be a combination of single solitons and composite solitons. From the time-frequency analysis of Toda solitons in Section 3.2.1, Toda solitons are unlimited in frequency and time, but since Toda solitons are of finite energy, they are limited in finite bandwidth and duration at some level ε. For the single soliton described in (3.3), the 99% energy bandwidth is $W = 0.3937\beta$ with respect to $\varepsilon = 1\%$ as calculated in Section 3.2.1. Thus, the sampling interval must satisfy $T_s < \frac{1}{0.7874\beta}$ considering the 99% energy bandwidth. In soliton systems, to provide reasonable transmission energy and bandwidth, generally the solitons with $\beta < 10$

are employed, in reference to the literature [2, 3, 4, 5]. Therefore, a sampling rate of $T_s < 0.1270$ is required for single soliton. For a composite soliton, the bandwidth is dependent on the different solitons that are overlapping and the relative phase between them, and an analytical solution is difficult to derive. Nevertheless, from numerical studies, the bandwidth of composite soliton has the same order of magnitude as a single soliton. Of course if specific solitons are assumed to propagate in the simulator, the sampling rate can be adjusted to the corresponding value of β. The smaller sampling interval provides better performance. However, the smaller T_s requires higher-speed operations. Design of a high-speed digital signal processing system requires less complexity than a high-speed analog system. According to the above, $T_s = 10^{-2}$ is chosen as the sampling interval in the general simulations to fit a large range of solitons in the digital soliton system simulator.

4.2.2 Lattice Length

As discussed previously, the ideal Toda lattice has an infinite number of nodes. A finite model is used to substitute for the ideal case in simulation. However the longer the circuit, the smaller the reflected signal from the terminal, but the more complex implementation. The MMSEs between input single soliton and the propagated signals at different nodes with different-length lattice is illustrated in Figure 4.1, where $T_s = 10^{-2}, L_{lpc} = 32$ and the parameter of input soliton is specified as $\beta = 1$. As shown in this figure, the performance at a given output node is improved with the addition of more nodes to the lattice. But when the number of nodes in the circuit increases to a certain number, the performance will be maintained to the same level even with more nodes added to the circuit. If the signal is outputted at the tenth node, lattices with more than thirty nodes provide the same performance, in terms of MMSE. In the same way, if the signal

is outputted at the thirtieth node, at least forty-node lattice is needed.

The time shifts between the input soliton and the output signals at every node with different-length lattice are shown in Figure 4.2. From (4.2), the theoretical time shifts at the mth node is

$$\Delta_m^s = 0.8814m \tag{4.3}$$

according to the parameters of the simulation. As illustrated in Figure 4.2, the numerical results closely approach the theoretical result, except for the last nodes due to the reflective signals from the terminating impedance.

According to the discussion above, how to choose the lattice length relates to the output node. And then where to output the signal at Toda lattice depends on the design of different systems.

4.2.3 Linear Predictor Order

In the digital soliton system simulator, linear predictors are used to cut delay-free directed loops to guarantee the realizability as discussed in Section 3.3.5.2. Qualitatively, a larger order predictor could provide a better performance to approximate the current output based on larger number of previous inputs. A larger order requires more memory, and a reasonable complexity versus performance balance should be achieved. The simulation parameters are as follows: $N = 50, T_s = 10^{-2}$ and $\beta = 1$. Here linear predictors in the model have different prediction orders at every experiment. The order $L_{lpc} = 32, 64, 128, 256$ are selected respectively. Figure 4.3 presents the performance curves of MMSEs between input single soliton and the propagated signal at each node. Notice that higher predictor order gives better MMSE performance for node number less than 35. Nodes further into the lattice are computed due to end reflections. Figure 4.4 illustrates the time shifts

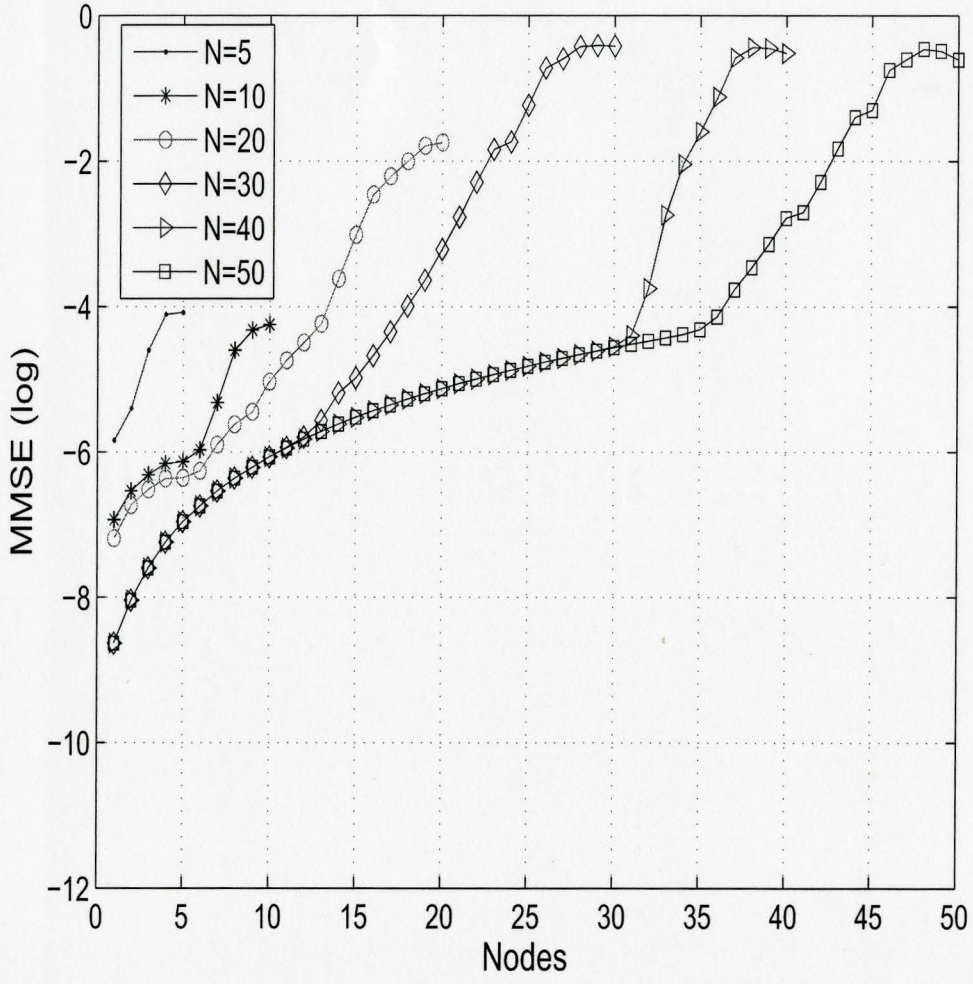

Figure 4.1: MMSEs at different node with different lattice length ($T_s = 10^{-2}, L_{lpc} = 32, \beta = 1$)

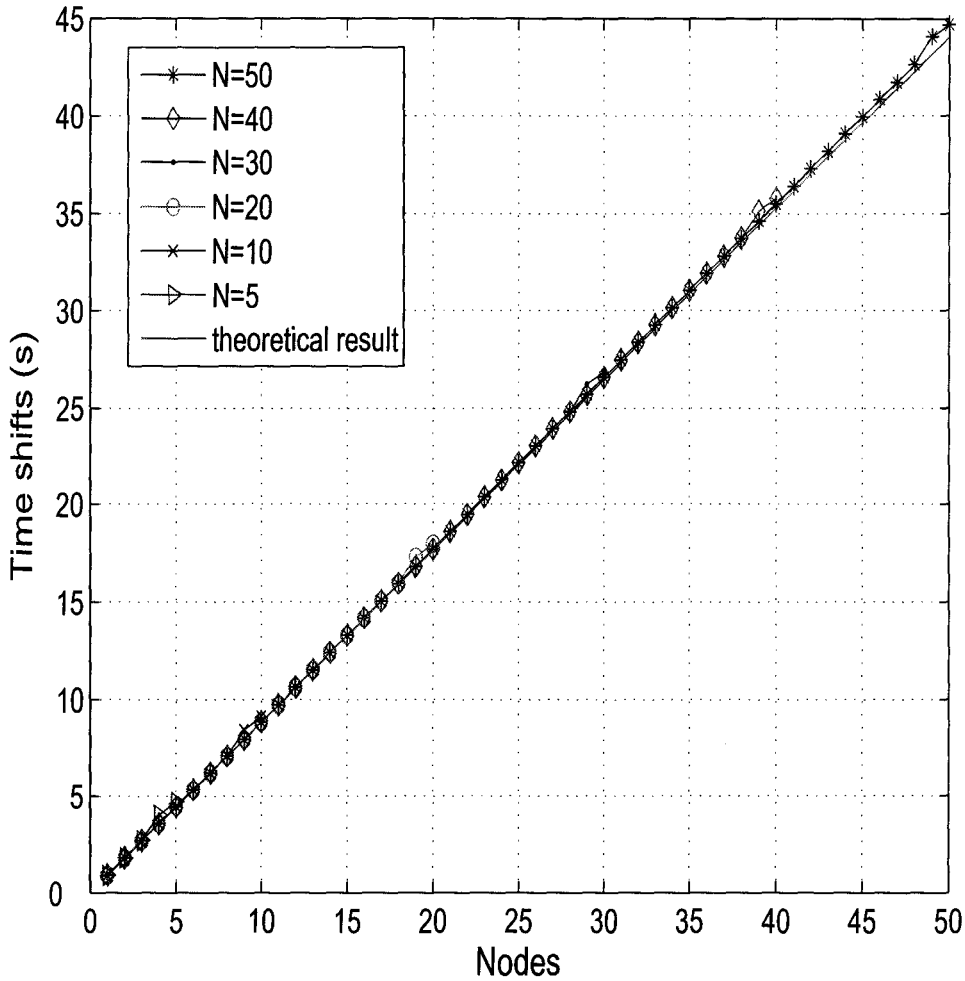

Figure 4.2: Time shifts at different node with different lattice length ($T_s = 10^{-2}, L_{lpc} = 32, \beta = 1$)

at every node with different order linear predictors. As shown in this figure, the numerical results with different order linear predictors are close to the theoretical result, which is described in (4.3), except for the last nodes due to the reflective signals from the terminal.

Different digital soliton systems have different performance requirements. Figure 4.3 is an important reference for deciding the linear predictor orders in different systems' simulation.

4.2.4 Computational Complexity Analysis

In this subsection, the computational and memory complexities per sample time are analyzed.

The L_{lpc}-th order linear predictor here applies Levinson-Durbin Algorithm [35] to compute the autocorrelation estimation equations, which requires $O(L_{lpc}^2)$ operations to get the L_{lpc} coefficients $a_i, \quad i = 2, \cdots L_{lpc} + 1$. The algorithm requires L multipliers for calculating the estimate of the next value

$$\widehat{s}_{L_{lpc}+1} = -\left(a_2 s_{L_{lpc}}\right) + -\left(a_3 s_{L_{lpc}-1}\right) + \cdots + \left(a_{L_{lpc}+1} s_1\right)$$

So a L_{lpc}th-order linear predictor requires $O(L_{lpc}^2)$ multiplication operations.

Moreover, the number of operations is proportional to the lattice length N. Therefore, the whole computational complexity of the digital Toda lattice is bounded by

$$C\left(N, L_{lpc}\right) = O\left(N L_{lpc}^2\right) \quad . \tag{4.4}$$

Notice that although L_{lpc} gives most benefit to performance, also increase the complexity greatly.

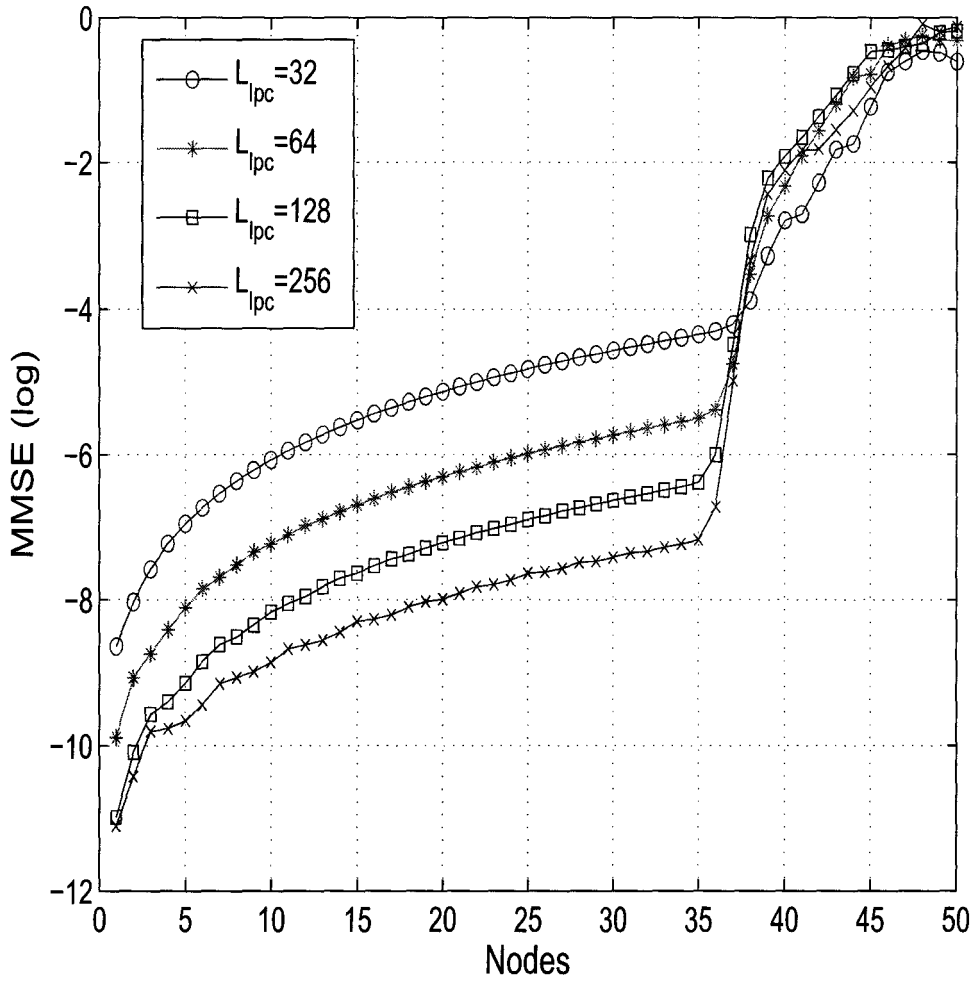

Figure 4.3: MMSEs at different node with different order linear predictor ($T_s = 10^{-2}, N = 50, \beta = 1$)

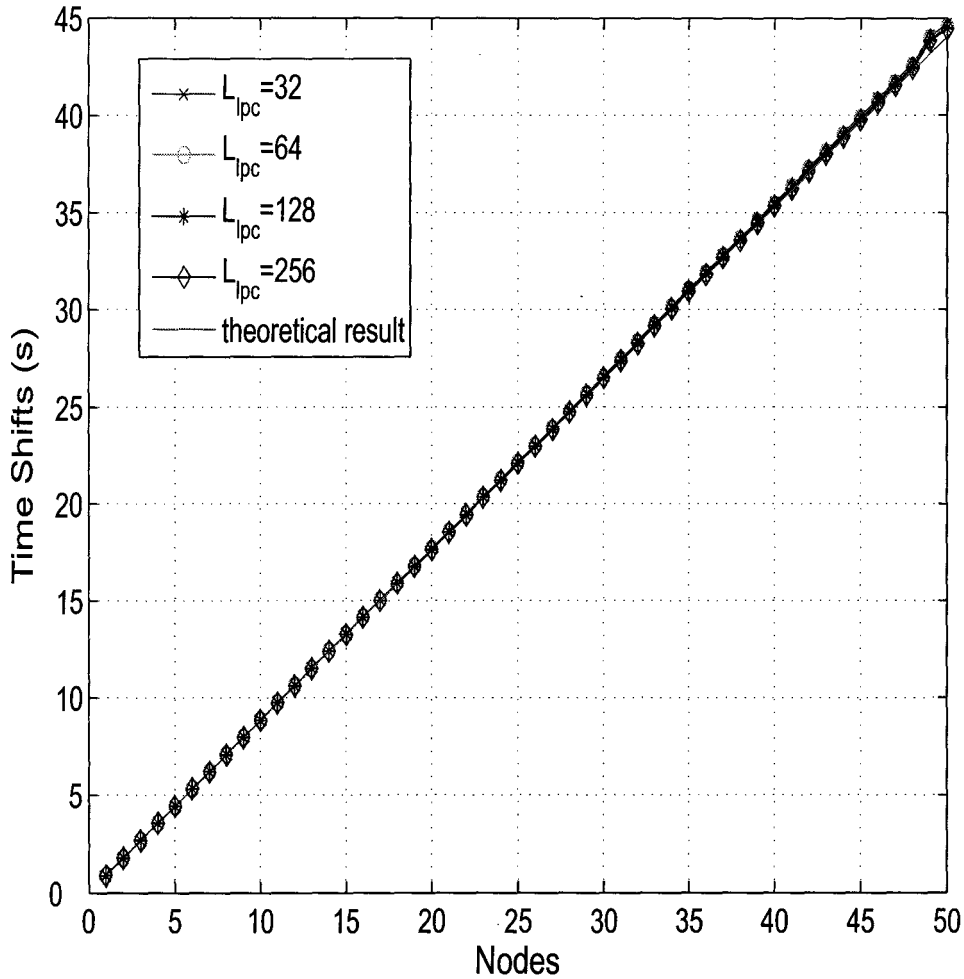

Figure 4.4: Time Shifts at different node with different order linear predictor ($T_s = 10^{-2}, N = 50, \beta = 1$)

A L_{lpc}th-order linear predictor requires L_{lpc} memories to store the previous inputs. At every node, two memory elements are included: a linear inductor and a nonlinear capacitor. In reference to Section 3.3.5, two memories are required to represent a node. Therefore, a N-node digital Toda lattice model with L_{lpc}th-order linear predictors requires

$$M\left(N, L_{lpc}\right) = N(L_{lpc} + 2) \tag{4.5}$$

memories.

When an example of soliton communication system is introduced in Section 4.4 to demonstrate this digital model, this form of complexities (4.4) and (4.5) will be employed to analyze the computational and momery complexities of the digital soliton communication system.

4.3 Verification of Soliton Properties

Based on the discussion of parameter design and the introduction to the simulation environment, a wave digital model of the Toda lattice was used to simulate a digital soliton system in Simulink. The underlying question is whether this model works for simulating the analog Toda lattice's properties. The following simulations are performed in Simulink, where the parameters are set as : the sampling rate $T_s = 10^{-2}$, linear predictor order $L = 256$, lattice length $N = 50$.

Considering the properties of soliton-supporting systems exemplified by the Toda lattice in Section 2.3.1, three significant characteristics should be checked to demonstrate that the digital model can function as a digital soliton system, namely (i) an input pulse dissolves into many solitons, each travels at its own velocity, (ii) a soliton of higher amplitude travels faster than one of lower amplitude, (iii) solitons

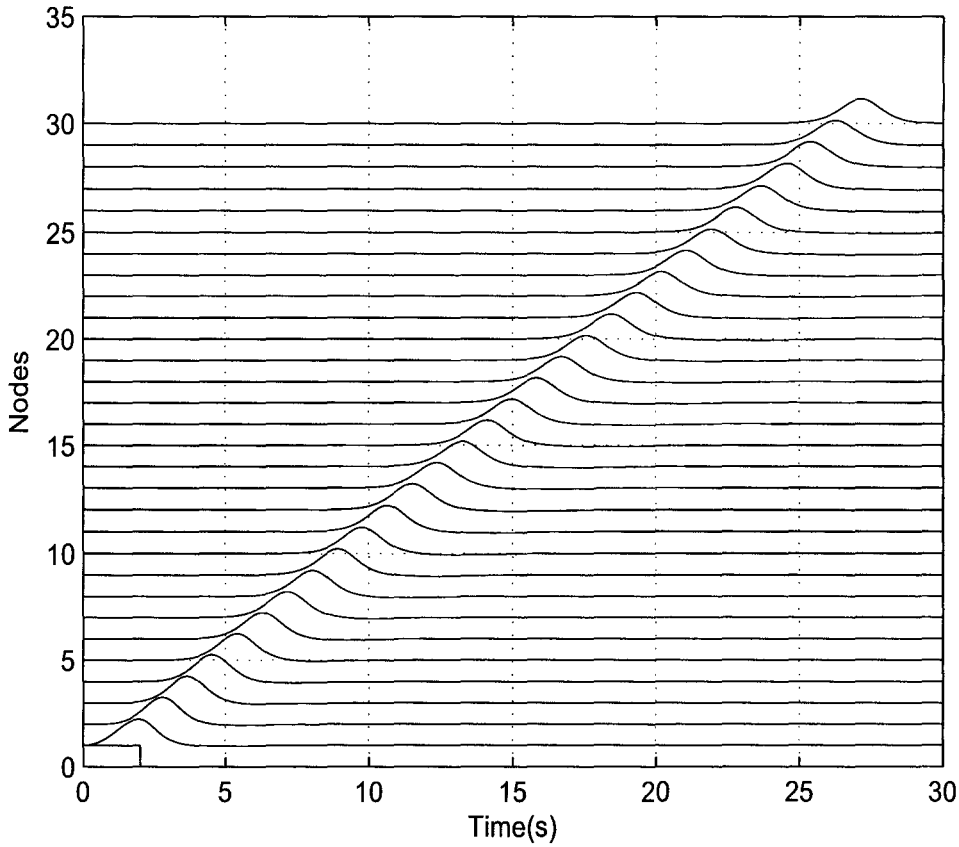

Figure 4.5: The propagation of input pulse in the digital Toda lattice (Amplitude=1 V, Duration=2 s $T_s = 10^{-2}, N = 50, L_{lpc} = 256$)

can pass through one another without changing their shapes and velocities, (iv) during overlap, their joint amplitude decreases [1].

Firstly, an input pulse signal will dissolve into solitons propagating along the soliton-supporting system. This property is illustrated in Figures 4.5, 4.6 and 4.7. As shown in Figures 4.5 and 4.6, rectangular pulses with different amplitudes and the same duration will dissolve into different solitons. Higher-amplitude pulses propagate as a soliton with higher amplitude, faster velocity, which indicates that

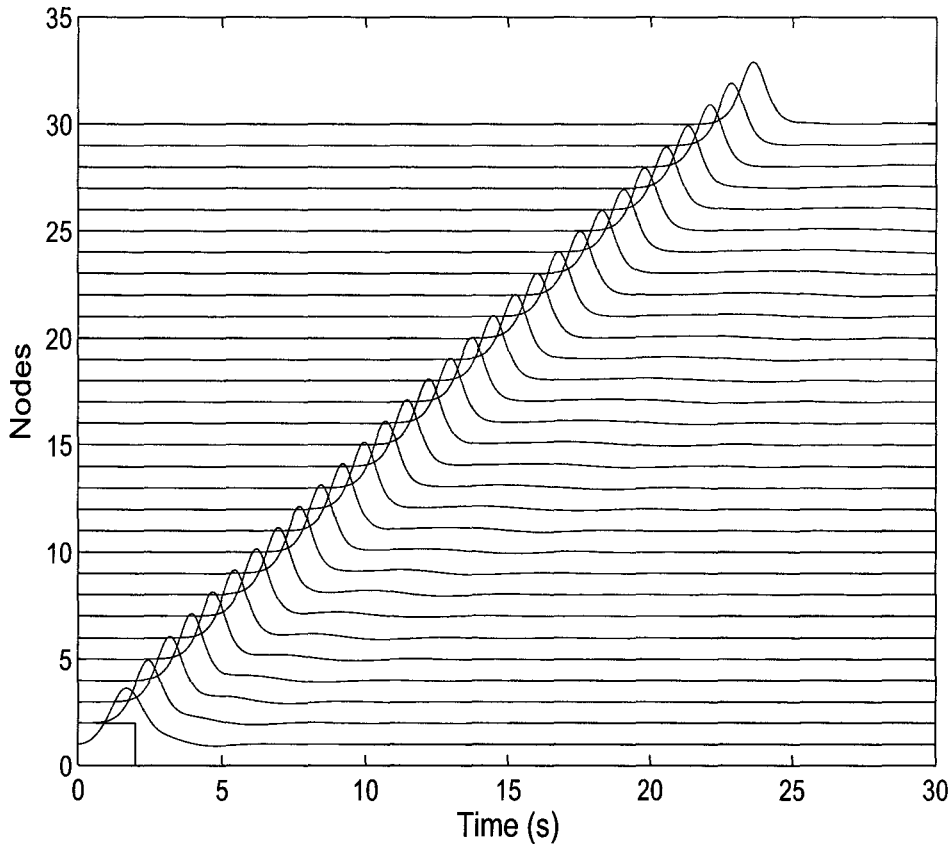

Figure 4.6: The propagation of input pulse in the digital Toda lattice (Amplitude=2 V, Duration=2 s $T_s = 10^{-2}, N = 50, L_{lpc} = 256$)

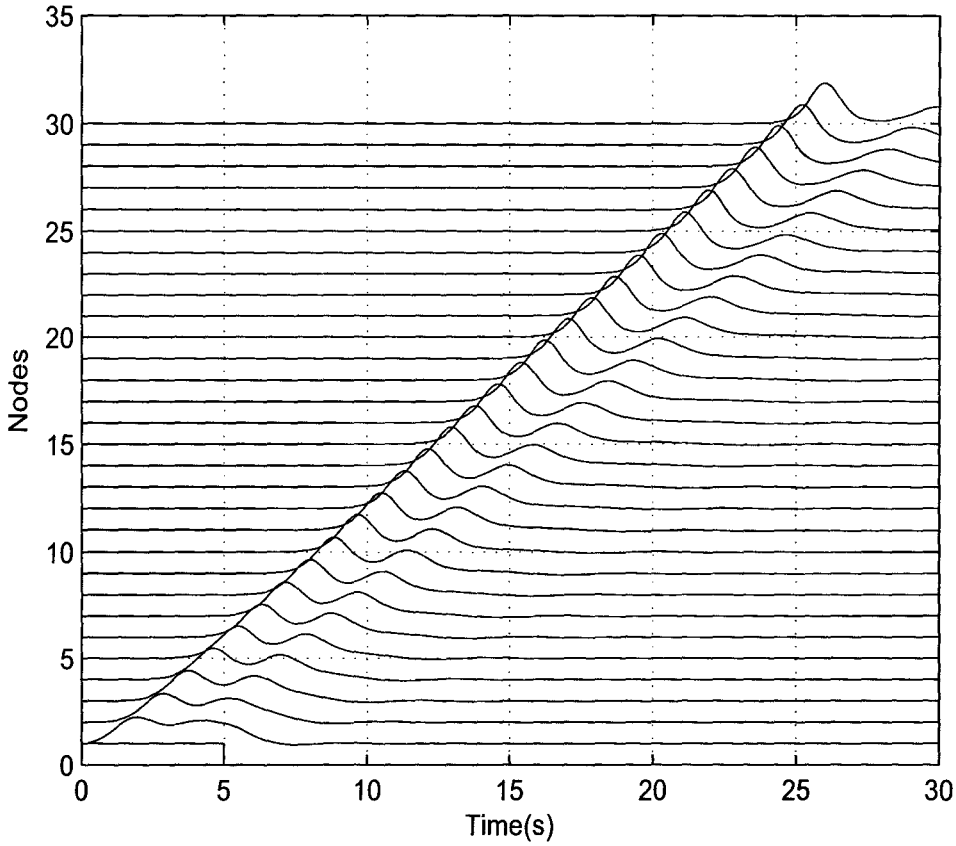

Figure 4.7: The propagation of input pulse in the digital Toda lattice (Amplitude=1 V, Duration=5 s $T_s = 10^{-2}, N = 50, L_{lpc} = 256$)

the parameter β of this soliton is larger. Similarly, the lower-amplitude pulse propagates as a soliton with smaller β. In Figure 4.7, the rectangular pulse with 2 volts amplitude and 5-seconds duration dissolves into two solitons. Comparing with Figure 4.6, two pulses with the same amplitude and different duration will dissolve in solitons of different numbers. In general, longer duration pulses dissolve into more solitons than shorter duration pulses.

The second important property of a Toda lattice circuit is that a Toda soliton can travel with invariant velocity and stable shape and a soliton of higher amplitude travels faster than one of lower amplitude. Such stability can be shown in Figures 4.8 and 4.9. An input Toda soliton propagates in this digital Toda lattice model with stable shape and invariant velocity. A soliton of higher amplitude in Figure 4.9 travels faster than one of lower amplitude in Figure 4.8.

The third property is that solitons can pass through one another without changing their shapes and velocities. The forth property requires that during the overlapping of two solitons, the joint amplitude of the signal decreases. These characteristics are illustrated in Figure 4.10.

A key property for communication systems are the noise dynamics of soliton systems. In [2], noise dynamics are analyzed in detail using inverse scattering theory. The Toda lattice can be viewed as low pass filters at each node for Gaussian noise. Figure 4.11 and Figure 4.12 show the stability of solitons in the presence of additive noise when propagating in this digital Toda lattice model.

These simulation results verify some important properties of the digital model and show it to be a good model of a Toda lattice. Thus, this model can function as a digital soliton system simulator successfully, avoiding the inherent problems of analog implementations.

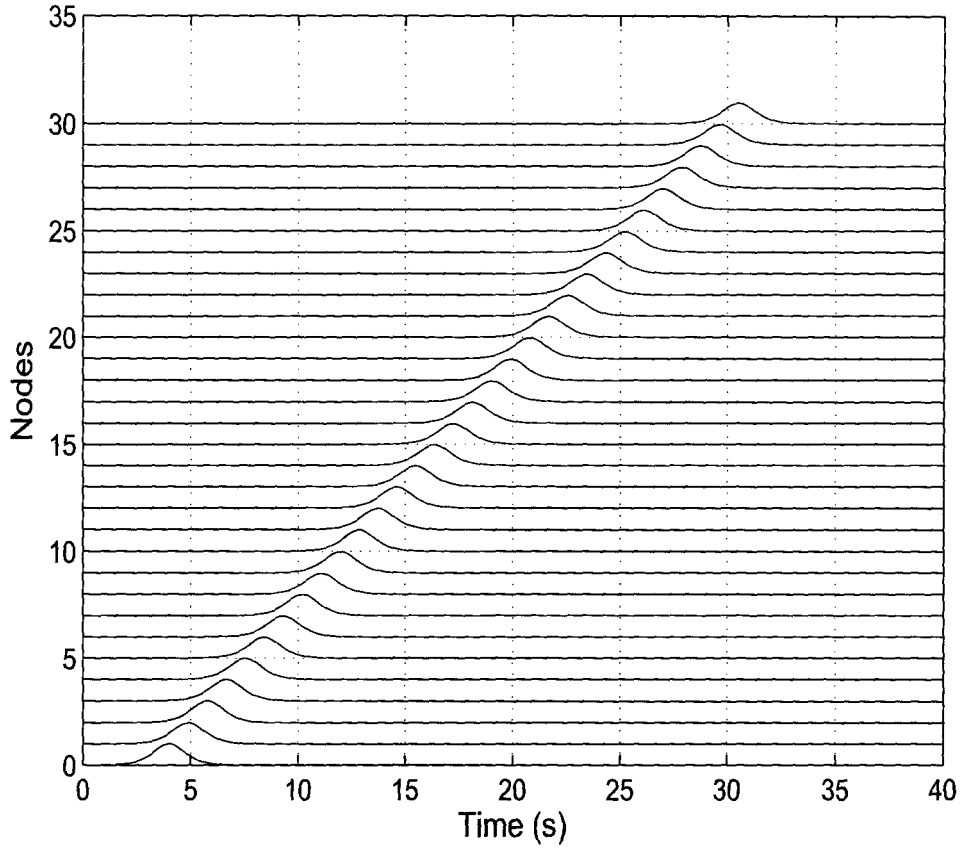

Figure 4.8: The propagation of single soltion in the digital Toda lattice ($\beta = 1, T_s = 10^{-2}, N = 50, L_{lpc} = 256$)

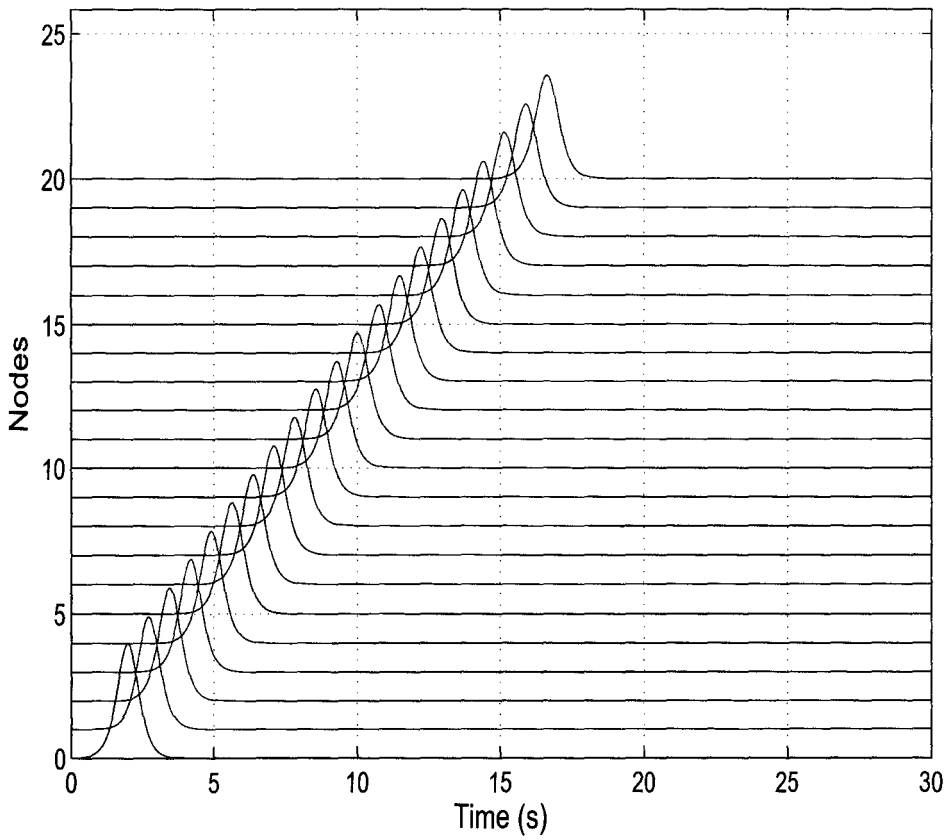

Figure 4.9: The propagation of single soltion in the digital Toda lattice ($\beta = 2, T_s = 10^{-2}, N = 50, L_{lpc} = 256$)

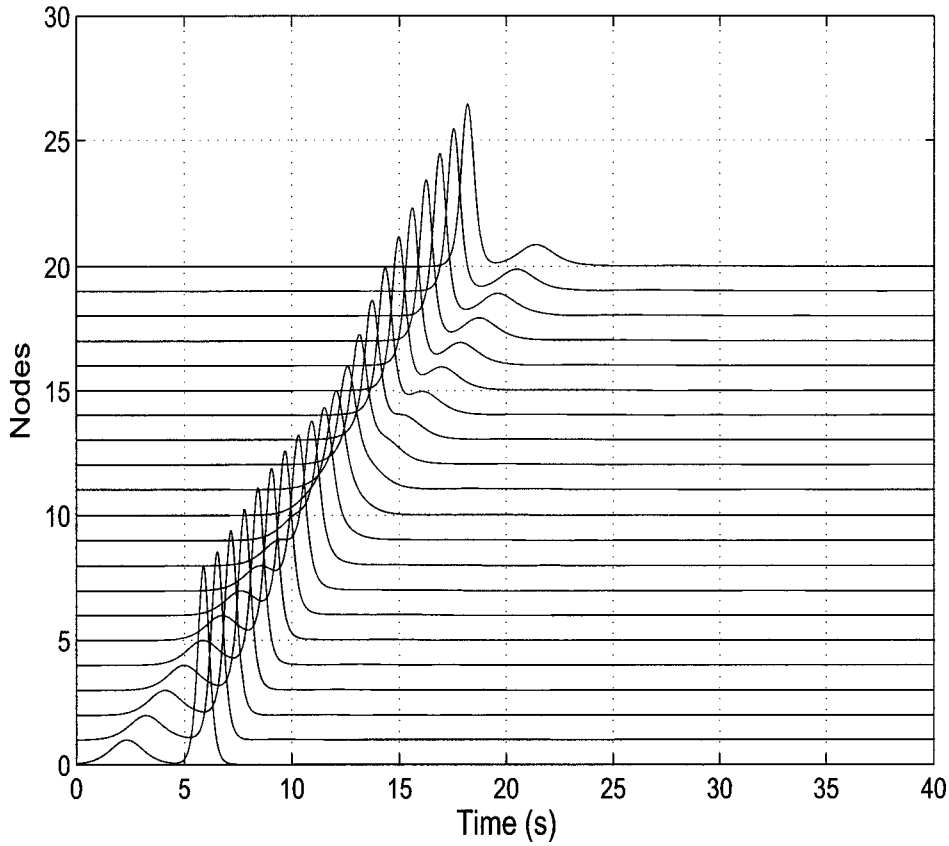

Figure 4.10: The propagation of two soltions in the digital Toda lattice ($\beta_1^2 = 1, \beta_2^2 = 8, T_s = 10^{-2}, N = 50, L_{lpc} = 256$)

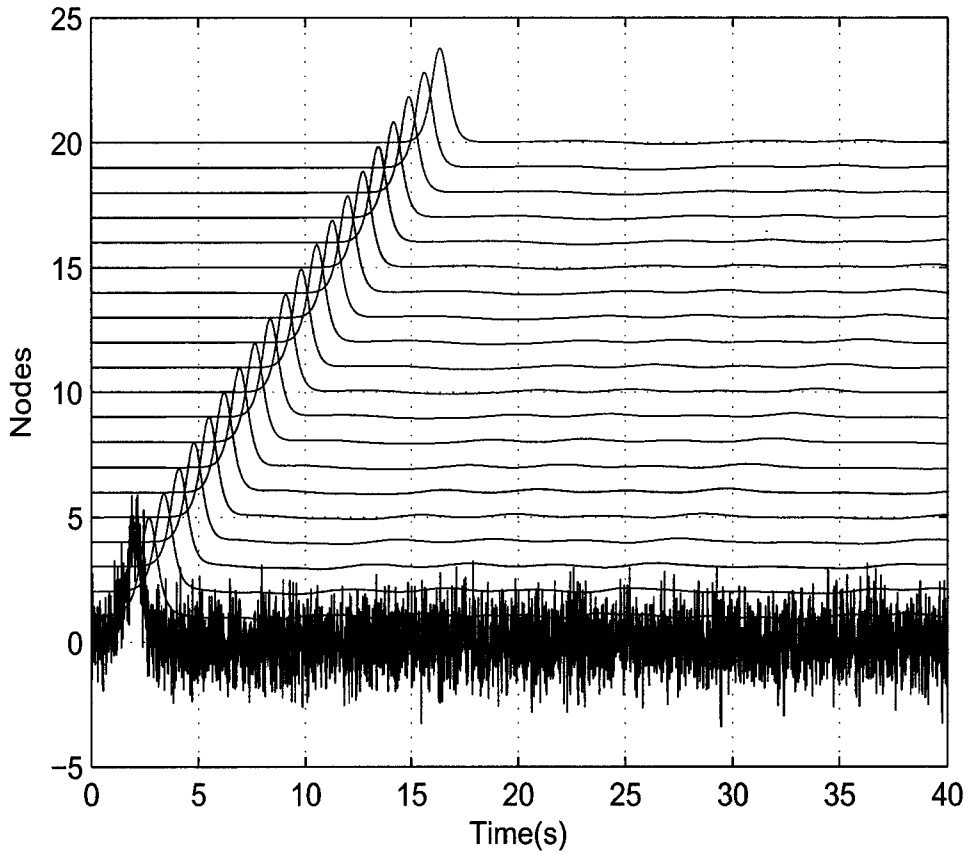

Figure 4.11: Noise dynamics in the digital Toda lattice with One soliton + additive Gaussian noise ($\mu = 0, \sigma^2 = 1$) input ($\beta = 2, T_s = 10^{-2}, N = 50, L_{lpc} = 256$)

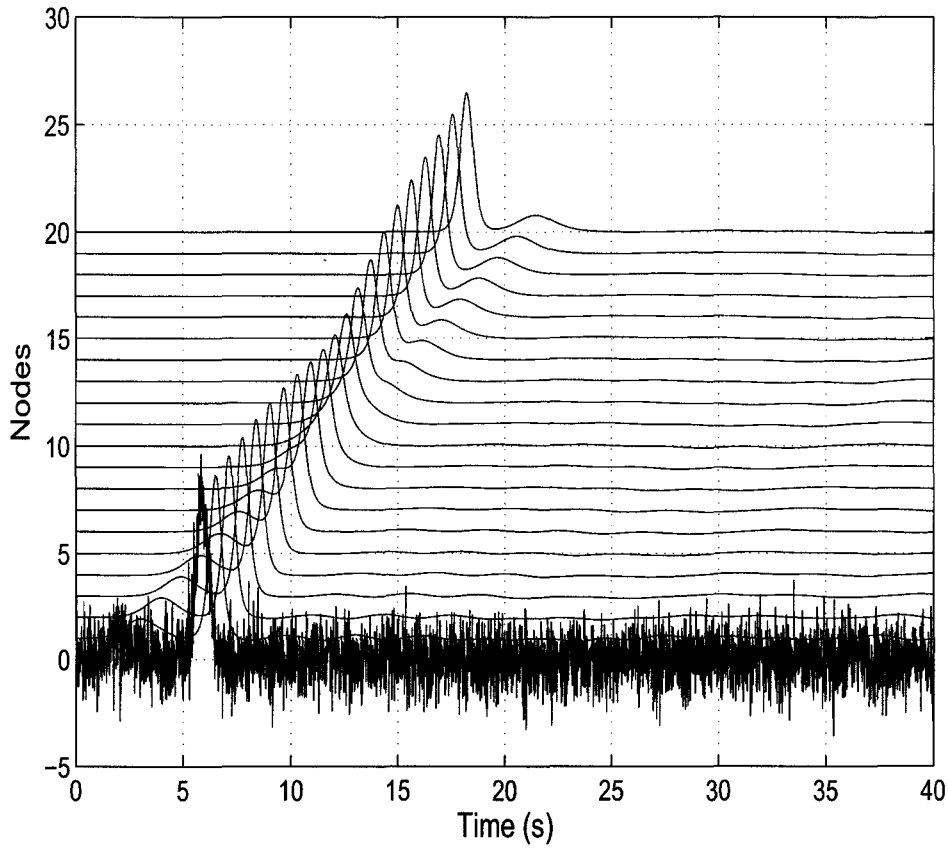

Figure 4.12: Noise dynamics in the digital Toda lattice with two solitons + additive Gaussian noise ($\mu = 0, \sigma^2 = 1$) input ($\beta_1^2 = 1, \beta_2^2 = 8, T_s = 10^{-2}, N = 50, L_{lpc} = 256$)

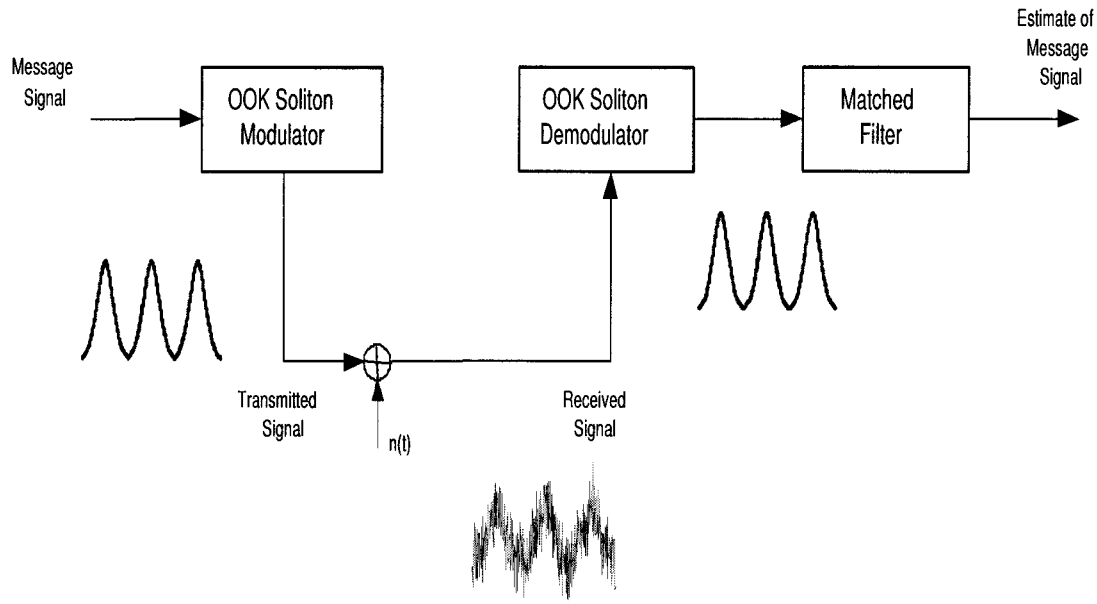

Figure 4.13: OOK soliton communication system

4.4 an Example of a Soliton Communication System

According to the discussion in the previous section, the digital soliton system simulator has been demonstrated to have good agreement with an analog Toda lattice circuit. In this section, an example of a soliton communication system, described in Section 3.2.2, is provided to compare the digital model with analog Toda lattice. Consider the soliton communication system in Figure 4.13, on-off keying (OOK) modulation is employed, and a soliton with $\beta = 2$ is used as carrier signal. The digital model established in Simulink acts as the digital modulator and demodulator. For comparison, an analog modulator and demodulator are simulated using the ordinary differential equation (ODE) functions in Matlab to solve (2.23) to represent analog Toda lattice.

Figure 4.14 presents bit error rate (BER) versus signal-to-noise ratio (SNR). The performance curve of OOK system with analog modulator and demodulator is computed using the technique in [19]. Here

$$SNR = 10\log\left(\frac{E_a}{\sigma^2}\right) \quad db \quad ,$$

where σ^2 is the power of AWGN, E_a is the average transmission energy of OOK communication system,

$$E_a = \frac{1}{2}\int_0^T s^2(t)dt \quad ,$$

where T is 99% energy duration of soliton carrier $s(t)$. The AWGN is modelled as i.i.d. Gaussian random sequence in Matlab, i.e. the sampled noise. Thus the effective white noise power for modelling in Matlab σ_m^2 should be

$$\sigma_m^2 = \sigma^2 T_s \quad ,$$

where T_s is the sampling time and σ^2 is the noise in analog domain.

According to Section 4.2, the parameters of the simulation are as follows: $L = 1, V_0 = 1, C_0 = 1$, $T_s = 10^{-2}$, $L_{lpc} = 256$, $N = 30$. In reference to (4.4) and (4.5), the computational complexity of this model for simulation is approximated on the order of 10^6 operations per sample time and the number of memories required is on the order of 8000. However, as introduced in Section 4.1, this model can be translated to HDL, which can be implemented in FPGA, which is real-time system. Therefore the simulation time can be reduced significantly. The performance illustrated in Figure 4.14 shows that when SNR is small, the BER of the digital model approaches that of the analog model and when SNR is large than $8dB$, the performance of the digital model is a little better than that of analog model. Linear predictors are applied in the digital model to cut DFDLs. An

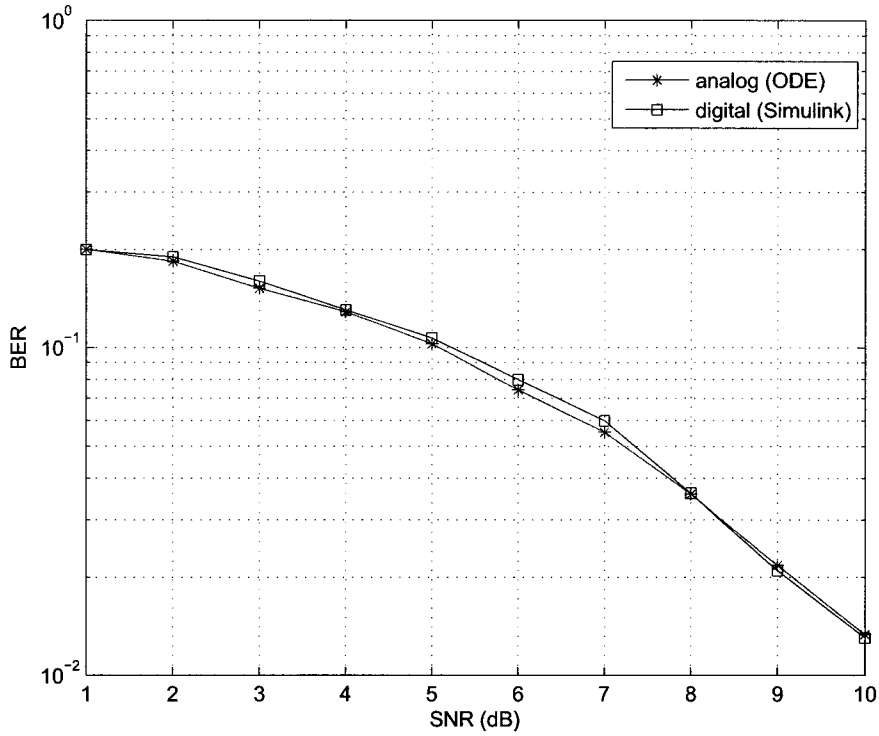

Figure 4.14: The performance comparison of analog [19] and digital OOK solition communication system

important property of the linear predictor is that it can smooth the input signal. Therefore, when SNR is larger, and the variance of the noise is smaller, the output signal from the linear predictor will be closer to the signal without noise. Figure 4.14 shows our digital model can work well as digital modulator and demodulator in a soliton communication systems.

4.5 Conclusions

In this chapter, the parameter design problem of the digital Toda lattice model is discussed and the simulation environment is specified. The models built in Simulink can be translated to HDL by additional tools, so the digital model can be implemented in a DSP, or FPGA. Therefore, significant speed improvement using hardware simulation can be achieved based on the design of a digital simulator in Simulink. The properties of the digital model are verified, and the digital model is shown to closely approximate an analog Toda lattice circuit. Finally, an example of an OOK soliton communication system is provided. The BER versus SNR curve shows when the digital model is applied in communication systems, the performance of the system approaches the one with an analog Toda lattice. In summary, the digital Toda model based on WDF principles can work as a simulator for analog soliton systems.

Chapter 5

Conclusions and Discussions

Since soliton signals have some unique properties, solitons and soliton systems have become of significant interest for a variety of applications, especially in signal processing and communications. However, all the soliton systems are physical systems, and are thus analog. Analog systems are sensitive to random disturbances and component variations, whereas digital systems are more robust. In this thesis, a digital soliton system simulator is designed by wave digital principles and implemented in Simulink [57]. This digital soliton system simulator is a specialized soliton signal generator and processer in digital domain, which can be applied in digital signal processing or digital communication systems.

5.1 Discussions on the Digital Soliton System Simulator

The design and implementation of a digital soliton system is presented in this thesis to overcome many of the difficulties inherent to analog soliton systems. The Toda lattice circuit is considered since digital circuit design methods can be applied to

approach a digital model that has nearly equivalent functions with the analog Toda lattice circuit.

The analog Toda lattice LC circuit is nonlinear. Digital implementation of analog filters can be approached in the time domain or in the frequency domain. For a linear time-invariant (LTI) system, the impulse response or transfer function can describe the system completely. Therefore, the general methods to design a digital circuit from the corresponding LTI analog prototype are usually achieved by the transformation of the impulse response from continuous time domain to discrete time domain or the transfer function from analogous complex frequency $s-$domain to discrete complex frequency $z-$domain. However, since the convolution law does not apply for nonlinear systems, there is no impulse response or transfer function to describe the nonlinear analog circuit. Thus, the usual methods for the LTI cases are not directly available to this nonlinear case. Wave digital filter (WDF) theory is a digital circuit design technique based on the topological structure of the circuit [27]. A WDF can be regarded as a digital representation of a classical network by modelling every element and interconnection. It is a physical modelling methodology based on the topology. Thus, WDF techniques are applied to design the digital model of the Toda lattice circuit in this thesis.

By means of wave digital circuit theory, a new digital representation of the Toda lattice circuit is proposed in Chapter 3. The detailed design procedure of this wave digital model is addressed. This digital model of a soliton system can be employed as a digital soliton system simulator, which has the potential to be applied in the research of soliton systems, such as in optical communications, and soliton multiplexing systems.

To verify the properties of the digital soliton system simulator, the designed model is implemented in Simulink [57]. After the simulation environment is specified, and the parameters are selected due to the various requirements, the model

can be exploited for simulation. Numerical results are given to verify some important properties of the digital model and show it to be a good digital model of an analog Toda lattice.

As an example of an application, a soliton communication system with on-off keying (OOK) modulation scheme is simulated with the digital soliton system simulator as the modulator and demodulator. For comparison, analog Toda lattice circuits are simulated using the ordinary differential equation (ODE) functions in Matlab to act as analog modulator and demodulator. The performance curve of bit error rate (BER) relative to signal-to-noise ration (SNR) shows the performance of applying the digital soliton system simulator approaches the communication system of applying the analog Toda lattice. Thus, the digital soliton system simulator can work as well in soliton communication systems, avoiding the inherent problems of analog implementations.

5.2 Future Work

In the realization of this digital soliton system simulator, wave digital filter theory is employed. An important problem of delay-free directed loops (DFDLs) is encountered in the implementation of this nonlinear ladder-type circuit which includes a nonlinear element at every node. In this thesis, linear predictors are added to cut the DFDLs. However many memories and multiplication operations are required for this method to solve DFDL problem. A promising future direction is to find a lower complexity method to cut DFDLs while maintaining the same performance level.

The motivation of this work is to realize a digital soliton system, which is more robust than its analog counterpart. Therefore, it can facilitate the applications of soliton systems to practical systems through the ability for rapid simulation.

Furthermore, this digital model built in Simulink can be translated to C code by the Target Language Compiler (TLC) in real-time workshop to accelerate the simulation speed. The code can be downloaded and executed in a digital signal processor (DSP) to execute the real-time simulations. Therefore, more work can be done to get a digital model of C code to be utilized in DSPs. In addition, more work is required to translate the Simulink models to a Hardware Description Language (HDL) for implementation on a field-programmable gate array (FPGA) [52, 53]. This will provide a further increase in rate of simulation of such systems while maintaining robustness over analog soliton systems.

Appendix A

Block Diagrams of the Digital Model in Simulink

As proposed in Chapter 4, the digital soliton system simulator is built in Simulink. The important models are illustrated here.

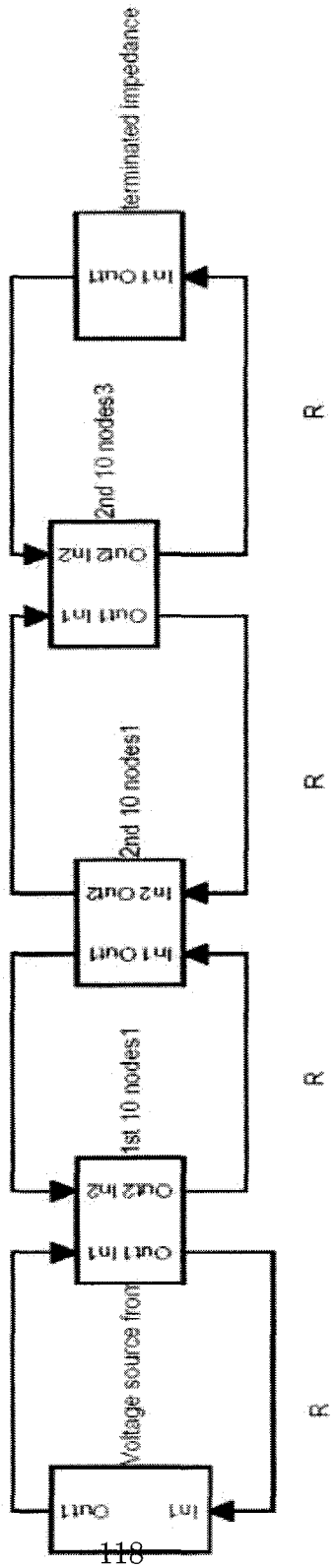

Figure A.1: The 30-node digital Toda lattice model

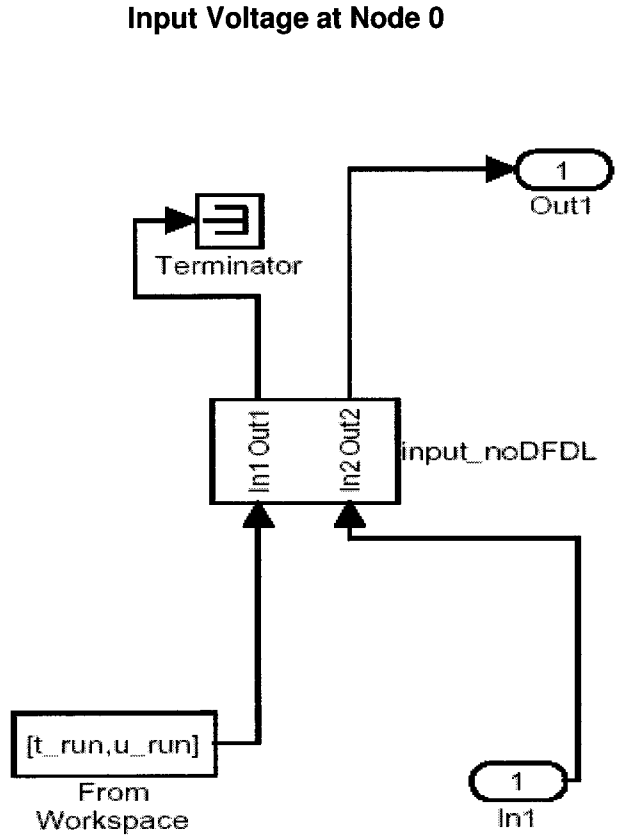

Figure A.2: The input voltage and terminating impedance block model

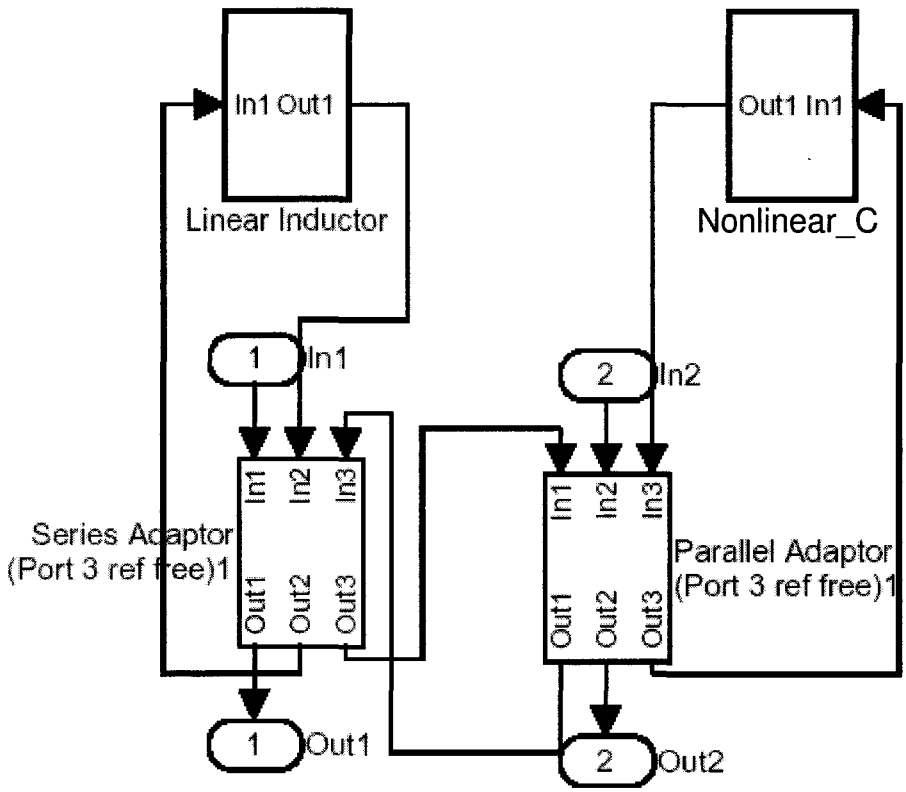

Figure A.3: The one node block model

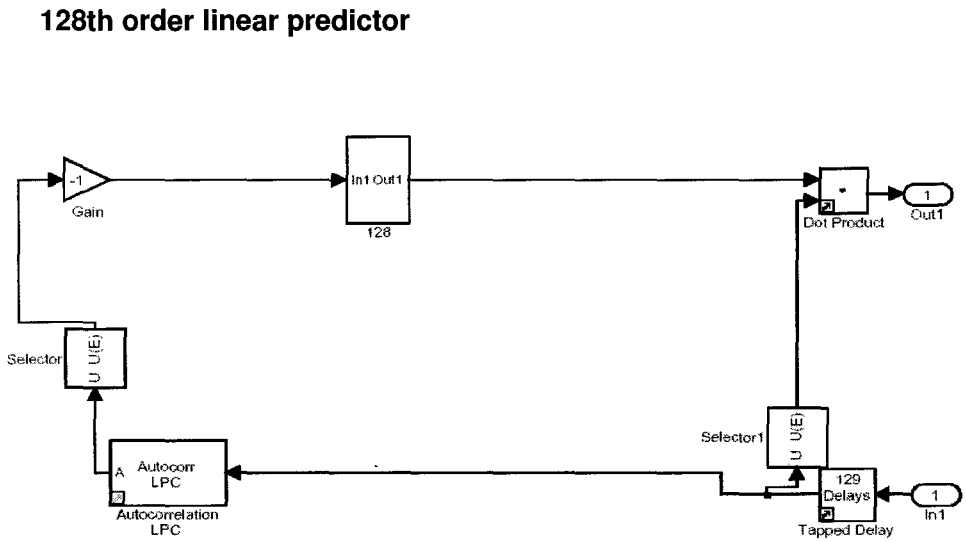

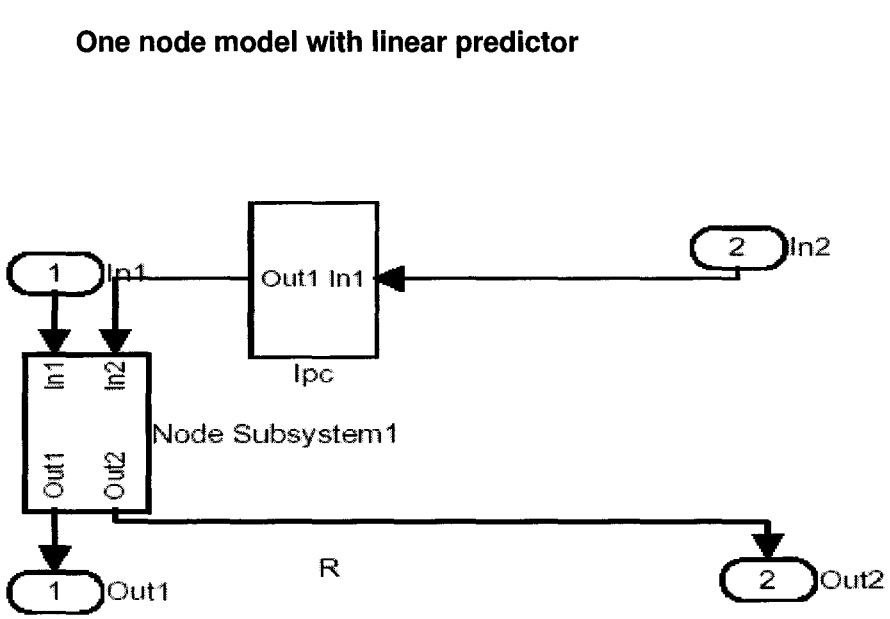

Figure A.4: The one node with linear predictor model

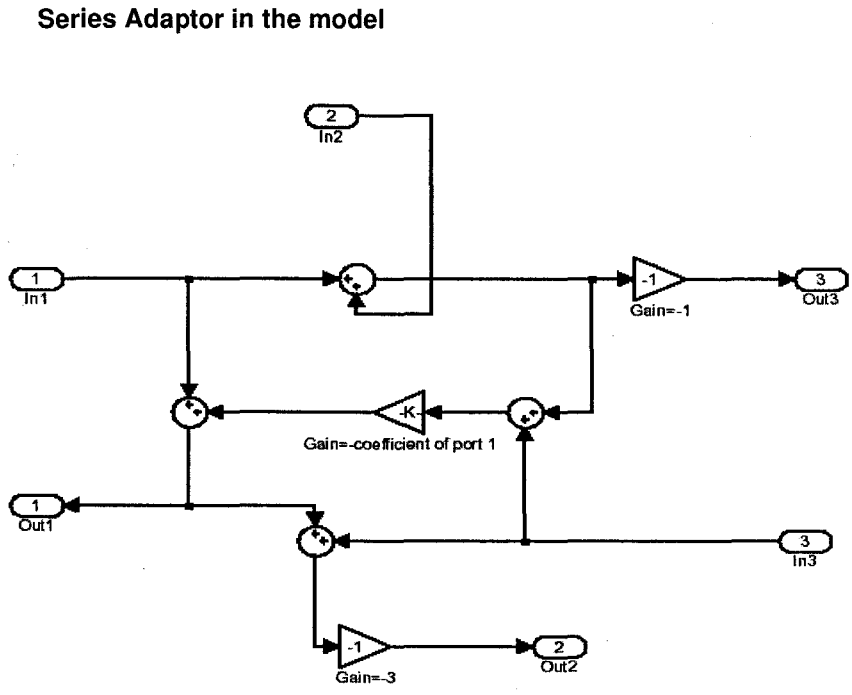

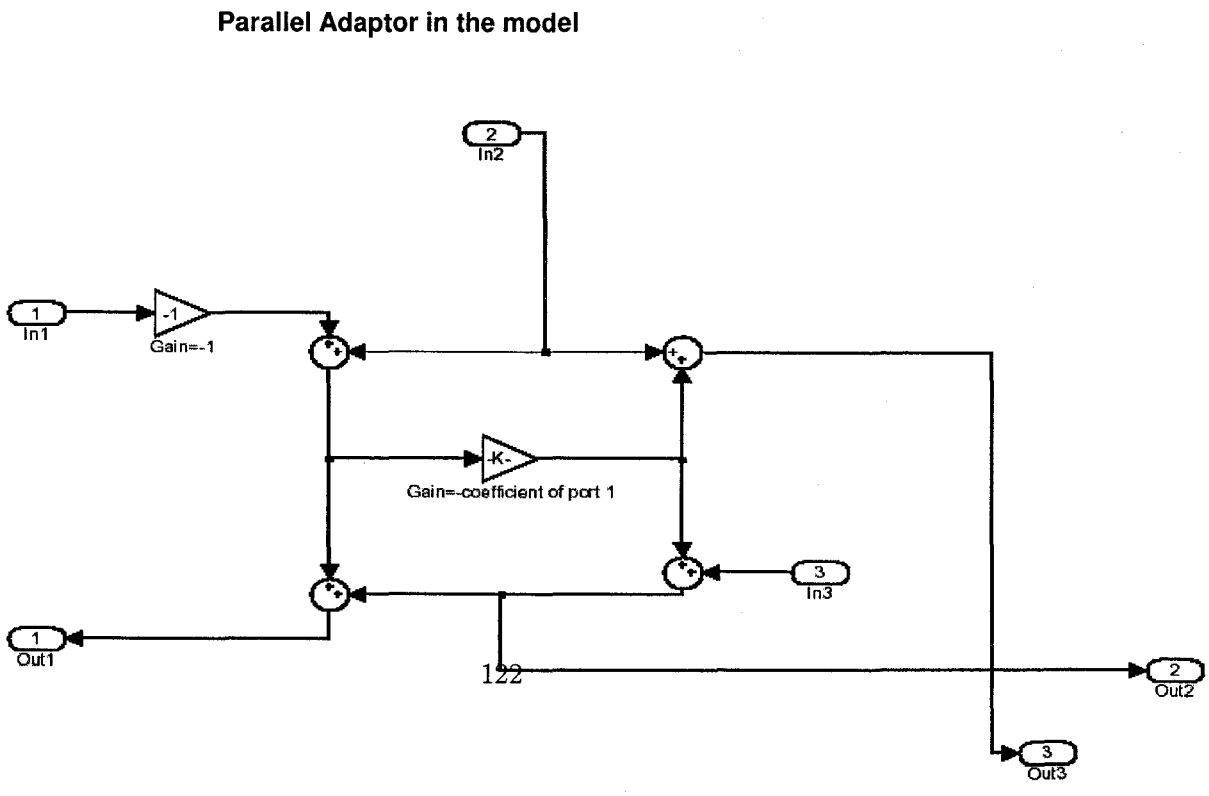

Figure A.5: The block models of series and parallel adaptors

The output voltage at n-th node

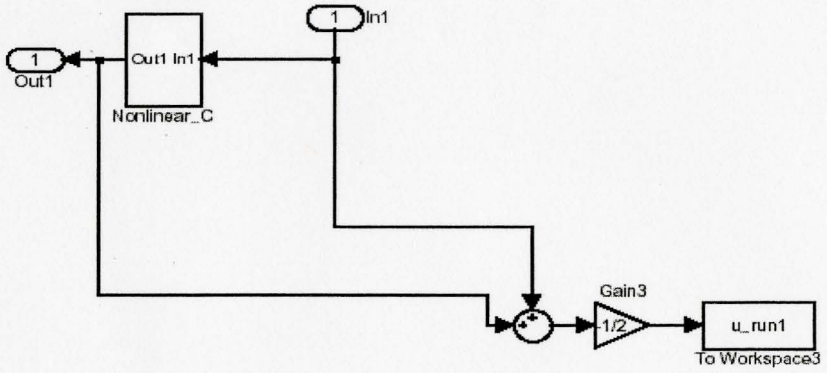

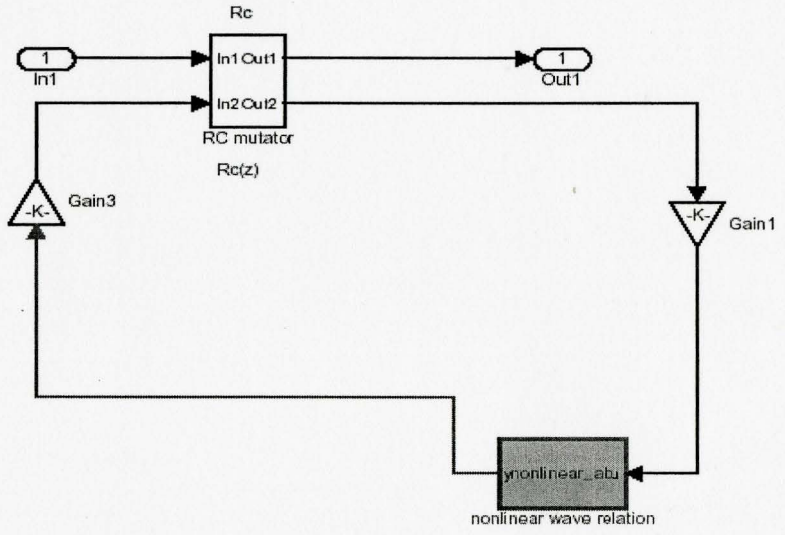

The RC mutator model

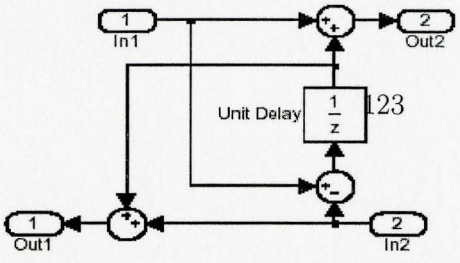

Figure A.6: The block models of nonlinear capacitor and the RC mutator

Bibliography

[1] P.G. Drazin and R.S. Johnson, *Solitons: An Introduction*, Cambridge Texts in Applied Mathematics,Cambridge University Press, New York, 1989.

[2] A.C. Singer, *Signal processing and communication with solitons* , Ph.D. dissertation, Mass. Inst. Technol., Cambridge, 1996.

[3] A.C. Singer, A.V. Oppenheim, G.W.Wornell, *Detection and estimation of multiplexed soliton signals* , IEEE Transactions on Signal Processing, Volume 47, Issue 10, Page(s): 2768-2782, Oct. 1999

[4] A.C. Singer, *Detection and estimation of soliton signals* , IEEE International Conference on Acoustics, Speech, and Signal Processing, Volume 3,Page(s): 1625 - 1628, May 1996

[5] A.C. Singer, *Signaling techniques using solitons* , International Conference on Acoustics, Speech, and Signal Processing, Volume 2, Page(s): 1336-1339, May 1995

[6] M. Toda, *Theory of Nonlinear Lattices*, No. 20 in Springer Series in Solid-State Science, New York, Springer-Verlag, 1981

[7] R. Hirota and K. Suzuki, *Theoretical and experimental studies of lattice solitons in nonlinear lumped networks*, Proceedings of the IEEE, volume 61, Page(s): 1483-1491, Oct. 1973

[8] K. Suzuki, R Hirota and K. Yoshikawa , *Amplitude modulated soliton trains and coding-decoding applications* , Int. J. Electron, volume 34, no.6, Page(s): 777-784, 1973

[9] K. Suzuki, R. Hirota and K. Yoshikawa , *The properties of phase modulated soliton trains* , Jpn. J. Appl. Phys, volume 12, no.6, Page(s): 361-365, Mar. 1973

[10] M. Nakazawa, K. Suzuki, H Kubota, E. Yamada and Y. Kimura, *Dynamic optical soliton communication* , IEEE Journal of Quantum Electronics, volume 26, Issue 12 Page(s): 2095-2102, Dec. 1990

[11] A. Hasegawa, *Soliton-based optical communications: an overview* , IEEE Journal of Selected Topics in Quantum Electronics, Volume: 6, Issue: 6, Page(s): 1161-1172, Nov/Dec 2000

[12] A.C. Scott, F.Y.F. Chu and D.W. McLaughlin, *The soliton: A new concept in applied science* , Proceedings of the IEEE, Volume 61, Issue 10, Page(s): 1443 - 1483, Oct. 1973

[13] J.S. Russell, *Report on waves* , Proc. Roy. Soc. Edinburgh, Page(s): 319-320, 1844

[14] E. Fermi, J. Pasta and S. Ulam, *Studies of nonlinear problems* , in Collected Papers of E.Fermi, Volume 2, Page(s): 977-988, 1965

[15] N.J. Zabusky and M.D. Kruskal, *Interaction of solitons in a collisionless plasma and the recurrence of initial states* , Physical Review Letters, Volume 15, Page(s): 240-243,1965

[16] M. Toda, *Nonlinear lattice and soliton theory* , IEEE Transactions on Circuits and Systems, Volume 30, Issue 8, Page(s): 542-554, Aug 1983

[17] H. Nagashima and Y. Amagishi, *Experiment on the toda lattice using nonlinear transmission lines*, Journal of the Physical Society of Japan, Volume 45, No. 2, Page(s): 680-688, Aug 1978

[18] N. Doran and K. Blow, *Solitons in optical communications* , Journal of the Quantum Electronics, Volume 19, Issue 12, Page(s): 1883-1888, Dec 1983

[19] R. Chai, *Properties and Applications of Toda Solitons*, Ph. D. Thesis, McMaster University, 2007

[20] R. Chai and K.M. Wong, *Application of solitons in multiplexing*, Proc. IWDDC, Edinburgh, UK, November 2004.

[21] P. Rosenau, *Nonlinear dispersion and compact structures*, Physical Review Letters, Volume 73, Issue 13, Page(s): 1737-1741, Sep. 1994

[22] *http://www.playstation.com/*, Sony Computer Entertainment Inc. 2007

[23] *http://www.xbox.com*, Microsoft Corporation. 2007

[24] F. Gardner, *A transformation for digital simulation of analog filters* , IEEE Transactions on Communications, Volume 34, Issue 7, Page(s): 676-680, Jul 1986

[25] A. Fettweis, *Filter having frequency-dependent transmission propereies for electric analog signals*, U.S. Patent 3 967 099, German Patent 2 027 303, first filed in West Germany, June 3, 1970

[26] A. Fettweis, *Digital circuits and systems*, IEEE Transactions on Circuits and Systems, Volume 31, Issue: 1, Page(s): 31- 48, Jan 1984

[27] A. Fettweis, *Wave digital filters: theory and practice* , Proceedings of the IEEE, Volume 74, Issue 2, Page(s): 270-327, Feb. 1986

[28] V. Belevitch, *Classical Network Theory*, San Francisco, CA : Holden-Day 1968

[29] C.R. Paul and S.A. Nasar, *Introduction to Electromagnetic Fields*, Second edition, New York: McGraw-Hill, 1987

[30] K. Meerkotter and T. Felderhoff, *Simulation of nonlinear transmission lines by wave digital filter principles*, IEEE International Symposium on ISCAS '92. Proceedings., Volume 2, Page(s): 875-878, May 1992

[31] K. Meerkotter and R. Scholz, *Digital simulation of nonlinear circuits by wave digital filter principles*, IEEE International Symposium on Circuits and Systems, Page(s): 720-723, May 1989

[32] T. Felderhoff, *Jacobi's method for massive parallel wave digital filter algorithm*, IEEE International Conference on Acoustics, Speech, and Signal Processing, Volume 3, Page(s): 1621 - 1624, May 1996

[33] A. Sarti and G.D. Poli, *Toward nonlinear wave digital filters*, IEEE Transactions on Signal Processing, Volume 47, Issue 6, Page(s): 1654-1668, June 1999

[34] R. Rabenstein, S. Petrausch, A. Sarti, G.D. Sanctis, C. Erkut and M. Karjalainen, *Blocked-based physical modeling for digital sound synthesis*, IEEE Signal Processing Magazine, Volume 24, Issue 2, Page(s): 42 - 54, 2007

[35] J. Makhoul, *Linear prediction: a tutorial review*, Proceedings of the IEEE, Volume 63,Issue 4, Page(s): 561-580, April 1975

[36] S.G. Krantz and H.R. Parks, *The Implicit Function Theorem*, Birkhauser Boston, 2002

[37] J.K. Zhang, *Notes of Digital Signal Processing*, Department of Electrical and Computer Engineering, McMaster University, 2006

[38] T. Felderhoff, *A new wave description for nonlinear elements*, Int. Symp. Circuits System, Atlanta, GA, Page(s): 221-224, May 1996

[39] S. Haykin, *Communication systems*, 4th ed.,New York : Wiley, c2001.

[40] C.E. Shannon, *Communication in the presence of noise*,Proceedings of the IRE, Volume 37, Issue 1, Page(s): 10-21, Jan. 1949

[41] C.E. Shannon, *A mathematial theory of communication*, The Bell System Technical Journal, Volume 27, Page(s): 379-423, 623-656, Oct.1948

[42] J.G. Proakis, *Digital Communications*, 4th ed.,Boston : McGraw-Hill, c2001

[43] S. Hranilovic, *Notes of Information Theory and Coding*, Department of Electrical and Computer Engineering, McMaster University, Winter 2006

[44] A. Papoulis, *Signal Analysis*, McGraw-Hill, 1977.

[45] D. Slepian, *On bandwidth*, Proceedings of the IEEE, Volume 64, Issue 3, Page(s): 292-300, March 1976

[46] G. Borin, G. D. Poli and D. Rocchesso, *Elimination of delay-free loops in discrete-time models of nonlinear acoustic systems* , IEEE Transactions on Speech and Audio Processing, Volume 8, Issue 5, Page(s): 597-605, Sept. 2000

[47] F. Avanzini, F. Fontana and D. Rocchesso, *Efficient computation of nonlinear filter networks with delay-free loops and applications to physically-based sound models* ,Multidimensional Systems, The Fourth International Workshop, Page(s): 110-115, July 2005

[48] J. Szczupak and S. Mitra, *Detection, location, and removal of delay-free loops in digital filter configurations* , IEEE Transactions on Acoustics, Speech, and Signal Processing, Volume 23, Issue 6, Page(s): 558-562, Dec 1975

[49] A. Härmä, *Implementation of recursive filters having delay free loops* , Proceedings of the 1998 IEEE International Conference on Acoustics, Speech, and Signal Processing, Volume 3, Page(s): 1261 - 1264 , May 1998

[50] F. Fontana, F. Avanzini and D. Rocchesso, *Computation of nonlinear filter networks containing delay-free paths* ,Proceedings of Conference on Digital Audio Effects(DAFX-04), Naples, Italy, Page(s): 113-118, 2004

[51] S.K. Mitra, *Digital Signal Processing: A Computer-Based Approach*, 3rd ed. NY : McGraw-Hill Higher Educagion, c2006.

[52] J. Hwang, B. Milne, N. Shirazi and J. Stroomer, *System level tools for DSP in FPGAs*, Proceedings of the 11th International Conference on Field-Programmable Logic and Applications, Volume 2147, Page(s): 534-543, 2001

[53] M.A. Shanblatt and B. Foulds, *A Simulink-to-FPGA implementation tool for enhanced design flow*, Microelectronic Systems Education, Proceedings of 2005 IEEE International Conference, Page(s): 89-90, June 2005

[54] M. Matar, M. Abdel-Rahman and A. Soliman, *Developing an FPGA coprocessor for real-time simulation of power systems*, 2004 International Conference on Electrical, Electronic and Computer Engineering, Page(s): 791-794, Sept. 2004

[55] V. Singh, A. Root, E. Hemphill, N. Shirazi and J. Hwang, *Accelerating bit error rate testing using a system level design tool*, Field-Programmable Custom Computing Machines, 11th Annual IEEE Symposium, Page(s): 62-68, April 2003

[56] S. Haykin, *Adaptive Filter Theory*, 3rd ed. Englewood Cliffs, NJ: Prentice-Hall, 1995.

[57] *Matlab 7.1.0.246 (R14) Service Pack 3, Simulink Version 6.3 (R14SP3)*, The Mathworks, Inc. 2005